CDF note 9406
July 24, 2008

A Search for $ZH \rightarrow l^+l^-b\bar{b}$ in 2.4 fb^{-1} using a Neural Network discriminant

Richard Hughes, Ben Kilminster, Brandon Parks, Brian Winer
Ohio State University
Rob Harr , Shalhout Shalhout
Wayne State University
Bo Jayatilaka, Ashutosh Kotwal, Ravi Shekhar
Duke University
Daniel Whiteson
UC Irvine

Abstract

We search for the Higgs Boson in 2.4 fb^{-1} from the process $ZH \rightarrow l^+l^-b\bar{b}$ in both ee and $\mu\mu$ channels. Since the previous 1 fb^{-1} analysis we have developed looser lepton identification, by making use of a secondary Z selection trigger path. We introduce new loose plug and loose central electron categories. We correct the two candidate Higgs jets with an Artificial Neural Network which assigns $\not\!\!E_{\mathrm{T}}$ to the jets according to their $\not\!\!E_{\mathrm{T}}$ projections and relative ϕ. To maintain signal efficiency and improve signal discrimination, we employ an additional neural network trained to discriminate event kinematics of ZH compared to the main $Z+jets$ background and the kinematically different $t\bar{t}$ background.

1 Introduction

The search for the Higgs boson in the standard model expected $ZH \to l^+l^-b\bar{b}$ process, where l can be an electron or a muon, has a small cross-section compared with $ZH \to \nu\bar{\nu}b\bar{b}$ and $WH \to l^+\nu b\bar{b}$. However, it is the best constrained of the three processes since the final state particles are all measured, and there is both a Z mass resonance in the dilepton invariant mass distribution and a H mass resonance in the dijet invariant mass distribution. Further, any imbalance of calorimeter energy in the transverse direction $\not{E}_{\mathrm{T}}$ can be attributed mainly to downward fluctuations in the jet energies.

In this search we update the 1 fb^{-1} analysis described in Ref. [1]. The overview of the analysis is that we first identify a high P_T electron or muon, then we require a second lepton, of the same flavor, with their invariant mass being consistent with a Z boson. While we don't explicitly search for taus, we retain in our signal region Higgs events produced in association with $Z \to \tau\tau$. Next we identify events with two or more high E_T jets. We correct the jet energies by fitting for their most likely energy loss by utilizing the direction and magnitude of the MET, as well as its transverse projection onto the jets. This correction improves the resolution for identifying dijet resonances. Once the jets are corrected, the events have the same kinematic selection as our final signal region, and we use them to validate our analysis technique as a high statistics control region. Next we divide events into those with one tight secvtx b-tag and two loose secvtx b-tags. The final selected events are binned according to a 2D NN which is trained to simultaneously separate ZH from $t\bar{t}$, and ZH from Z+jets. Using the expected number of background events and their uncertainties, and the final output of the data, we are able to place an upper limit on the cross-section of ZH that could be contributing.

Many features of this analysis are the same as the previous analysis. The main differences are outlined here. The Monte Carlo is updated from Gen 5 to Gen 6 and now includes an estimate of the effect of extra interactions in the simulation. We now model Z+jets processes using Alpgen version 2 Monte Carlo, which is expected to more correctly add in the hard and soft radiation effects which produce the jets. We have added an additional trigger called Z_NOTRACK which selects events with two high E_T electromagnetic deposits in the central or plug regions. This complements the standard high P_T electron trigger which requires a central electron with a track. We make use of the Z_NOTRACK trigger by defining additional lepton categories with less restrictive selection criteria, therefore increasing Z acceptance. The dijet-$\not{E}_T$ corrections from the previous analysis [2] are updated with new MC and with an improved set of variables. Our final NN discriminant is trained for a Higgs mass of 120 and optimized to produce the best error in separating backgrounds. Kinematic selection of jets and b-tagging remain the same in this analysis. The basics of the NN design also remain the same although we allow the NNs to choose a new set of optimal input variables. Since the new Alpgen V2 MC better models the kinematics of Z+jets, we allow some variables to enter into the NN which were not previously used in the 1 fb^{-1} analysis due to poor modeling.

2 Data samples

Level 1 (L1_TWO_EM8)
Two EM energy clusters ET_CENTRAL or ET_PLUG = 8 GeV HAD_EM_CENTRAL = 0.125 HAD_EM_PLUG = 0.0625
Level 2 (L2_TWO_EM16)
Two central, forward, or plug seeds with shoulder energy Seed EM energy = 8 GeV Shoulder EM energy = 7.5 GeV E_T in two towers > 16 GeV $\|\eta\| < 3.6$
Level 3 (L3_TWO_ELECTRON)
Two EM objects each $E_T > 18$ GeV

Table 1: Z_NOTRACK trigger path

The data samples used include up to P15 which corresponds to the end of January 2008. They were taken with the inclusive high p_T lepton triggers: `ELECTRON_CENTRAL_18`, `CMUP_18` and `CMX_18` which require at least one central electron with $E_T > 18$ GeV, or a CMUP or CMX muon with $p_T > 18$ GeV. In addition, the Z_NOTRACK trigger is also used. The goodrun list version 21 is used [4], with good silicon required, and the CMX trigger is ignored for runs < 150145. The luminosity of the datasets is shown in Table 2. The trigger requirements for this trigger are defined in Table 1. The datasets used are defined in Tables 2 and 3.

3 Background model

Backgrounds to the signal process are mainly those with two leptons and two or more jets.

The main backgrounds are $Z + b\bar{b}$, $Z + c\bar{c}$, Z+mistagged light jets, $t\bar{t}$, ZZ, ZW, and WW, and fake Z+jets events mostly coming from W+jets where

data period(s)	**high P_t muon sample**
0	bhmukd
1-4	bhmukh
5-7	bhmuki
8-10	bhmumi
11-13	bhmumj
14-15	bhmumk

Table 2: High P_T muon datasets.

data period(s)	**high P_t electron sample**
0	bhelkd
1-4	bhelkh
5-7	bhelki
8-10	bhelmi
11-13	bhelmj
14-15	bhelmk

Table 3: High P_T electron datasets.

Good Run List	**Data Periods**	**Luminosity**	**Trigger(s)**
v21 good em,mu,si	0-15	2388.16 fb^{-1}	ELECTRON _ CENTRAL _ 18 Z _ NOTRACK
v21 good em,mu,si	0-15	2388.16 fb^{-1} 2336.55 fb^{-1}	CMUP _ 18 CMX _ 18

one lepton is faked. $Z \rightarrow \tau\tau+$ jets backgrounds are used in our model in order to reproduce the Drell Yan continuum at the low end of the dilepton mass window. Diboson processes, including ZH are modeled with PYTHIA. $Z+$ jets hard processes are modeled with sc alpgen, with PYTHIA for the hadronization and showering. Extra interactions are simulated using PYTHIA, and poisson distributed into events according to the measured instantaneous luminosities for a run range for which the Monte Carlo was simulated. Although the run range used for most of the MC is not of the same as that of the data, we check the MC modeling by comparing to MC events reweighted according to the number of vertices expected in the final data sample, and do not see a significant difference. We use data to model the mistags and the fake Zs as discussed later in the text. The signal MC datasets we use are listed in Table 4. The backgrounds are listed in Table 5.

$ZH \rightarrow \ell\ell b\bar{b}$ @ M_H	**MC Sample**
100	ahgt2k
105	ahgt2l
110	ahgt2m
115	ahgt2n
120	ahgt2o
125	ahgt1a
130	ahgt1b
135	ahgt1c
140	ahgt1d
145	ahgt1e
150	ahgt1f

Table 4: Signal MC.

4 Lepton selection

Our muon selection remains unchanged from the 1 fb^{-1} analysis [1], and is also documented in [5]. We select one tight muon from the high P_T CMX or

Process	**MC Sample(s)**
$(Z \to \ell\ell)$+ jets	xtop[0-9]p ytop[0-9]p ztop[2-4,7-9]p ztopp[0,1,5,6]p ztopl[0,1,2]p ztopm[0,1,2]p
$(Z \to \ell\ell)$+ hf jets	ztopc[0,1,2,5,6,7] ztopb[0,1,2,5,6,7] ztopbt ztopct
DiBoson	itopww itopwz itopzz
$t\bar{t}$	ttop75
$Z \to \tau\tau$	xtopt[0,1,2] ztopt[2,3,4] zttt[0-4]h

Table 5: Background MC datasets used.

CMUP trigger path. At least one muon must satisfy the trigger requirements. We apply the muon selection of Table 6. Our second muon is looser in P_T, and is not required to leave hits in any muon chambers. Our track definition is the same as the standard Deftrack definition, although we veto silicon-standalone tracks. Our loose muon selection is defined in Table 7.

Our electron selection is much looser than previously, and we will discuss it in detail here. In the previous analysis, we had tight central (TC), loose central (LC), loose plug (LP) types. We could form a Z boson with a TC and either a TC, LC, or TP. In our new analysis, we have additional electron categories, and we also define a more detailed dilepton selection. Our electron categories are listed in Table 8. The selection criteria for each electron type is defined in Tables 9, 10, 11, 12, 13, 14, 15, 16, and 17. The dilepton categories are composed of a subset of combinations of the defined lepton types and are listed in Table 18. For dilepton categories with tracks, we require them to have opposite curvature to reduce backgrounds.

For each electron type, we define scale factors using the method outlined in Ref. [6]. We define loose probe electrons in the central and plug regions, and after subtracting off background contamination from sidebands, compute scale factors in three Z mass regions (Table 19, We use the difference in the scale factors in these regions to compute the uncertainty on the scale factor (Table 20). For the CrkTrk category, we use scale factors found in Ref. [7]. For muons, we use values from the Joint Physics class.

We determine the fake rate for each of our electron types by using jet20, jet50, jet70, and jet100 data. We require $\not\!\!E_{\mathrm{T}} < 15$ GeV in order to remove real electrons from W processes. We also veto Z candidates which have two electrons. Our fake rates use denominators composing of all cone 0.4 jets with the required E_T cut and detector region of the electrons, after rejecting the leading jet firing the trigger. The numerators are defEm objects passing the electron selection and matched to the denominator jet within $\Delta R < 0.4$. We smear the denominator E_T to better model the E_T of the numerator object in jet data 4. We use variable-sized bins to maintain statistics, and we find that a 50% systematic uncertainty is required to span the fake rates coming from each jet sample. Our electron fake rate functions for each electron type are shown in Figures 1, 2, and 3. We apply the fake probabilities to all denominator pairs in our electron dataset. We check which fraction of Z events are accepted by each dilepton category, and evaluate the expected fake

Tight Muon Selection
$P_T > 20$ GeV
Had Energy < 6 GeV
Em Energy < 2 GeV
CMX $\rho > 140$ cm
$>=$ 3 axial and $>=$3 stereo segments
Isolation fraction < 0.1
$\lvert\Delta X\rvert_{CMU} < 3.0$ cm
$\lvert\Delta X\rvert_{CMP} < 5.0$ cm
$\lvert\Delta X\rvert_{CMX} < 6.0$ cm
Impact parameter $d_0 < 0.2$ w/Silicon hits (0.02 w/out)
Z_0 is within 60 cm of z=0

Table 6: The tight muon is currently the same as the Top group's tight selection for CMX and CMUP.

fraction for the category as shown in Table 21. The relative fake fractions demonstrate which categories have the highest non-Z background rates. The overall fake rate for $Z \rightarrow ee$ is 2.4%, and for $Z \rightarrow \mu\mu$ we use the same-sign sample to determine our fake rate of 1%. We demonstrate that there is no Z contamination in our fake estimate by showing the dilepton mass distribution for our expected fake background shape in Figures 5, and 6.

We apply trigger efficiencies to each dilepton combination according to the joint physics recommendations. However, since some dilepton categories can pass multiple triggers, and some dilepton categories have two leptons which can fire the same trigger, we are careful with the accounting, and determine a different trigger efficiency for each dilepton pair. Since there are multiple ways a Z candidate can be identified, the trigger efficiencies are typically close to 100%.

We compare our background model for the dilepton categories at the Z candidate level and find the dilepton mass distributions shown in Figures 7, 8, 9, and 10 . Agreement is satisfactory both in normalization and shape and improves as the dilepton categories are added together, and as additional event selection on the jets is applied.

Loose Muon Selection
$P_T > 10$ GeV *
Had Energy < 6 GeV
Em Energy < 2 GeV
Isolation fraction < 0.1
Impact parameter $d_0 < 0.2$ w/Silicon hits (0.02 w/out)
>=2 axial and >=2 stereo segments
>= 1 COT hits
No stub requirements *
Z_0 is within 60 cm of z=0

Table 7: The loose muon selection criteria based on CMIO muons.

TC	Tight-central
LC1	Loose-central 1
LC2	Loose-central 2
TP	Tight Plug Phoenix
LP	Loose Plug
LPPhx	Loose Plug Phoenix
LPNphx25	Loose Plug Non-phoenix, 25 GeV E_T cut
LPNphx25	Loose Plug Non-phoenix, 33 GeV E_T cut
CrkTrk	Crack Track, no Em requirement

Table 8: The electron types we consider in this analysis.

TC (Tight central) Selection
Region = 0
Fiducial = 1 or 2
$E_T \geq 18$
Trk $P_T \geq 9$ GeV
Not a conversion
$\|TrackZ_0\| \leq 60$ cm
≥ 2 Ax layers ≥ 10 hits
≥ 2 St layers ≥ 10 hits
HadEm $\leq 0.055 + 0.00045 \times$ En
Isol – $0.35 \times (N_{vtx} - 1) \leq 3 + 0.02 \times E_T$
$L_{shr} \leq 0.2$
$\frac{E}{P} \leq 2.5 + 0.015 \times E_T$ or TrkPt ≥ 50 GeV
$\|\Delta$ Z $\| \leq 3$ cm
-3 $\leq \Delta X \times Q \leq 1.5$
$\chi^2_{strip} \leq 25$

Table 9: Tight central (TC) electron selection.

LC1 (Loose central 1) Selection
Region = 0
Not a TC
$E_T \geq 18$
Trk $P_T \geq 9$ GeV
Not a conversion
$\|TrackZ_0\| \leq 60$ cm
HadEm $\leq 0.055 + 0.00045 \times$ En
Isol – $0.35 \times (N_{vtx} - 1) \leq 4 + 0.02 \times E_T$
$L_{shr} \leq 0.2$

Table 10: Loose central 1 (LC1) electron selection.

LC2 (Loose central 2) Selection
Region = 0
Not a TC or LC1
$E_T \geq 10$
Trk $P_T \geq 5$ GeV
$\lvert TrackZ_0 \rvert \leq 60$ cm
HadEm $\leq 0.055 + 0.00045 \times$ En
Isol – $0.35 \times (N_{vtx} - 1) \leq 4 + 0.02 \times E_T$

Table 11: Loose central 2 (LC2) electron selection.

TP (Tight plug) Selection
Region = 1
$E_T \geq 25$
Phoenix
$1.2 \leq \lvert\eta\rvert \leq 2.8$
if En $\leq$ 100 GeV, HadEm $\leq$ 0.05
if En > 100 GeV, HadEm $\leq 0.05 + 0.026 \times \log(\text{En})$
Isol – $0.35 \times (N_{vtx} - 1) \leq 1.6 + 0.02 \times E_T$
$\chi^2_{3x3} \leq 25$

Table 12: Tight plug (TP) electron selection.

LpPhx (Loose plug Phoenix) Selection
Region = 1
Not a TP
Phoenix
$E_T \geq 18$
if En $\leq$ 100 GeV, HadEm ≤ 0.05
if En > 100 GeV, HadEm $\leq 0.05 + 0.026 \times \log(\text{En})$
Isol $- 0.35 \times (\text{N}_{vtx} - 1) \leq 2.5 + 0.02 \times E_T$
$\frac{Isol}{E_T} < 0.1$

Table 13: Loose plug phoenix(LpPhx) electron selection.

LpNPhx25 (Loose plug Non-phoenix) Selection
Region = 1
Not a TP or LpPhx
Not a Phoenix
$E_T \geq 25$
if En $\leq$ 100 GeV, HadEm ≤ 0.05
if En > 100 GeV, HadEm $\leq 0.05 + 0.026 \times \log(\text{En})$
Isol $- 0.35 \times (\text{N}_{vtx} - 1) \leq 2.5 + 0.02 \times E_T$
$\frac{Isol}{E_T} < 0.1$

Table 14: Loose plug phoenix(LpNphx25) electron selection.

LpNPhx33 (Loose plug Non-phoenix) Selection
Region = 1
Not a TP or LpPhx or LpNPhx25
Not a Phoenix
$E_T \geq 33$
if En $\leq$ 100 GeV, HadEm $\leq$ 0.05
if En $>$ 100 GeV, HadEm $\leq 0.05 + 0.026 \times \log(\text{En})$
Isol $- 0.35 \times (\text{N}_{vtx} - 1) \leq 2.5 + 0.02 \times E_T$
$\frac{Isol}{E_T} < 0.1$

Table 15: Loose plug phoenix(LpNphx33) electron selection.

LP (Loose plug) Selection
Region = 1
Not a TP
$E_T \geq 18$
if En $\leq$ 100 GeV, HadEm $\leq$ 0.05
if En $>$ 100 GeV, HadEm $\leq 0.05 + 0.026 \times \log(\text{En})$
Isol $- 0.35 \times (\text{N}_{vtx} - 1) \leq 2.5 + 0.02 \times E_T$

Table 16: Loose plug (LP) electron selection.

CrkTrk (Crack Track) Selection
$\|Z_0\| \leq 60$ cm
$\|D_0\| \leq 0.2$ cm
≥ 3 Ax layers & ≥ 15 hits
≥ 3 St layers & ≥ 15 hits
Not a CMUP or CMX muon
Not Track Fiducial
Not a conversion
$P_T \geq 20$
$\frac{Isol}{P_T} < 0.1$ or $\frac{EmIsol4}{P_T} < 0.1$

Table 17: Crack Track (CrkTrk) electron selection.

Combination	**1st Lepton**	**2nd Lepton**	**Additional Cuts**
TcTc	Tc	Tc	opposite charge
TcLc	Tc	Lc1, Lc2	opposite charge
TcTp	Tc	Tp	none
TcLp	Tc	LpPhx, LpNphx25, LpNphx33, Lp	none
Lc1Lc1	Lc1	Lc1	opposite charge
TpLc	Tp	Lc1, Lc2	none
Lc1Lp	Lc1	LpPhx, LpNphx25, LpNphx33	none
TpTp	Tp	Tp	none
TpLp	Tp	LpPhx, LpNphx33	none
LpLp	LpPhx	LpPhx, LpNphx33	both $E_t >= 30$
TcCrkTrk	Tc	CrkTrk	opposite charge
MuonMuon	CMUP, CMX	CMUP,CMX,CMIO	opposite charge

Table 18: Allowed dilepton types considered in this analysis.

e Type	**66-116**	**76-106**	**86-96**
Tc	0.990196	0.988176	0.992926
Lc1	1.00644	1.0056	1.00404
Lc2	1.00128	1.00119	1.00073
Tp	0.921023	0.923176	0.913724
Lp	1.00304	1.00141	0.998939
LpPhx	0.944691	0.95437	0.937738
LpNphx25	1.0138	1.02989	1.01047
LpNphx33	1.01758	1.06056	1.0218

Table 19: Electron scale factors in different mass regions.

e Type	scale factor
Tc	$.9929 \pm 0.005$
Lc1	1.0040 ± 0.002
Lc2	1.0007 ± 0.0005
Tp	$.9137 \pm 0.010$
Lp	$.9989 \pm 0.002$
LpPhx	$.9377 \pm 0.017$
LpNphx25	1.0105 ± 0.019
LpNphx33	1.0218 ± 0.041

Table 20: Electron scale factors with uncertainties used in the analysis.

Combination	**% of Total Z's Candidates in data**	**% fakes**
TcTc	12.18	0.015
TcLc	5.73	4.06
TcTp	16.22	0.034
TcLp	15.87	3.5
Lc1Lc1	0.35	4.0
TpLc	4.24	8.1
Lc1Lp	2.34	14.75
TpTp	5.1	0.03
TpLp	5.2	0.09
LpLp	1.08	5.95
TcCrkTrk	5.73	4.8
MuonMuon	25.9	0.27
All	100	2

Table 21: For each dilepton category, we list the percentage of Zs in data, as well as the expected fake percentage.

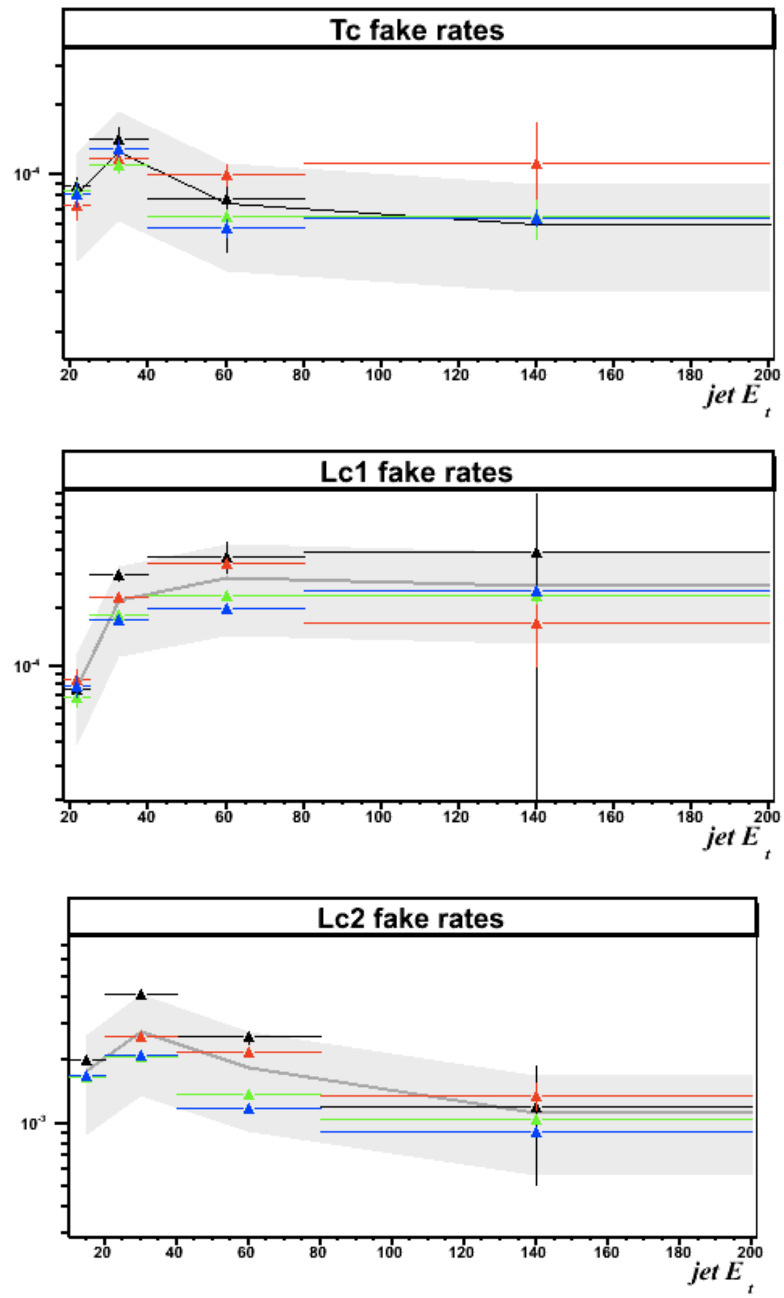

Figure 1: Fake rates for Tc, Lc1 and Lc2 type electrons. The mean fake rate from jet20 (black) , jet50 (red), jet70 (green) and jet100 (blue) data is applied to the high P_t electron data. The 50 % error band is shown in grey.

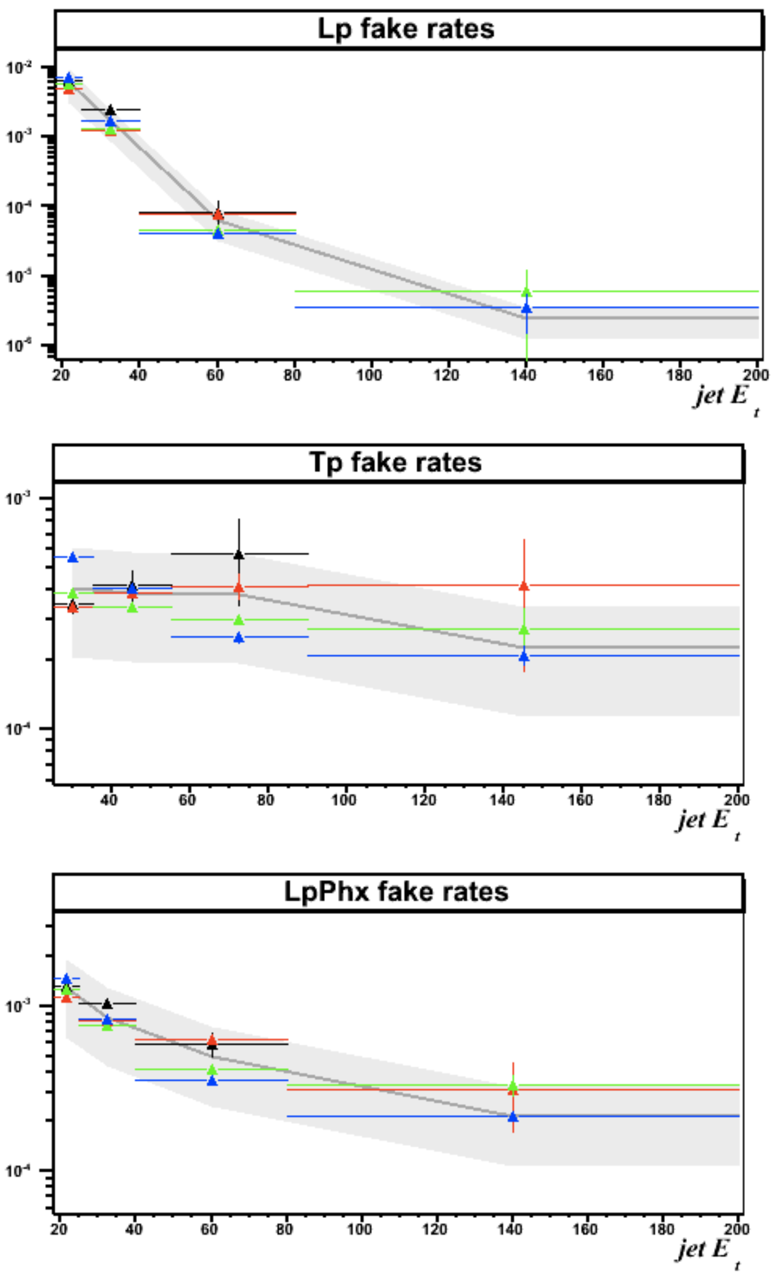

Figure 2: Fake rates for Lp, Tp and LpPhx type electrons.

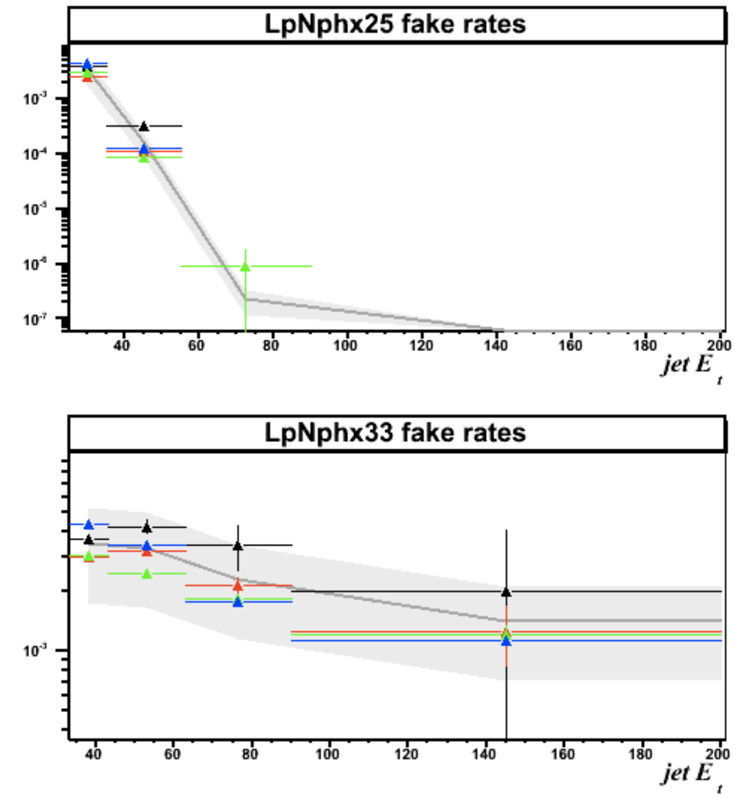

Figure 3: Fake rates for Lp, Tp and LpPhx type electrons.

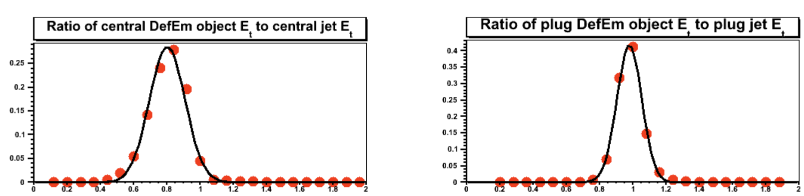

Figure 4: Ratio of Em object E_t to jet E_t in jet triggered data.

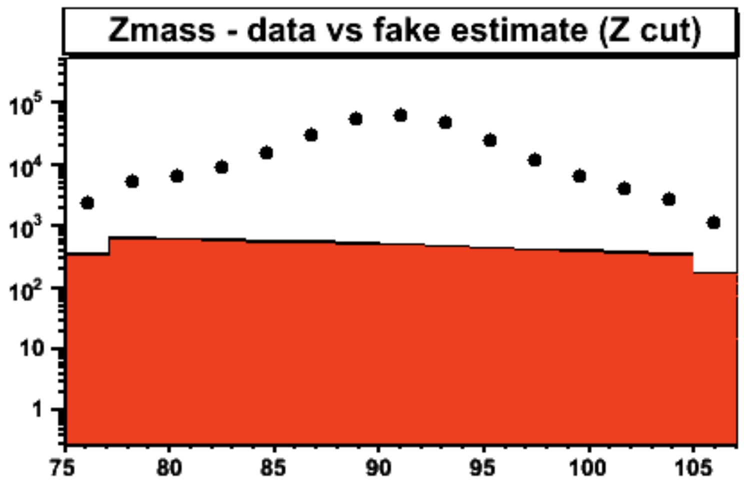

Figure 5: Fake component (red) of total data (black) for $Z \to ee$.

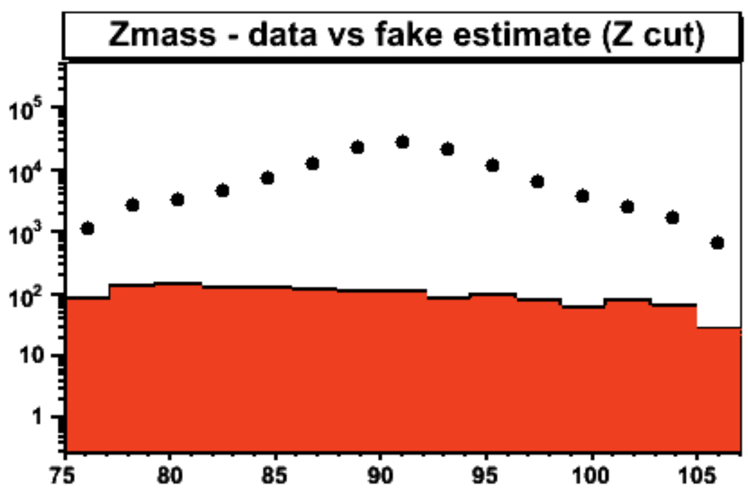

Figure 6: Fake component (red) of total data (black) for $Z \to \mu\mu$ and CrkTrk

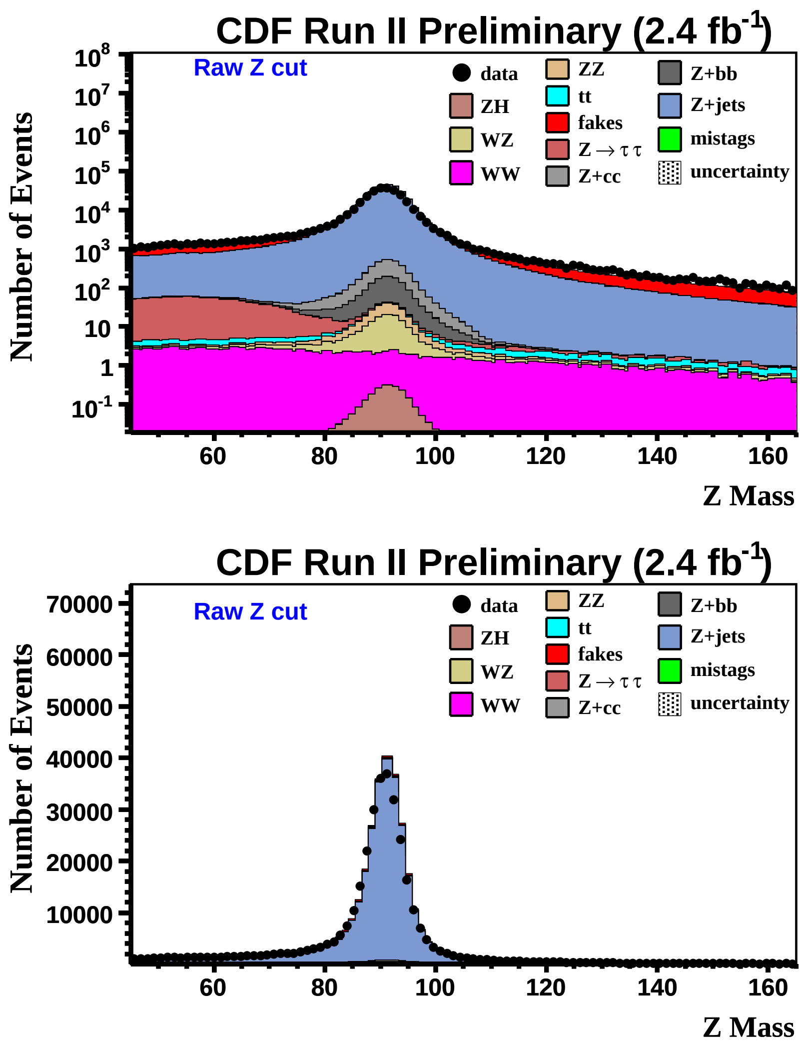

Figure 7: Z mass for $Z \to ee$.

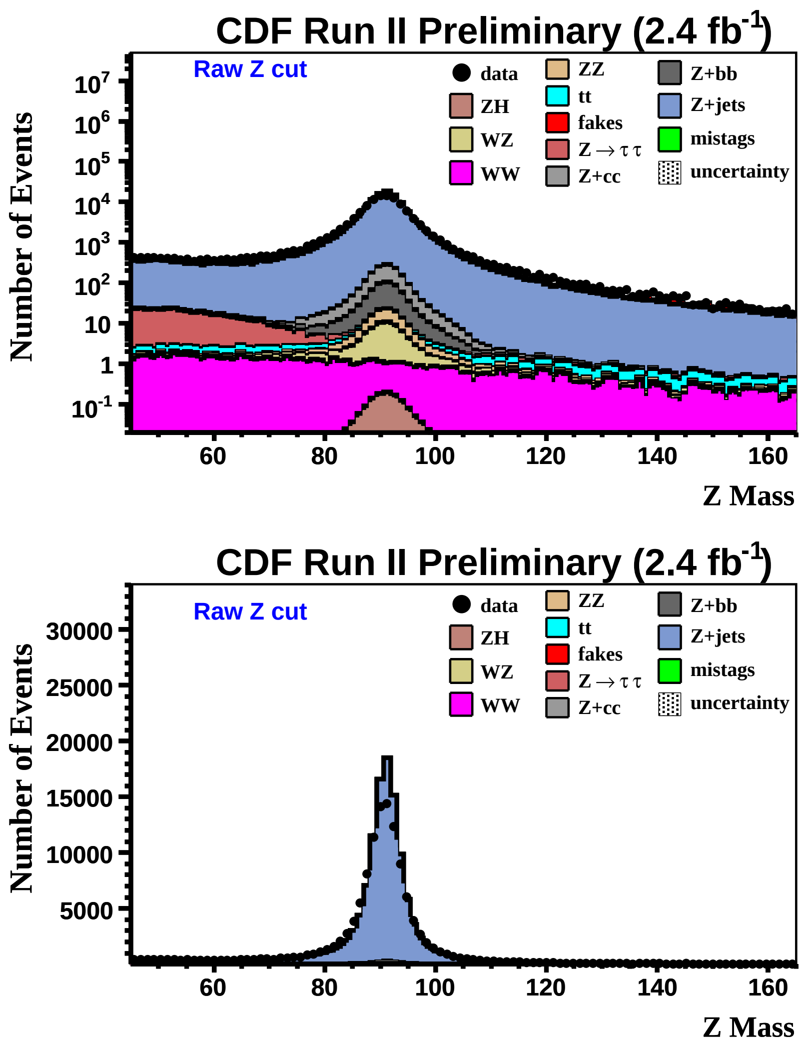

Figure 8: Z mass for $Z \to \mu\mu$.

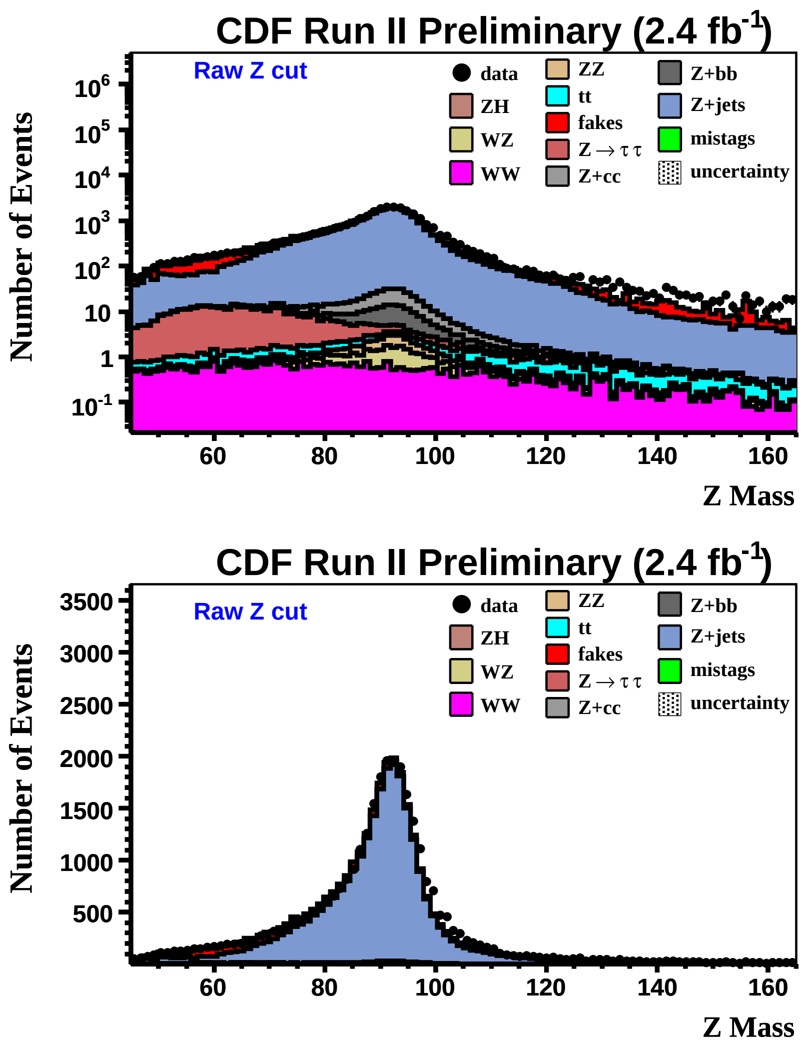

Figure 9: Z mass for $Z \rightarrow e\ CrkTrk$.

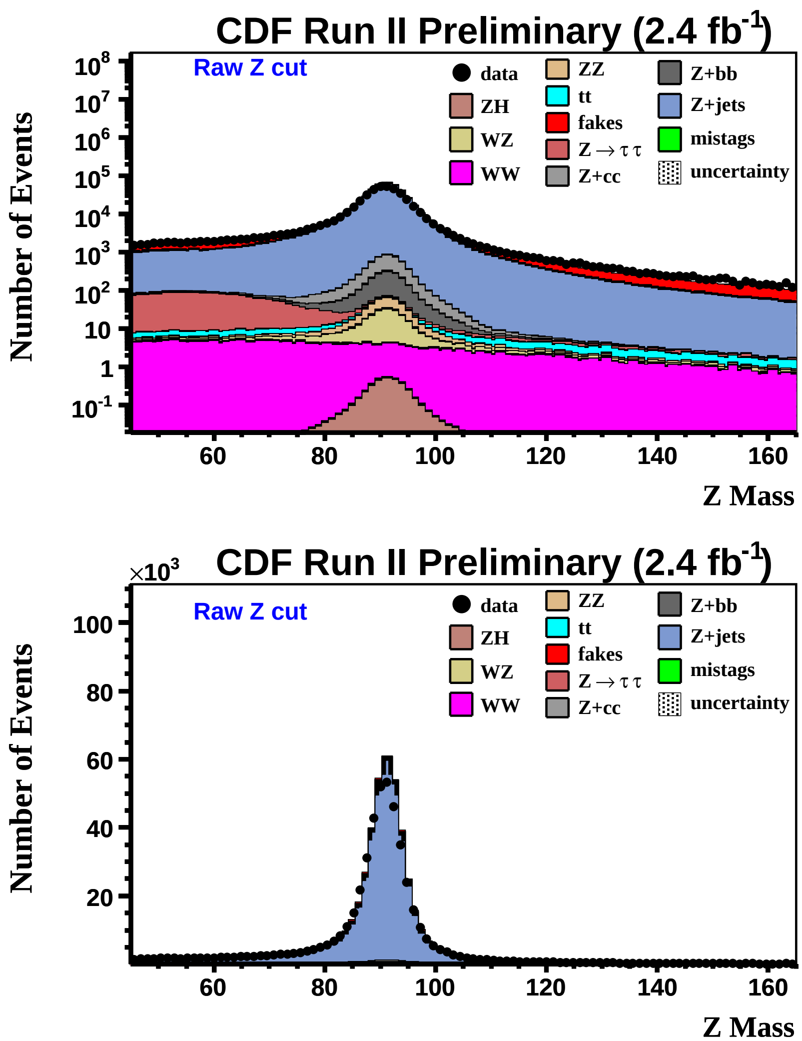

Figure 10: Z mass for all Z types.

+

Selection
Kinematic selection to get pretagged control region
Allowed dilepton category from Table 18 ΔZ_0 of leptons < 4 cm Z mass window 76 GeV - 106 GeV 2 or more Cone 0.4 jets L5 $E_T > 15$ GeV, $\|\eta\| < 2$ 1 or more jets with L5 $E_T > 25$ GeV
Additional b-tagging selection for signal region
2 or more loose SECVTX tags If not found 1 or more tight SECVTX tags (with b-tagged jet $E_t \geq 25$)

Table 22: Summary of event selection.

5 Event selection

After we select Z candidates, we apply additional selection, as in Table 22. The agreement of our preselection is shown in Table 23 and in the Appendix.

After tagging our event sample is divided into four categories in order to maintain high $\frac{S}{\sqrt{B}}$. The events are assigned a category by Z type as shown in Table 24. The final tag categories are *Double Tag High*, *Single Tag High*, *Double Tag Low* and *Single Tag Low*.

6 Jet energy resolution corrections

We correct jet energies with the $\not\!\!E_{\mathrm{T}}$ direction and magnitude, and projections onto the jet directions as in the procedure in Ref. [2].

Corrections were redone to use Gen 6 MC. In order to sample a wide range of jet E_Ts in order to prevent overcorrecting low E_T jets, we train over Higgs masses (50 - 200 GeV, in 10 GeV steps). We configure the NN slightly differently than previously. We use relative $\Delta\phi$ between jets and $\not\!\!E_{\mathrm{T}}$ direction rather than absolute ϕ. We also use a signed $\not\!\!E_{\mathrm{T}}$ projection to correct jets,

Event Totals			
sample	**Z**	**1 jet**	**2 jet Et 25**
ZH	3.5	3.46	2.76
tt	54.66	54.25	45.36
WW	82.09	26.01	5.5
WZ	189.92	144.74	84.86
ZZ	206.33	135.46	81.65
Z $\rightarrow \tau\tau$	158.74	28.51	4.27
Z+jets (bb)	1540.56	836.86	243.86
Z+jets (cc)	3363.1	1643.27	474.06
mistags / Z + jets	399711	60352.1	7140.82
fakes	8252.99	2697.17	591.58
Total Background	413563	65921.8	8674.72
Data	420900	70228	9035

Table 23: Preselection event totals.

High	Low
TcTc	Lc1Lc1
TcLc	TpLc
TcTp	Lc1Lp
TcLp	TpTp
μ μ	TpLp
	LpLp
	TcCrkTrk

Table 24: Z type and $\frac{S}{\sqrt{B}}$ category.

L5 Jet 1 E_T
L5 Jet 2 E_T
Jet 1 η
Jet 2 η
$\Delta\phi(jet1, jet2)$
$\Delta\phi(\not{E}_{\rm T}, jet1)$
$\Delta\phi(\not{E}_{\rm T}, jet2)$
Jet 1 Projection onto $\not{E}_{\rm T}$
Jet 2 Projection onto $\not{E}_{\rm T}$
$\not{E}_{\rm T}$ magnitude

Table 25: Variables used to correct jet energies to parton level.

rather than our an unsigned projection. This has the advantage of not applying the same correction to jets both pointed in the opposite direction and the same direction as the $\not{E}_{\rm T}$ direction.

The variables used to train the dijet mass correction NN are shown in Table 25. The NN corrections provide major improvement with respect to the Level 5 corrections in terms of the jet energy resolution, as well as providing a better estimate of the parton P_T. This leads to a truer and narrower reconstructed dijet mass. We evaluate the improvement for different Higgs masses in terms of 2σ fits to the dijet mass resolution, as shown in Table 26. Also shown in Table 27 are the means from the fits, showing that the NN does not overcorrect or undercorrect the jet energies. We test the linearity of the corrections in terms of mean reconstructed mass for a given input Higgs mass, and find the corrections to be more linear than the previous Gen 5 corrections.

7 Background modeling of data

After applying dijet energy corrections, we test our background model in events before applying the b-tag requirements. We show variables which will later be incorporated into the NN.

Higgs mass	L5 jetcorr	Gen 5 NN	Gen 6 NN
110	17.2 %		10.8 %
120	17.7 %	10.5%	10.5 %
130	17.3 %		9.7 %
150	16.8 %	10.0%	9.5 %

Table 26: Comparison of dijet mass resolution using different correction algorithms..

Higgs mass	L5 jetcorr	Gen 5 NN	Gen 6 NN
110	91 GeV		111
120	100	118	120
130	107		130
150	124	141	147

Table 27: Comparison of mean of dijet mass fit using different correction algorithms..

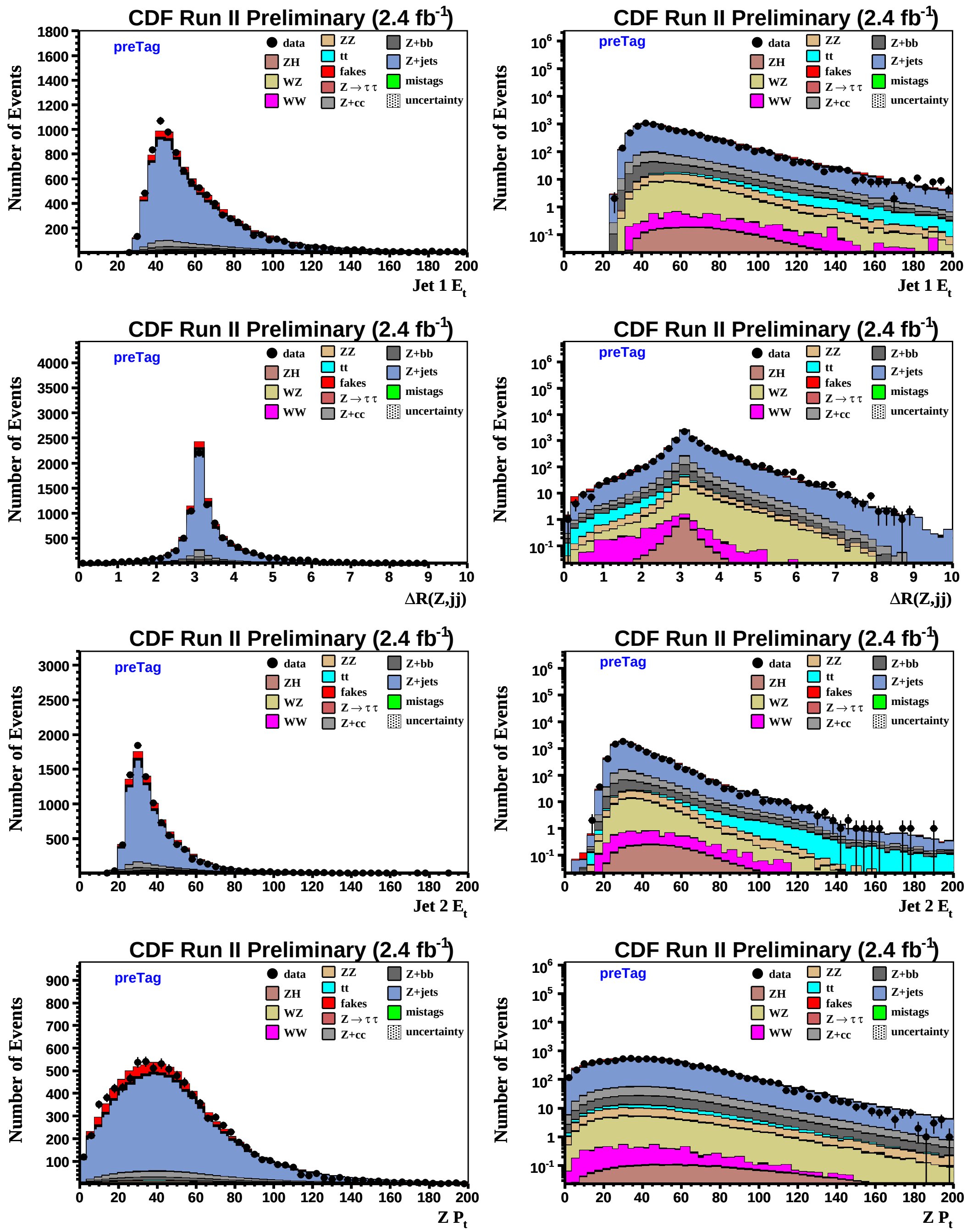

Figure 11: Pre-Tag NN inputs : Shape comparisons for all Z categories.

8 Neural Network signal-background discriminant

We develop a 2D NN using the same techniques as the 1 fb^{-1} analysis. We consider 29 input variables, after dijet energy corrections are applied, and iteratively add in the best variables until adding additional variables does not improve the training error.

Our final NN configuration uses the inputs listed in Table 28. In Figures 11 through 14 and in the Appendix, we show agreement of our NN discriminants using the pretagged data, which is dominated by Z+light jets. Two dimensional NN output distributions for pretag data and MC are shown in fiigres 15 through 17. Projections are shown in Figures 18 and 19.

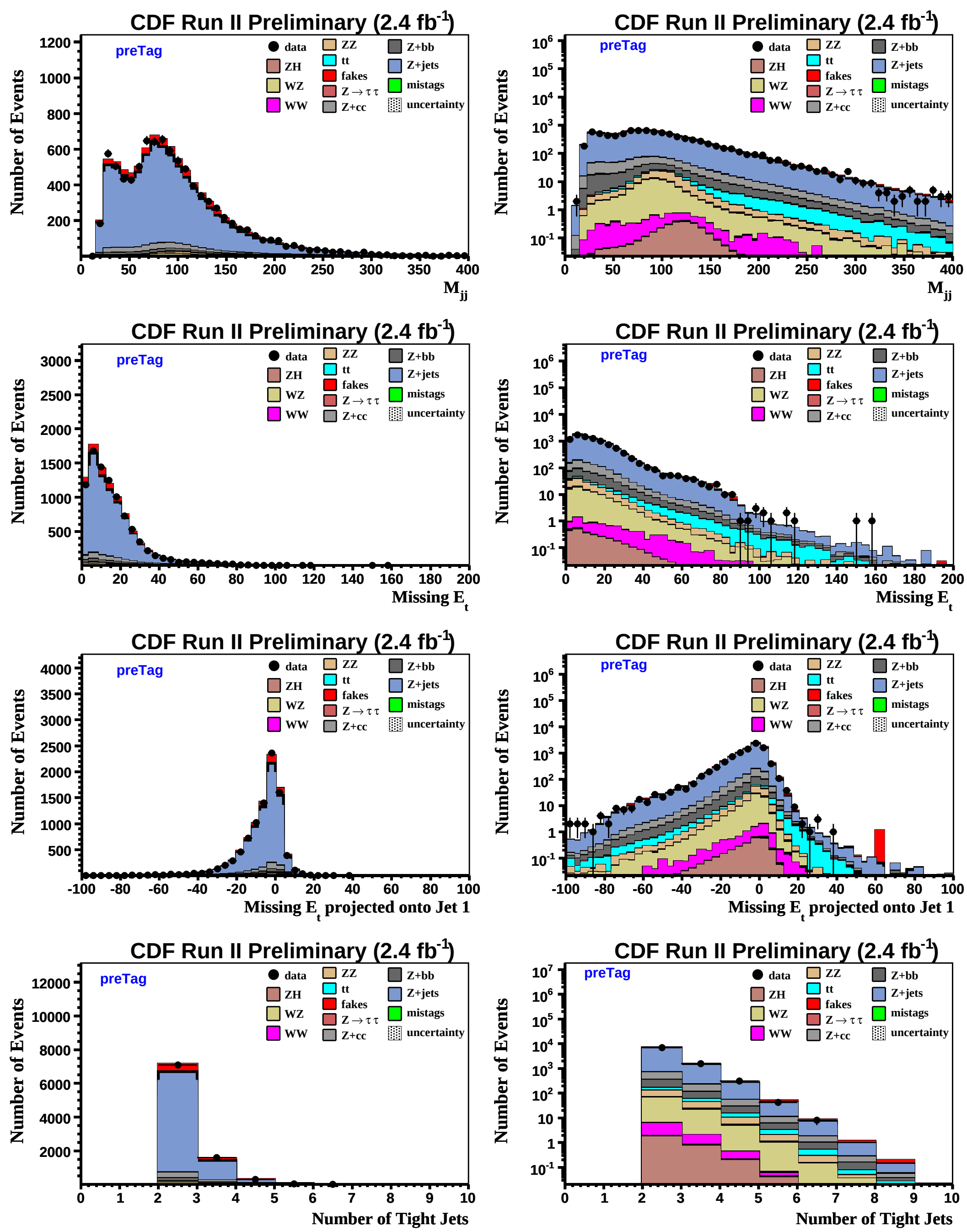

Figure 12: Pre-Tag NN inputs : Shape comparisons for all Z categories.

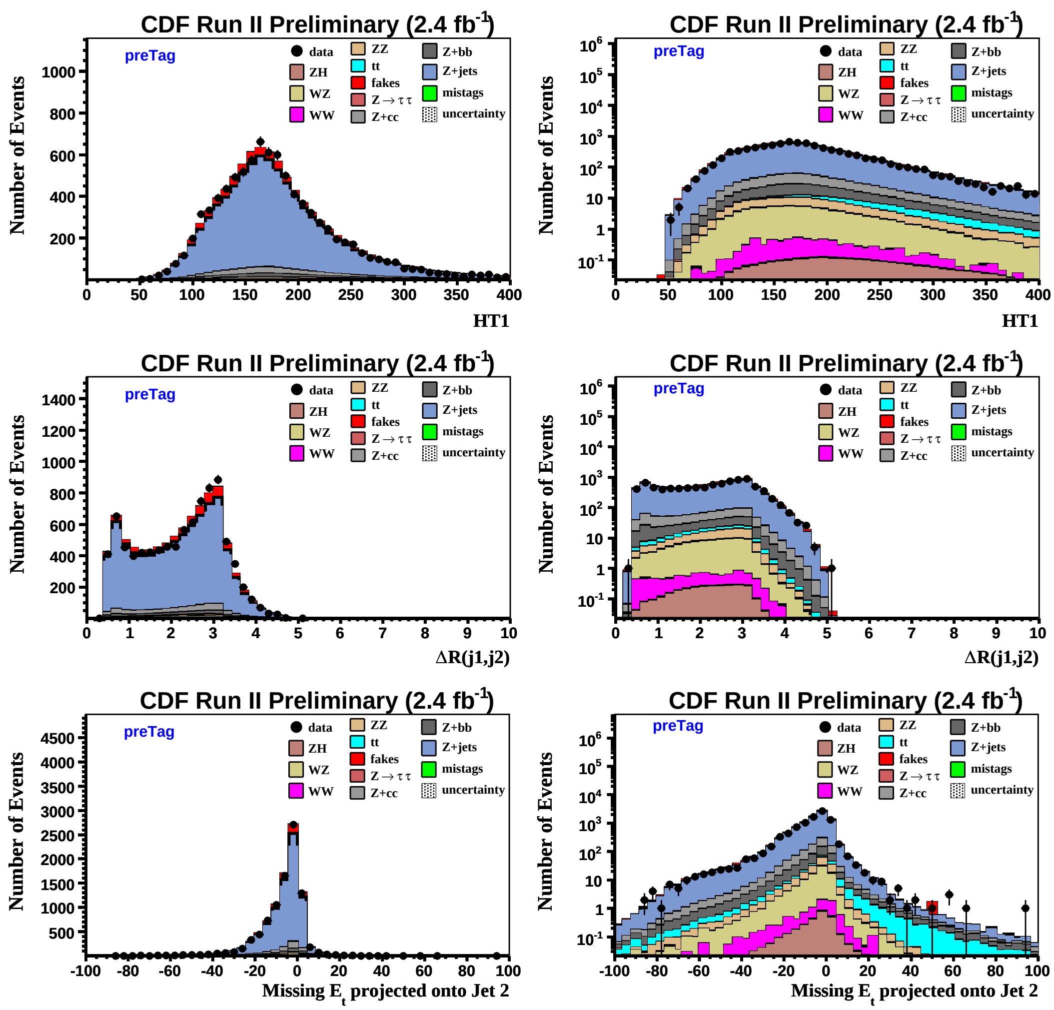

Figure 13: Pre-Tag NN inputs : Shape comparisons for all Z categories.

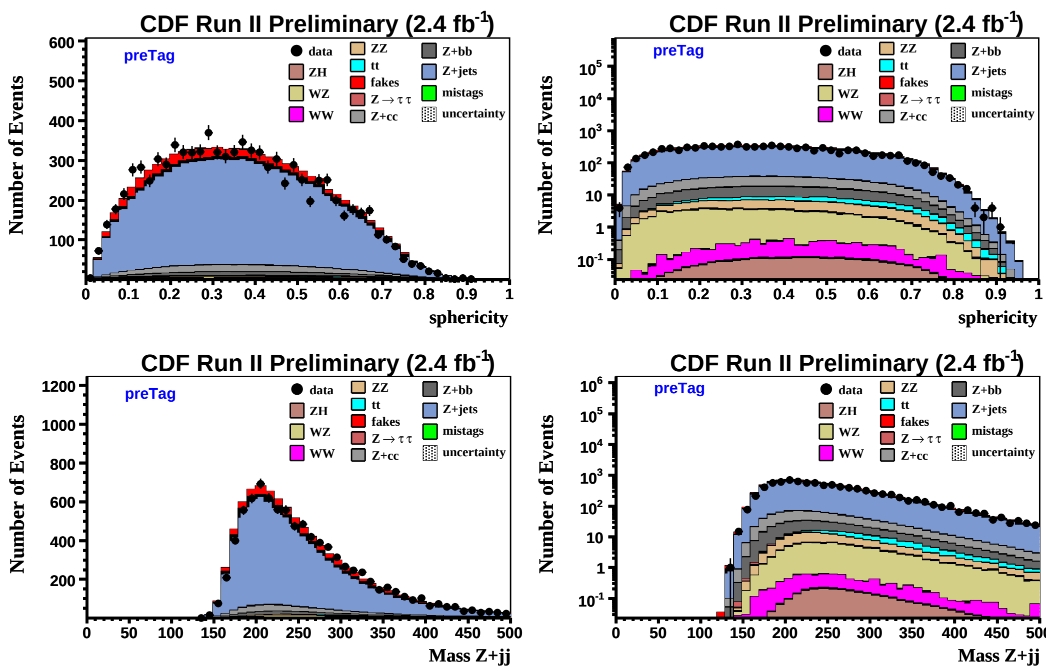

Figure 14: Pre-Tag NN inputs : Shape comparisons for all Z categories.

NN Inputs	**Error**
jet 1 E_t	0.3485
$\Delta R(Z, jj)$	0.3019
jet 2 E_t	0.2783
Z P_t	0.2548
M_{jj}	0.2326
Missing E_t	0.2257
MET projected onto jet 1	0.2196
Number of Tight Jets	0.2126
HT1	0.2082
$\Delta R(jet1, jet2)$	0.2073
MET projected onto jet 2	0.206
sphericity	0.2053
Mass Z+jj	0.2042

Table 28: NN inputs added in sequentially shown with average testing error.

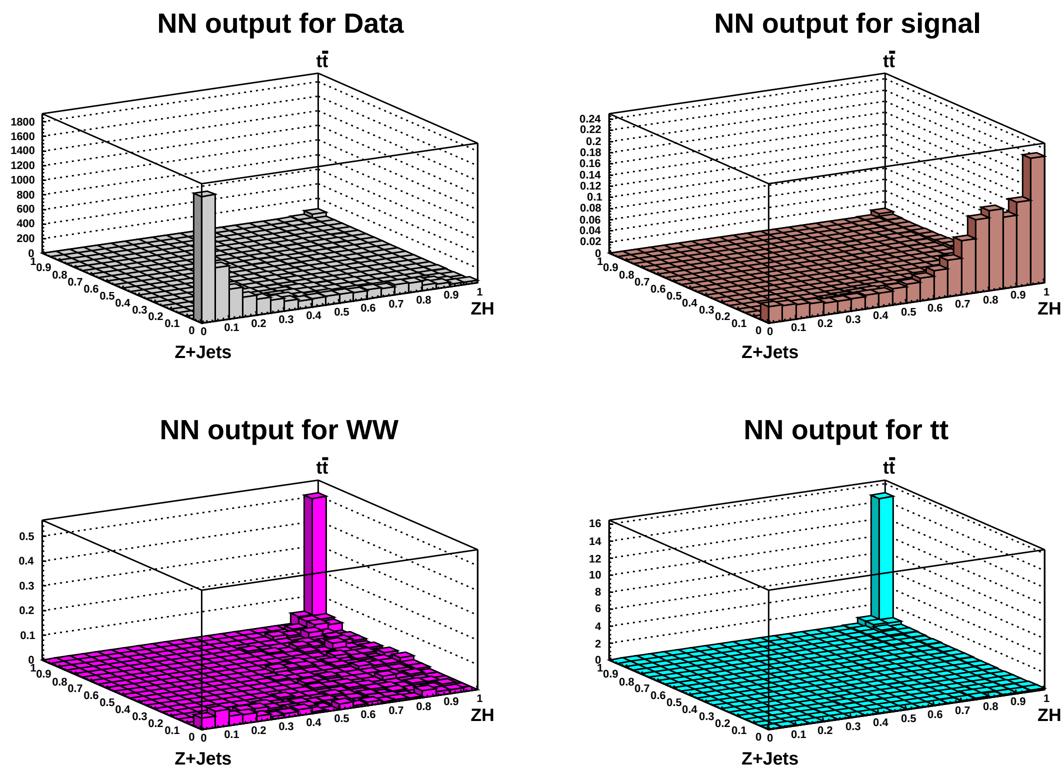

Figure 15: Pre-Tag NN outputs

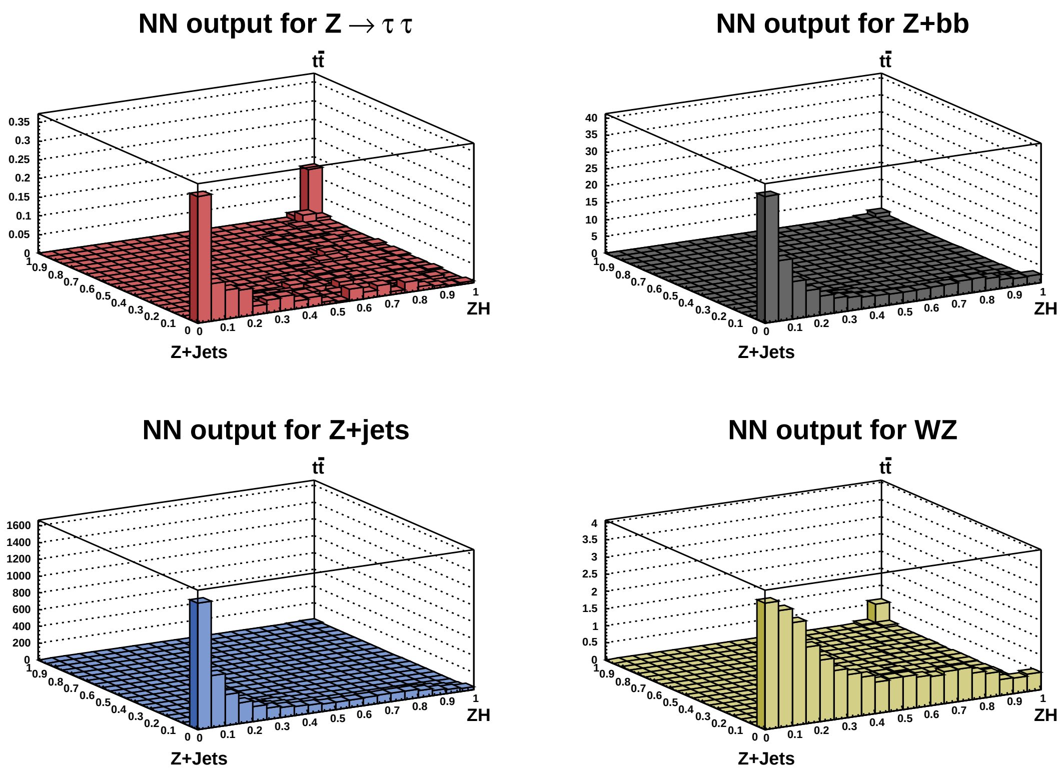

Figure 16: Pre-Tag NN outputs

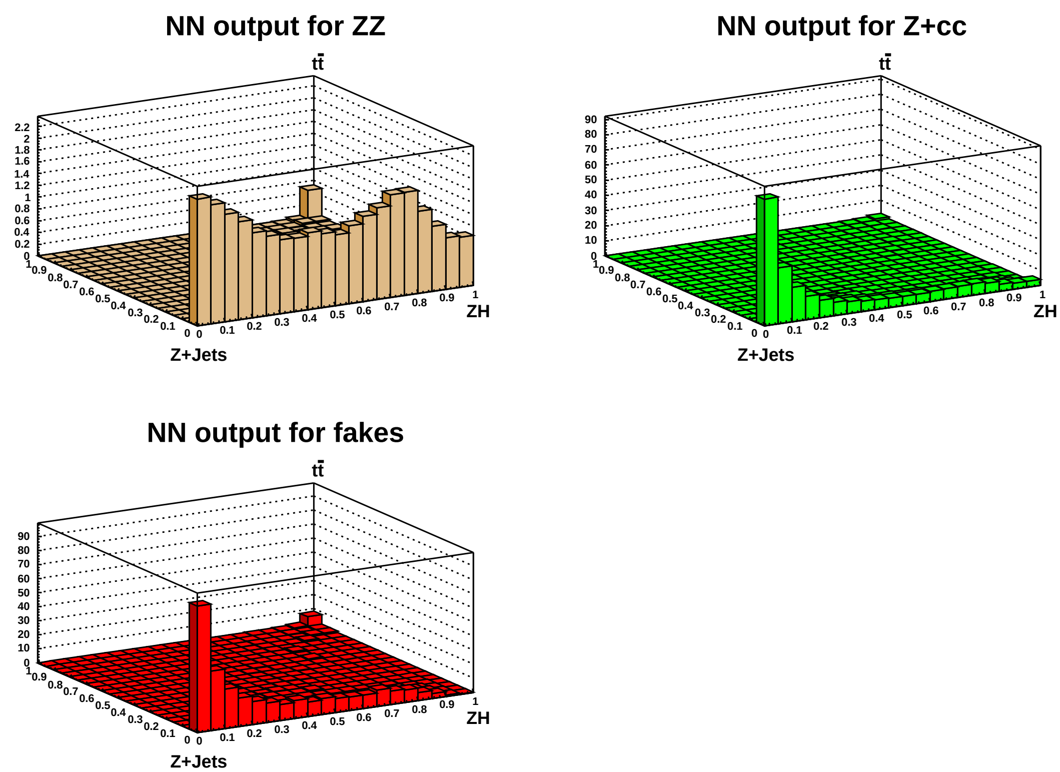

Figure 17: Pre-Tag NN outputs

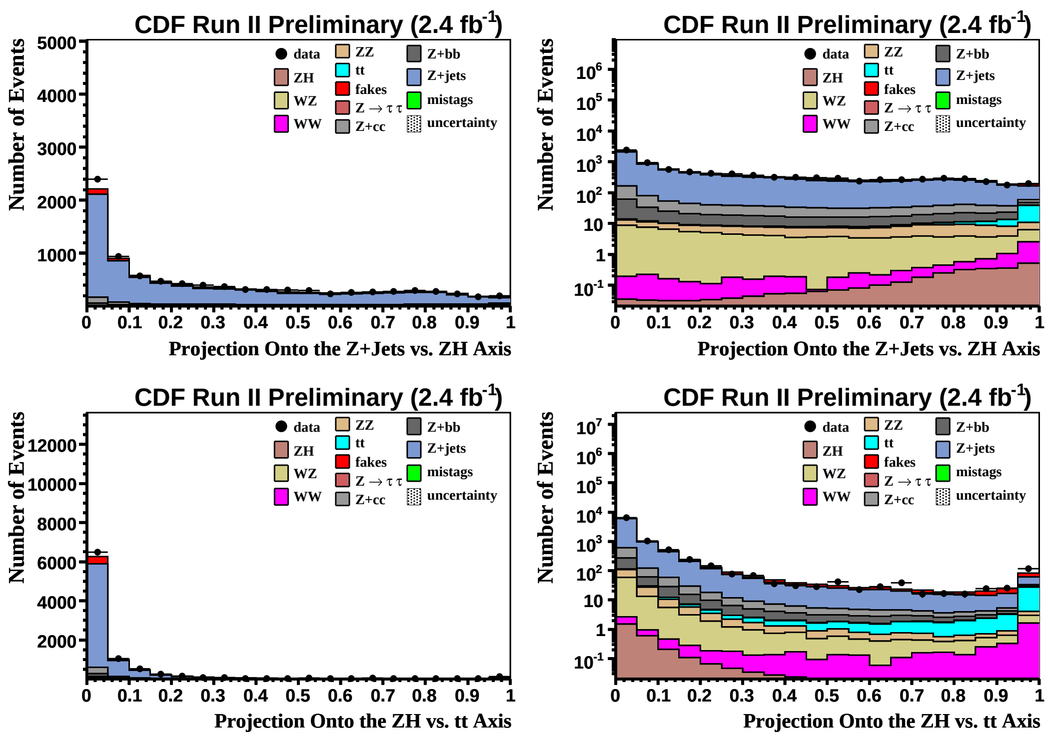

Figure 18: Pre-Tag NN output projections.

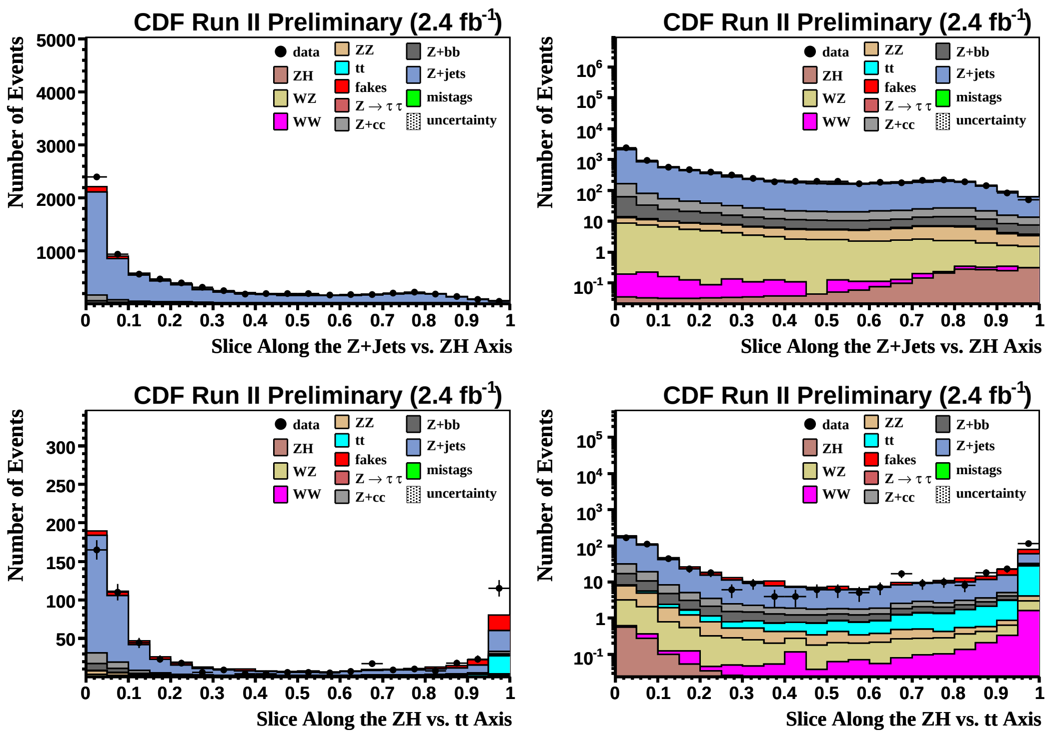

Figure 19: Pre-Tag NN output projections with $y \leq 0.1$ in the Z+Jets vs. ZH projections and $x \geq 0.9$ in the ZH vs. $t\bar{t}$ projections.

Fractional systematic uncertainty		Samples affected
Tevatron Luminosity	0.05	All MC
CDF Luminosity	0.04	All MC
Z+h.f cross-section	0.40	$Z + bb$, $Z + cc$
$t\bar{t}$ cross-section	0.20	$t\bar{t}$
Diboson cross-sections	0.115	ZZ, ZW, WW
Mistag errors		Mistags
Lepton ID	1%	All MC
B-tag scale factor	0.042 (0.105)	All single tag MC (All double tag MC)
Fakes	0.50	Fake ee, $\mu\mu$
JES	Hist. shape & Acc.	All MC
ISR & FSR	Hist. shape & Acc.	Signal MC
PDF reweighting	0.00	

Table 29: Summary of systematic uncertainties in terms of fractional acceptance change on samples.

9 Systematics

Our systematics are basically the same as from the 1 fb^{-1} analysis, and are listed in Table 29.

10 Results

After applying b-tagging our final event totals are shown in tables 30 and 31. Since the event yields in data agree with the events expected by our background model, we do not find a significant excess in the counting experiment. We show the agreement in the tagged regions for the NN inputs in both single-tagged and double-tagged events in Figures 20 through 27. The projected NN output distributions for the signal regions are shown in Figures 28 through 35. Since the cross-section for ZH is small, we do not expect a visible excess with this dataset, and so we quantify the maximum allowed ZH contamination in the data. We use the mclimit machinery for this, and do a binned fit of the 2D NN distribution, including systematics. Table 32, 33, 34, Figure 36 and Figure 37 show our expected limits assuming no Higgs production, and our observed limits for ZH production in the data with and without systematics.

Event Totals		
sample	**Single Tag (high)**	**double Tag (high)**
ZH	0.86 ± 0.07	0.45 ± 0.04
tt	11.36 ± 2.39	6.14 ± 1.29
WW	0.11 ± 0.02	0.01 ± 0
WZ	2.37 ± 0.35	0.13 ± 0.02
ZZ	6.31 ± 0.95	2.23 ± 0.31
Z $\rightarrow \tau\tau$	0.03 ± 0.01	0 ± 0
Z+jets (bb)	53.41 ± 22.43	13.41 ± 5.5
Z+jets (cc)	25.67 ± 10.78	1.92 ± 0.79
mistags / Z + jets	84.21 ± 36.21	2.11 ± 0.93
fakes	13.5 ± 6.75	0.82 ± 0.41
Total Background	197.84 ± 44.53	27.23 ± 5.8
Data	205	24

Table 30: Event totals for single and double tag (high).

Event Totals		
sample	**Single Tag (low)**	**double Tag (low)**
ZH	0.14 ± 0.01	0.07 ± 0.01
tt	5.49 ± 1.15	2.51 ± 0.53
WW	0.06 ± 0.01	0 ± 0
WZ	0.63 ± 0.09	0.02 ± 0
ZZ	1.19 ± 0.18	0.41 ± 0.06
Z $\rightarrow \tau\tau$	0.05 ± 0.02	0 ± 0
Z+jets (bb)	11.15 ± 4.68	2.8 ± 1.15
Z+jets (cc)	5.49 ± 2.31	0.37 ± 0.15
mistags / Z + jets	29.34 ± 12.61	0.62 ± 0.27
fakes	12.36 ± 6.18	0.54 ± 0.27
Total Background	65.89 ± 15.03	7.33 ± 1.33
Data	74	15

Table 31: Event totals for single and double tag (low).

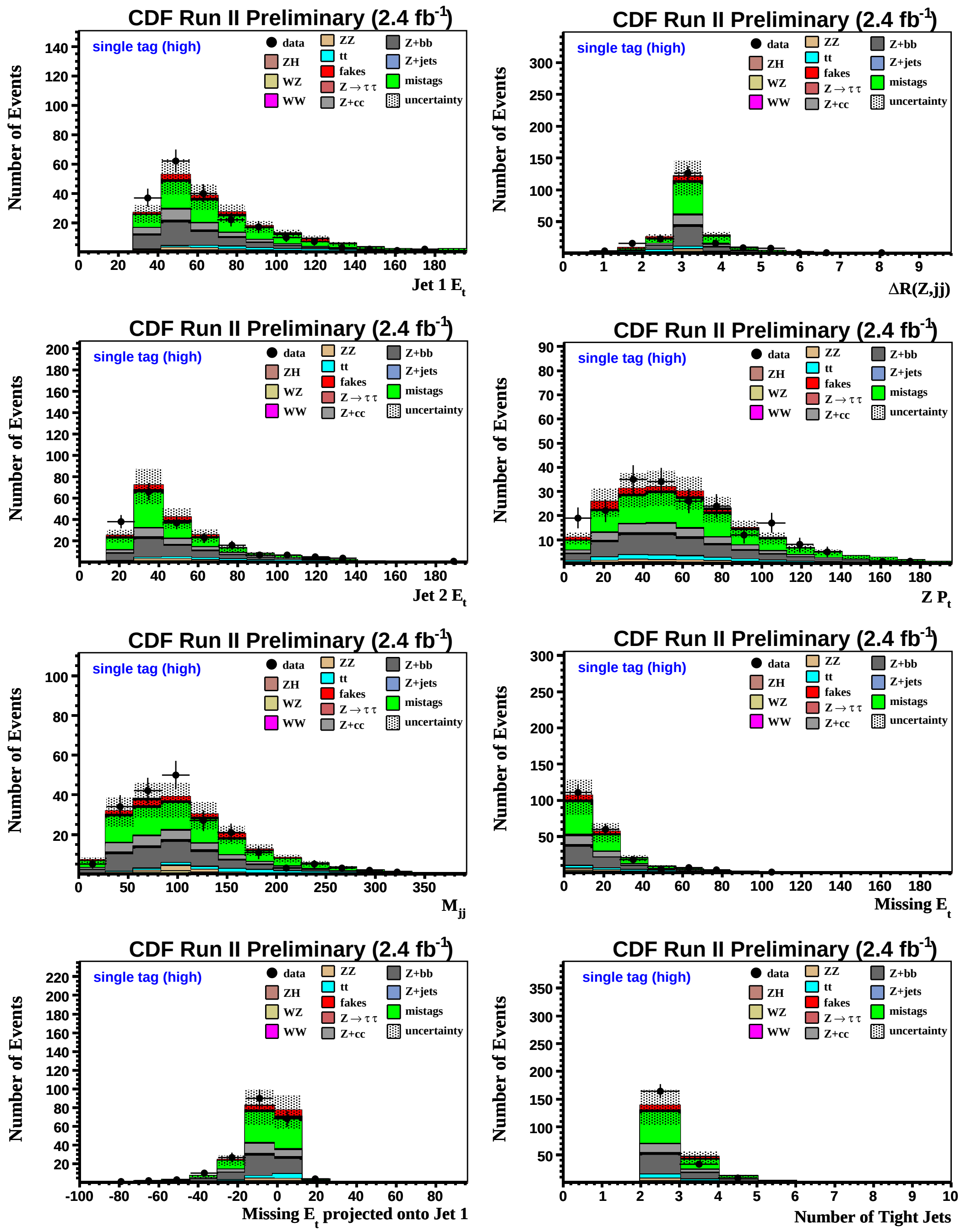

Figure 20: Single-Tag High NN inputs.

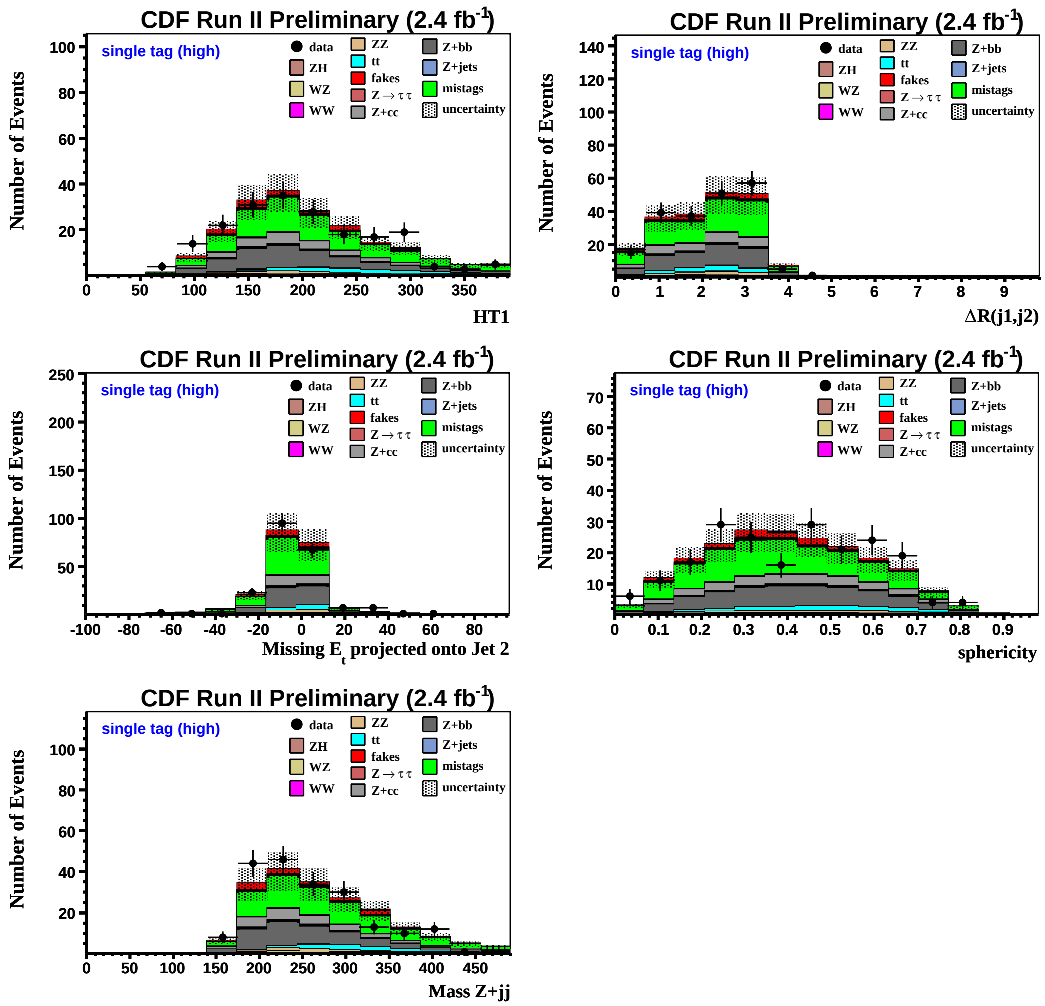

Figure 21: Single-Tag High NN inputs.

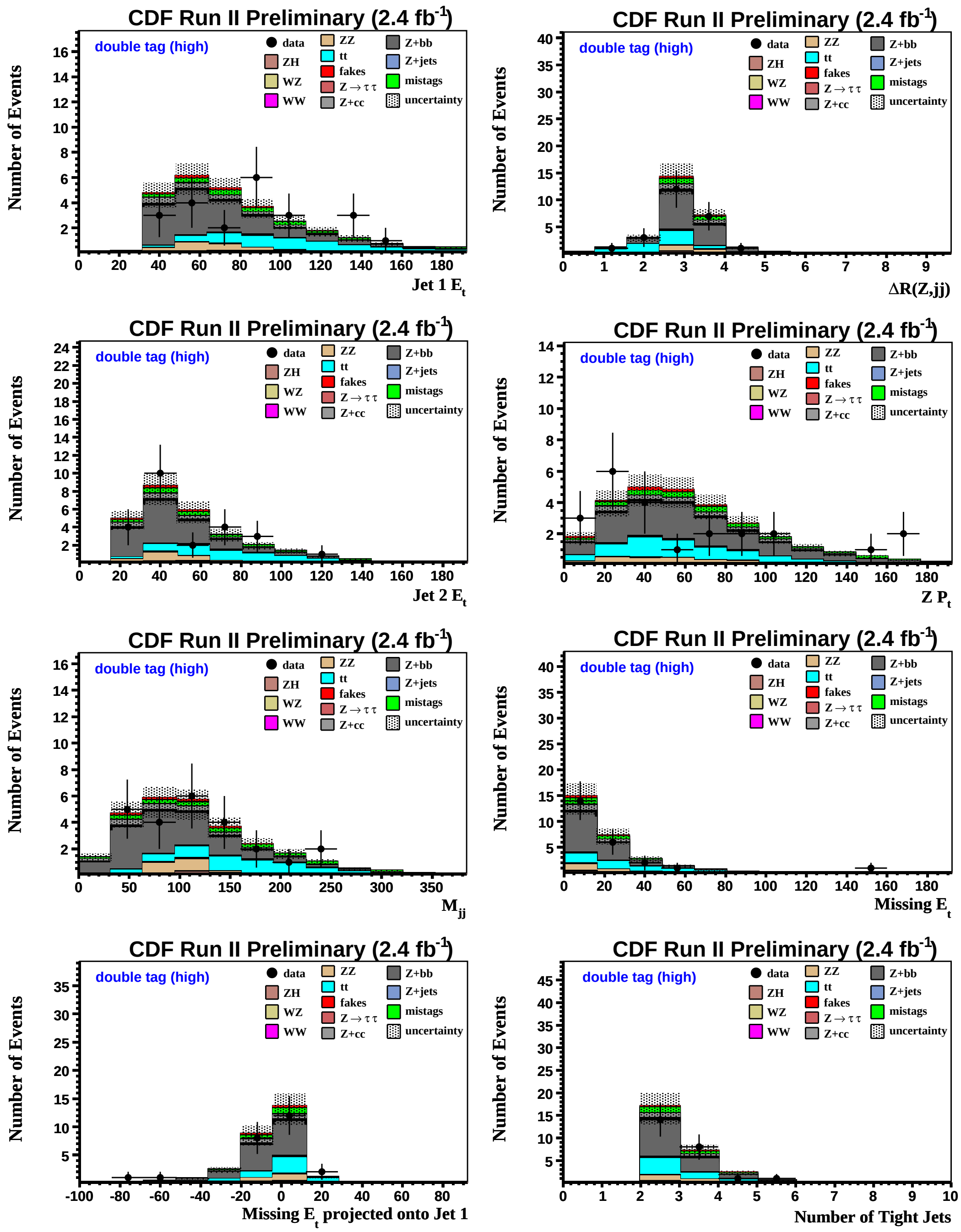

Figure 22: Double-Tag High NN inputs.

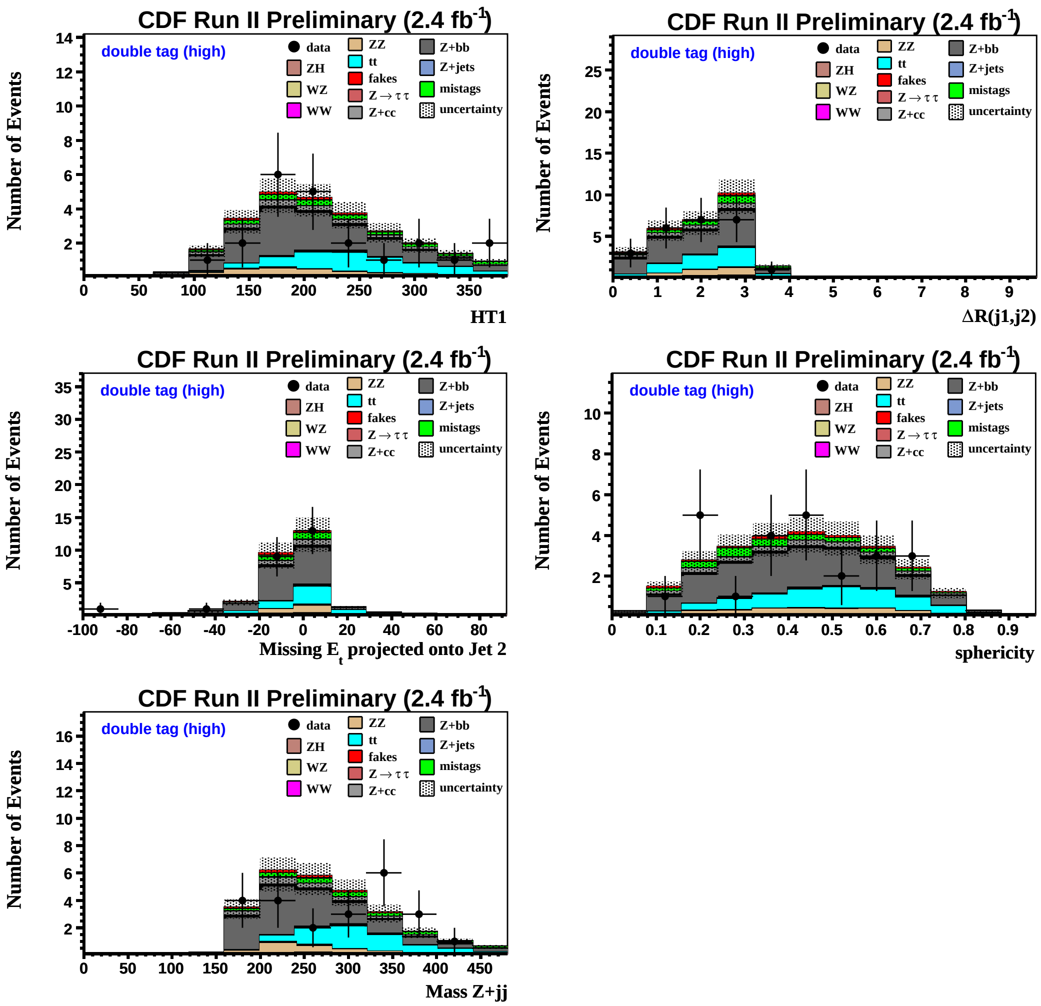

Figure 23: Double-Tag High NN inputs.

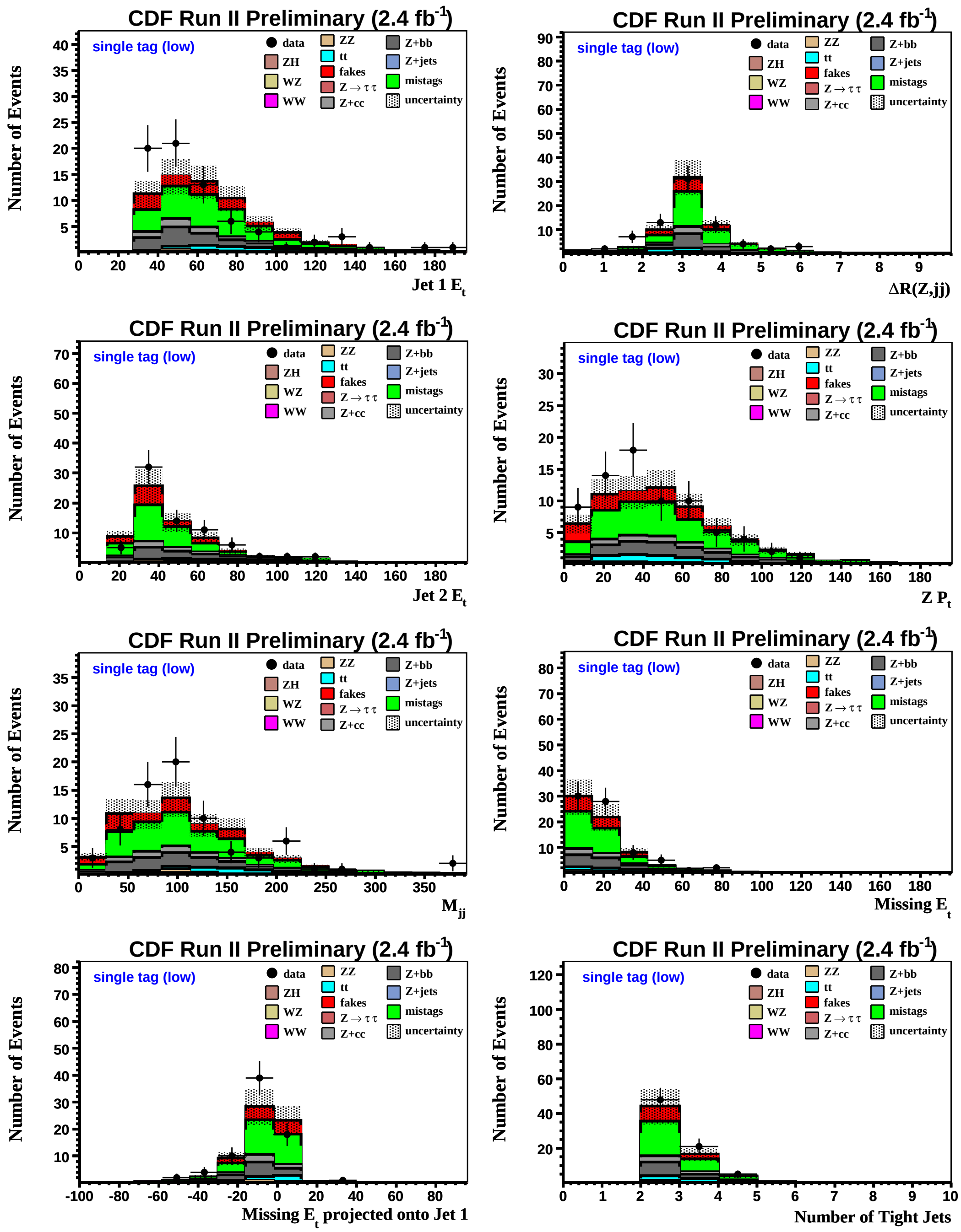

Figure 24: Single-Tag Low NN inputs.

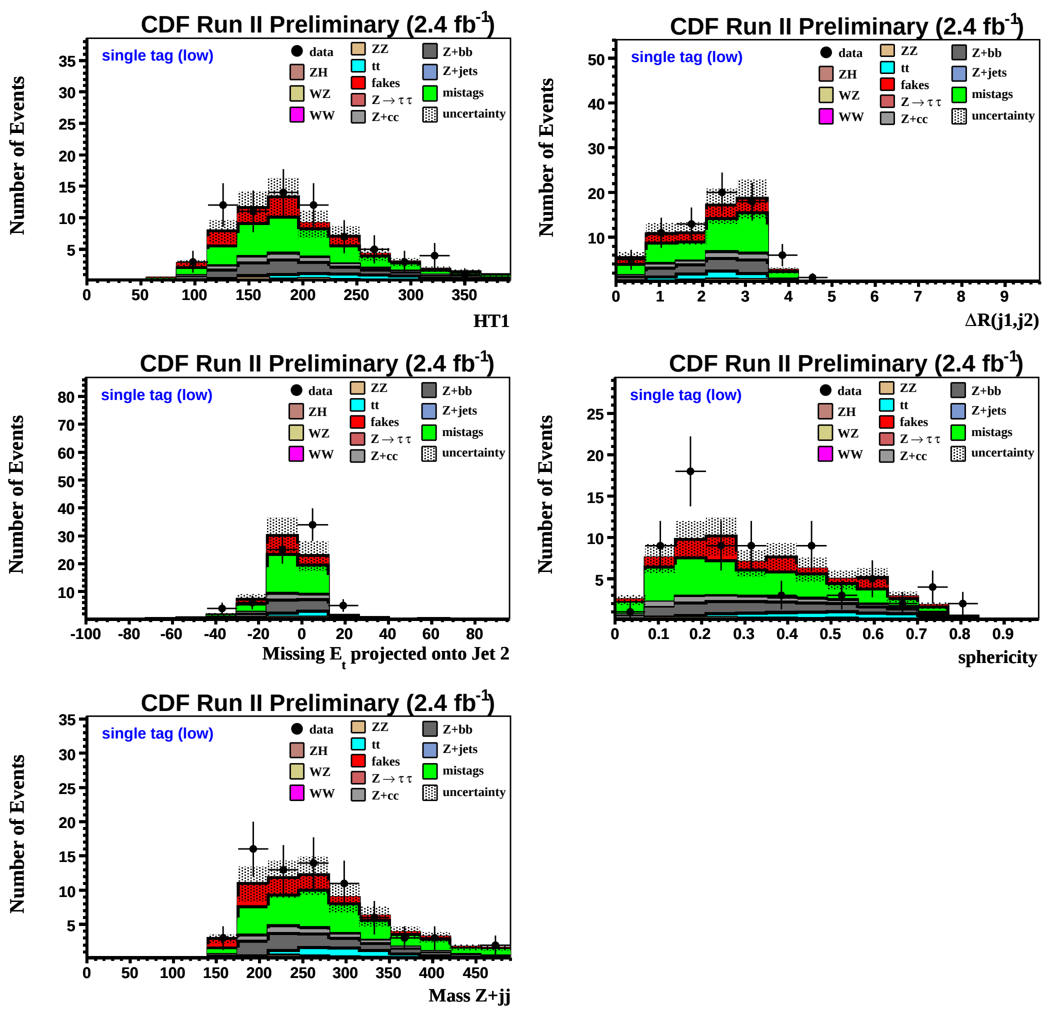

Figure 25: Single-Tag Low NN inputs.

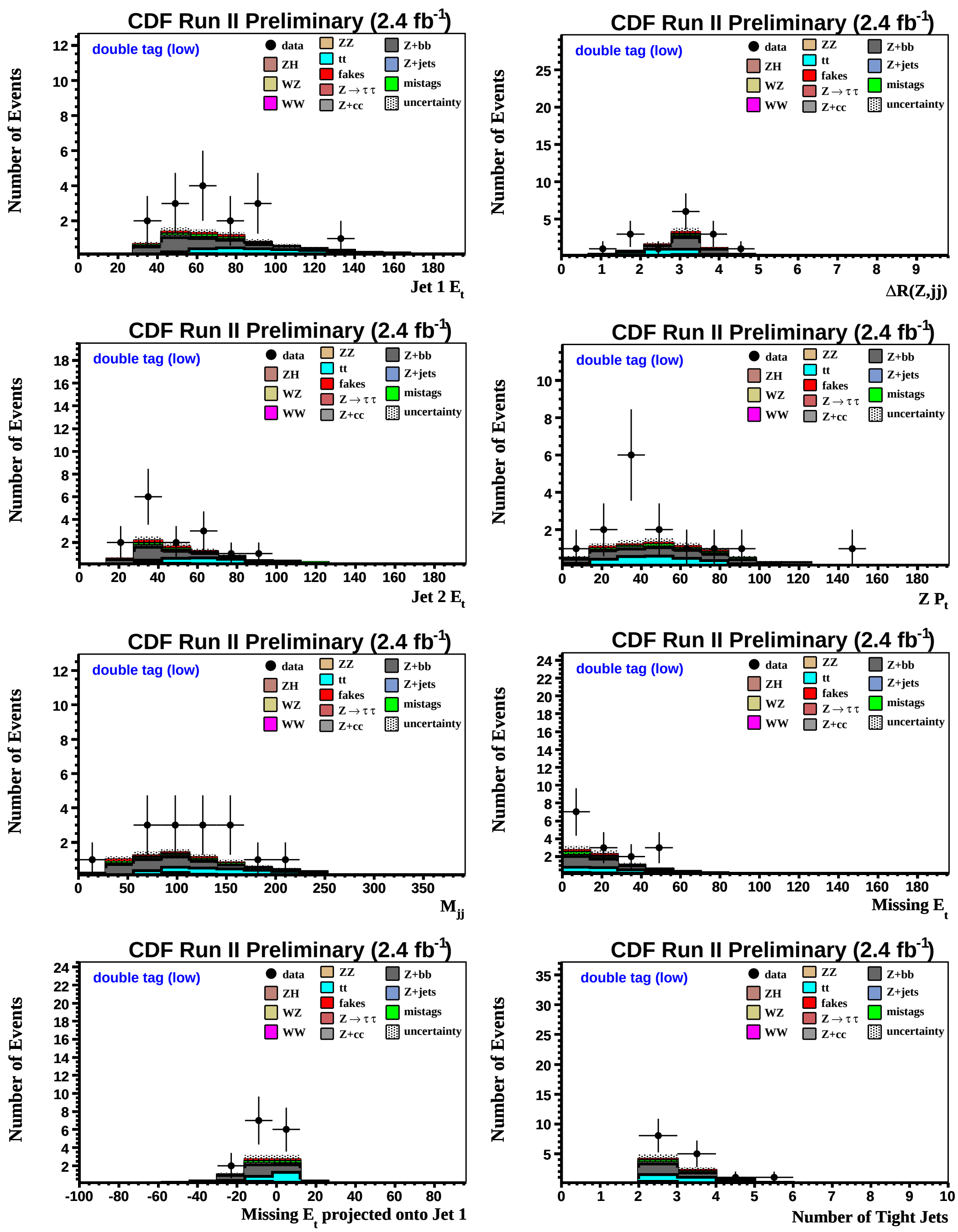

Figure 26: Double-Tag Low NN inputs.

Expected (Observed) Limits **@ M_H = 120 GeV/c^2**	
without systematics	with systematics
11.78 (13.44)	14.51 (13.36)

Table 32: Expected and Observed limits for one mass point.

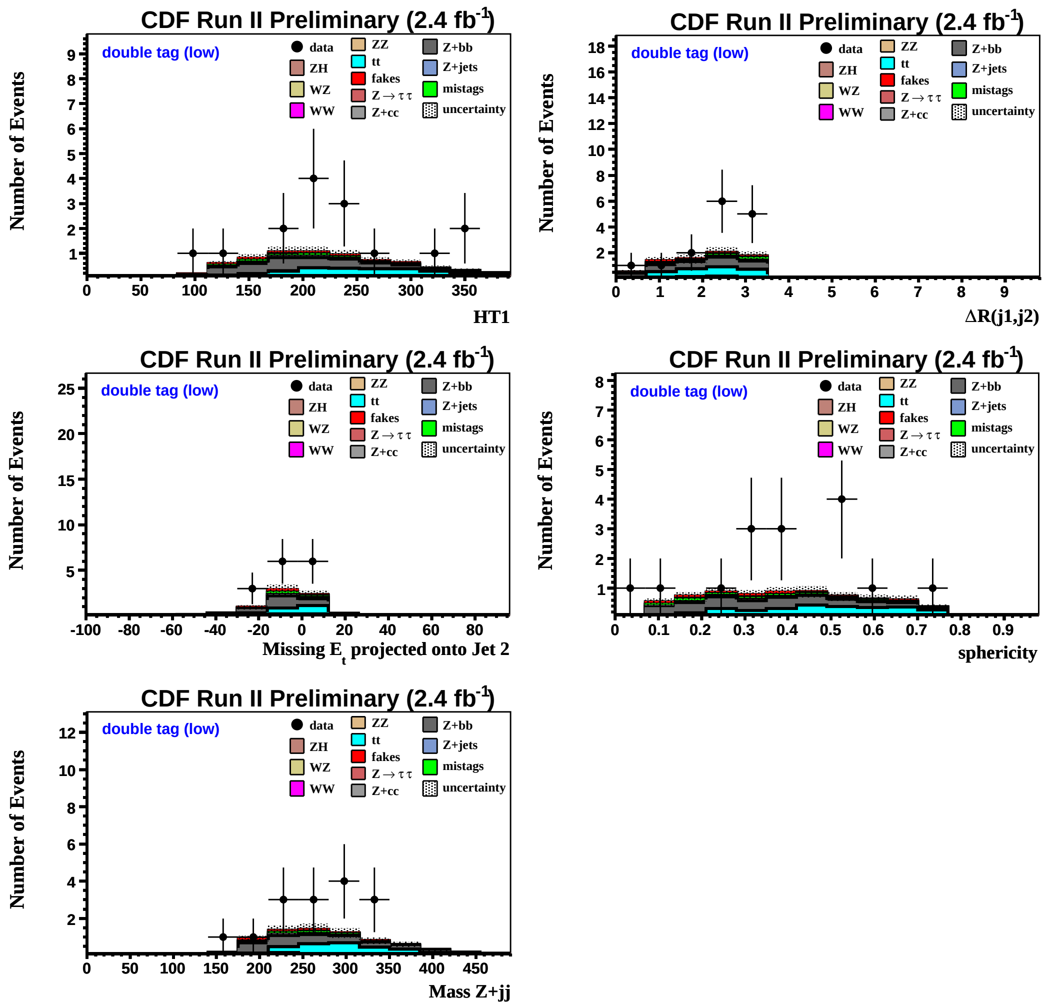

Figure 27: Double-Tag Low NN inputs.

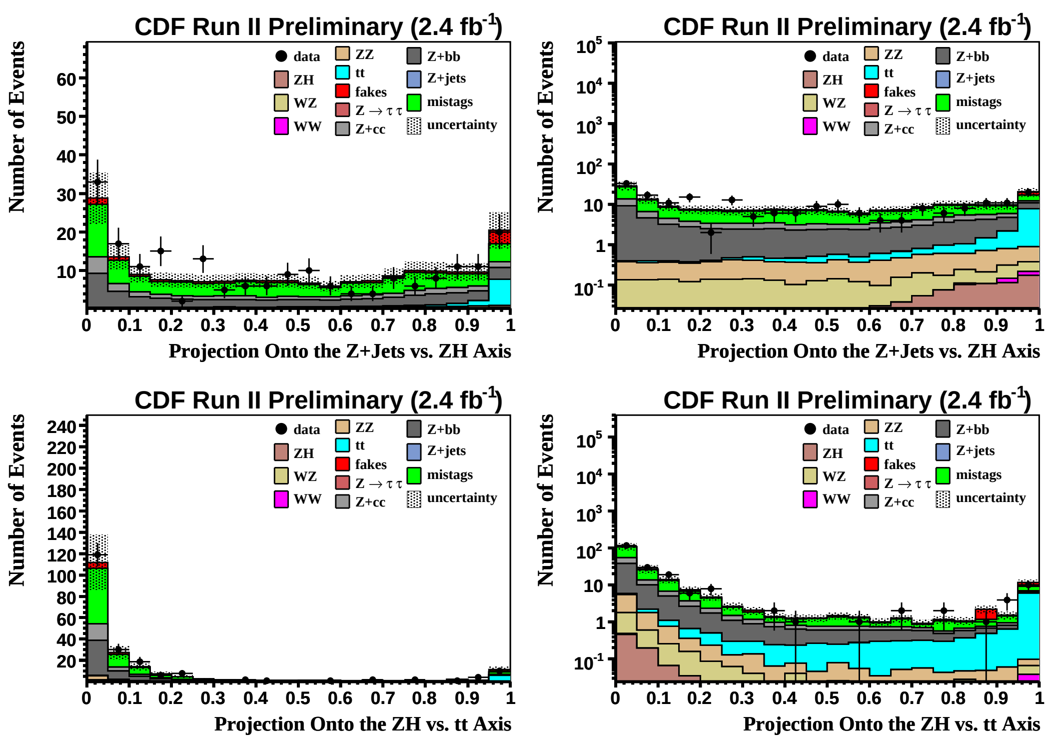

Figure 28: Single Tag (high) NN output projections.

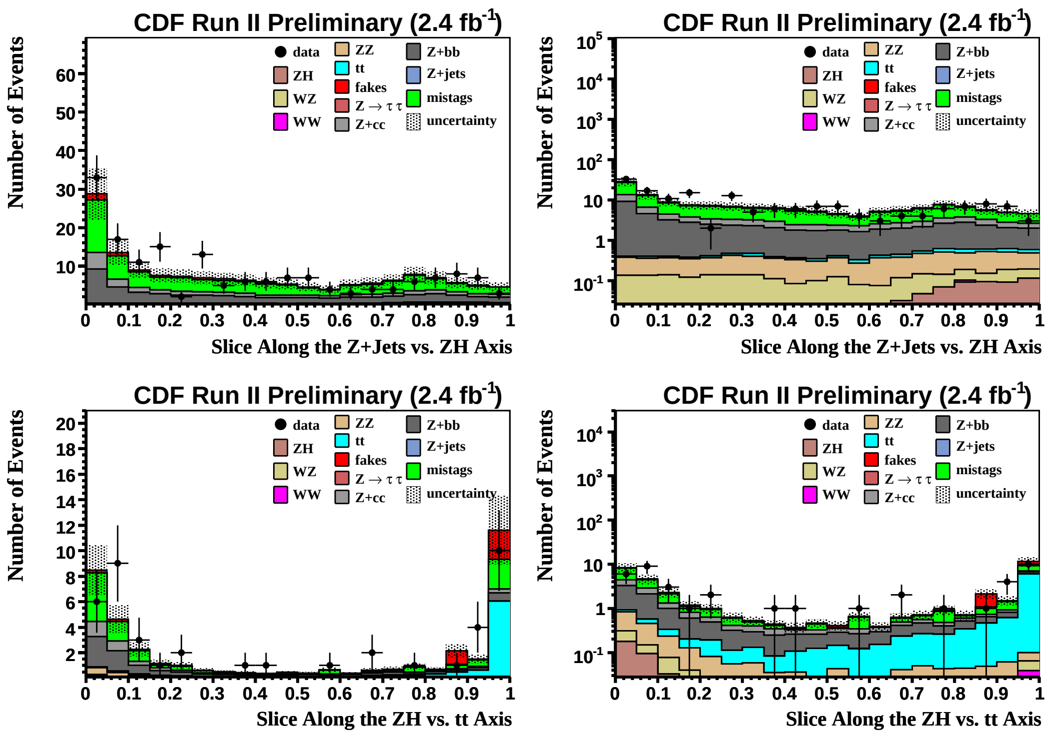

Figure 29: Single Tag (high) NN output projections with $y \leq 0.1$ in the Z+Jets vs. ZH projections and $x \geq 0.9$ in the ZH vs. $t\bar{t}$ projections.

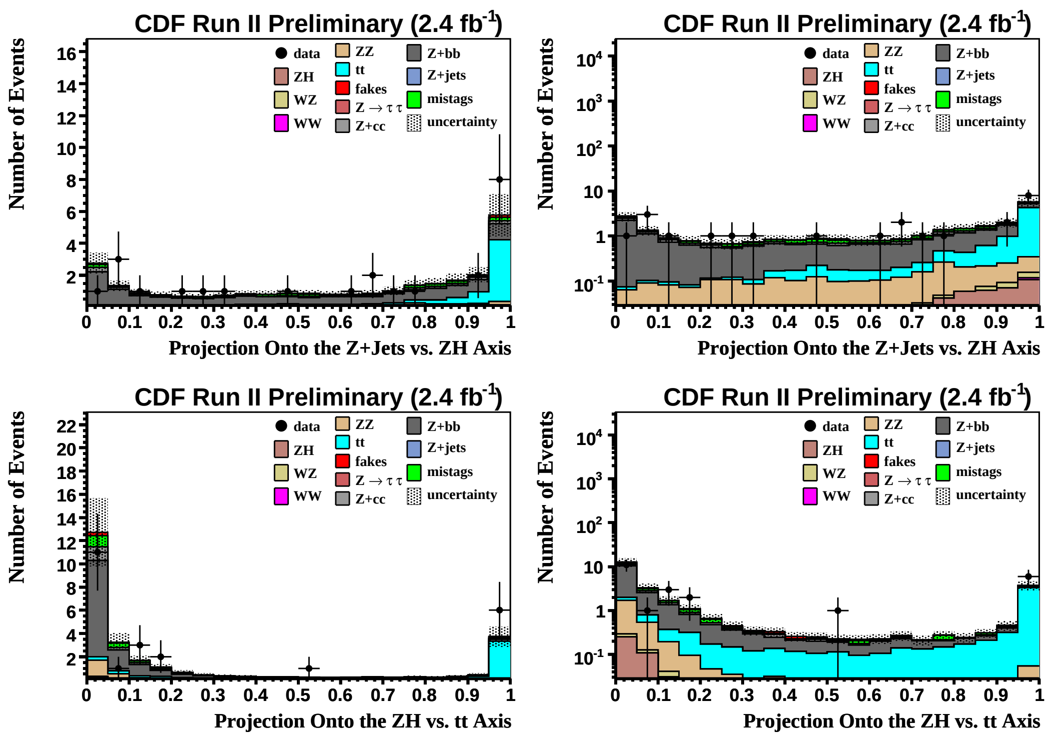

Figure 30: Double Tag (high) NN output projections.

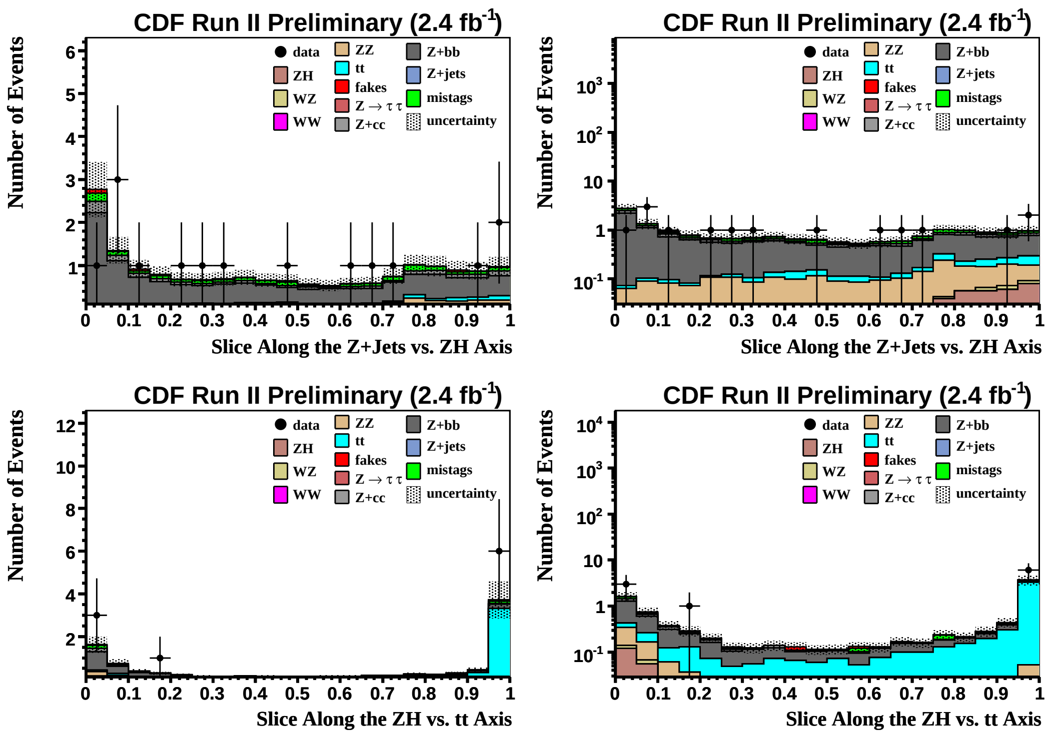

Figure 31: Double Tag (high) NN output projections with $y \leq 0.1$ in the Z+Jets vs. ZH projections and $x \geq 0.9$ in the ZH vs. $t\bar{t}$ projections.

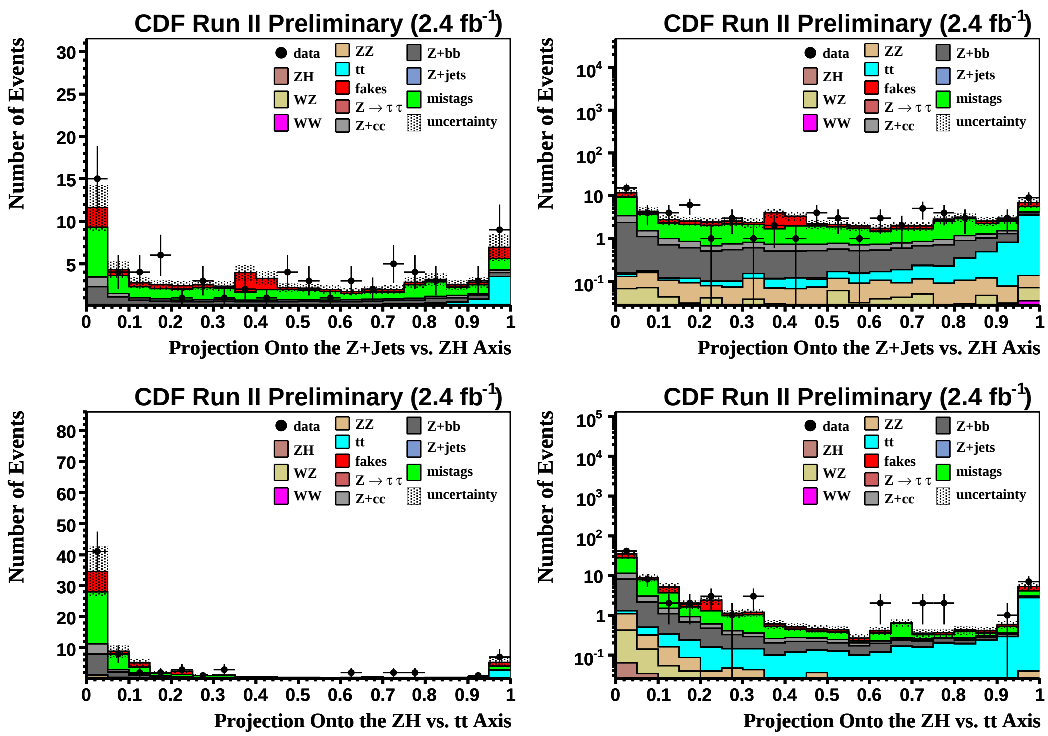

Figure 32: Single Tag (low) NN output projections.

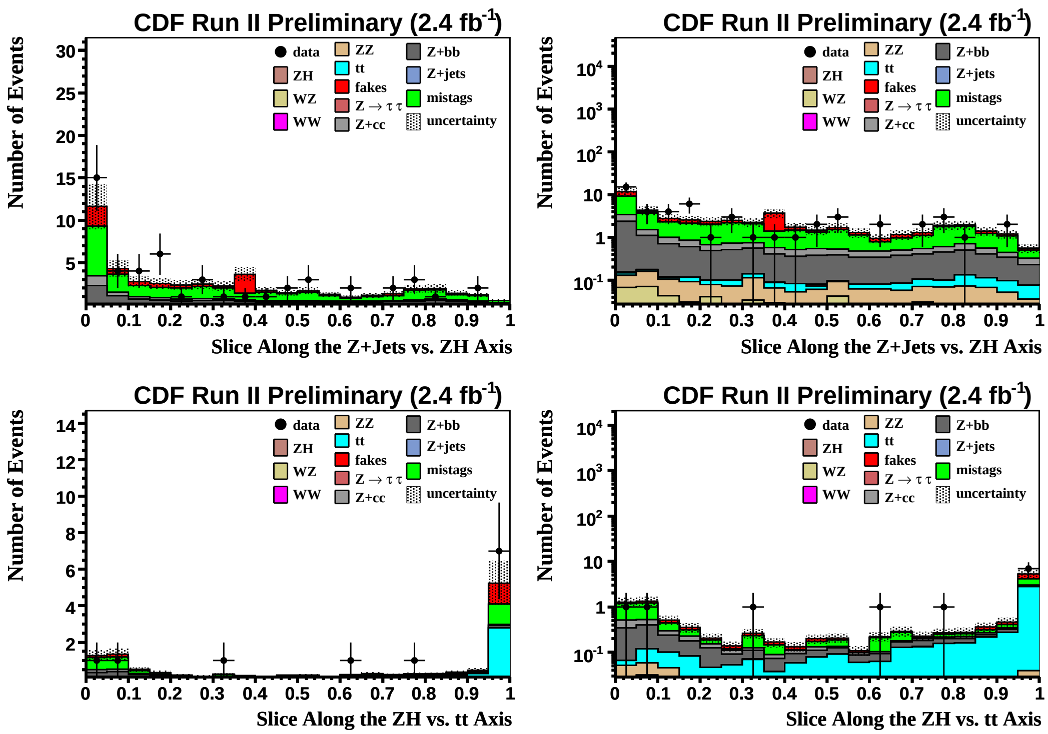

Figure 33: Single Tag (low) NN output projections with $y \leq 0.1$ in the Z+Jets vs. ZH projections and $x \geq 0.9$ in the ZH vs. $t\bar{t}$ projections.

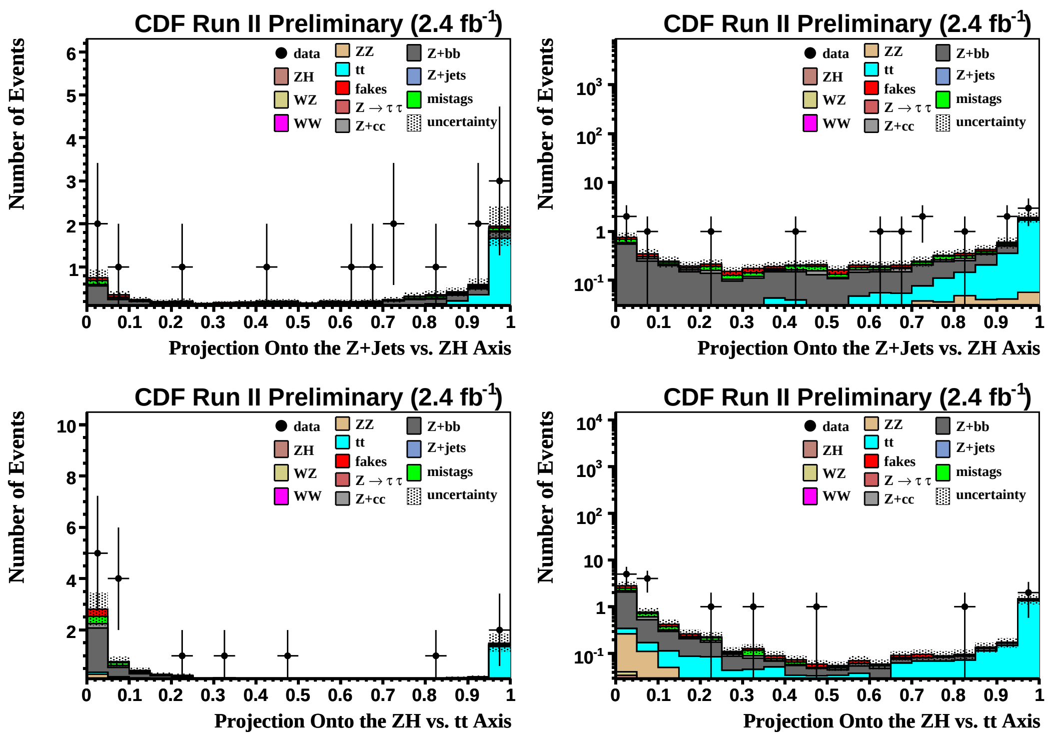

Figure 34: Double Tag (low) NN output projections.

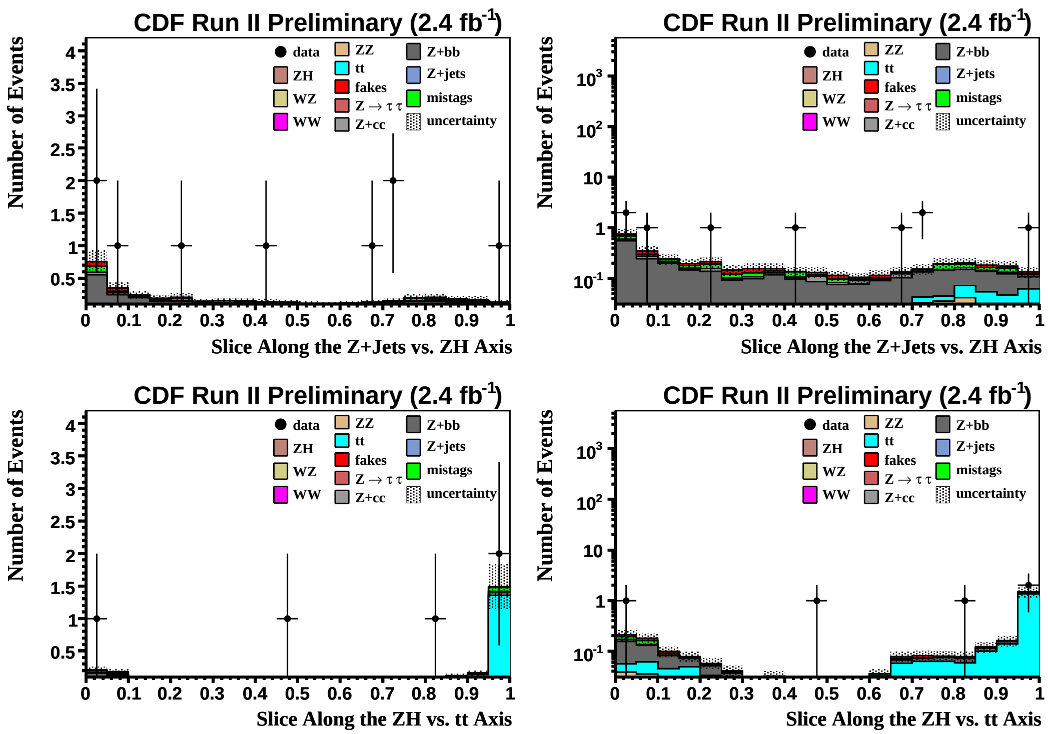

Figure 35: Double Tag (low) NN output projections with $y \leq 0.1$ in the Z+Jets vs. ZH projections and $x \geq 0.9$ in the ZH vs. $t\bar{t}$ projections.

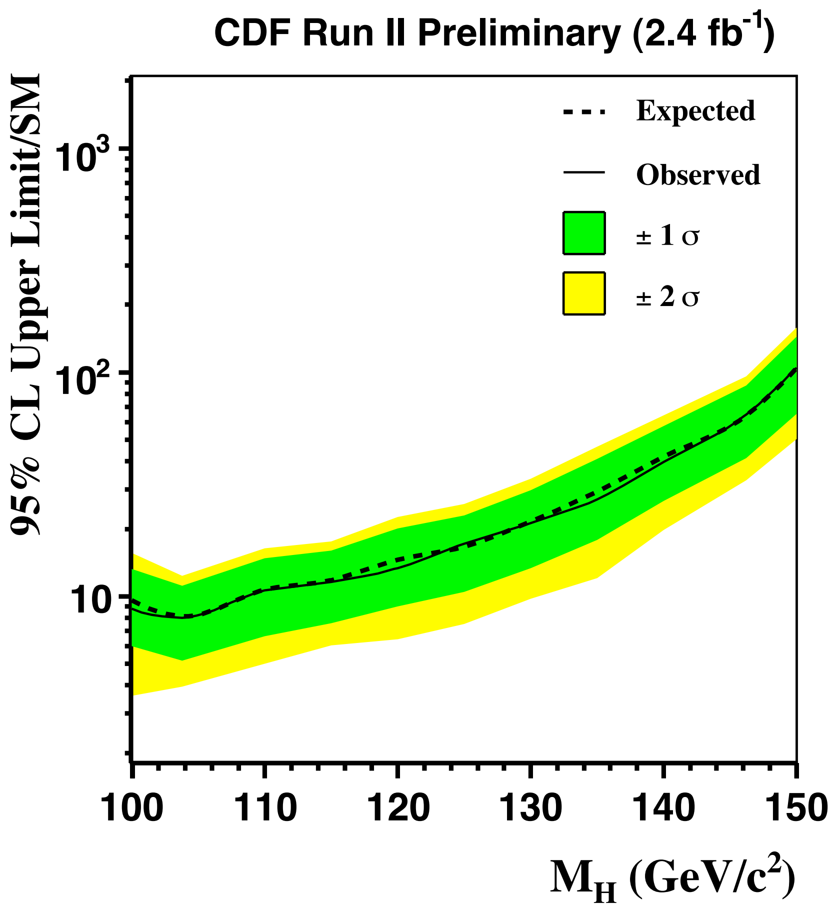

Figure 36: Combined expected and observed limits.

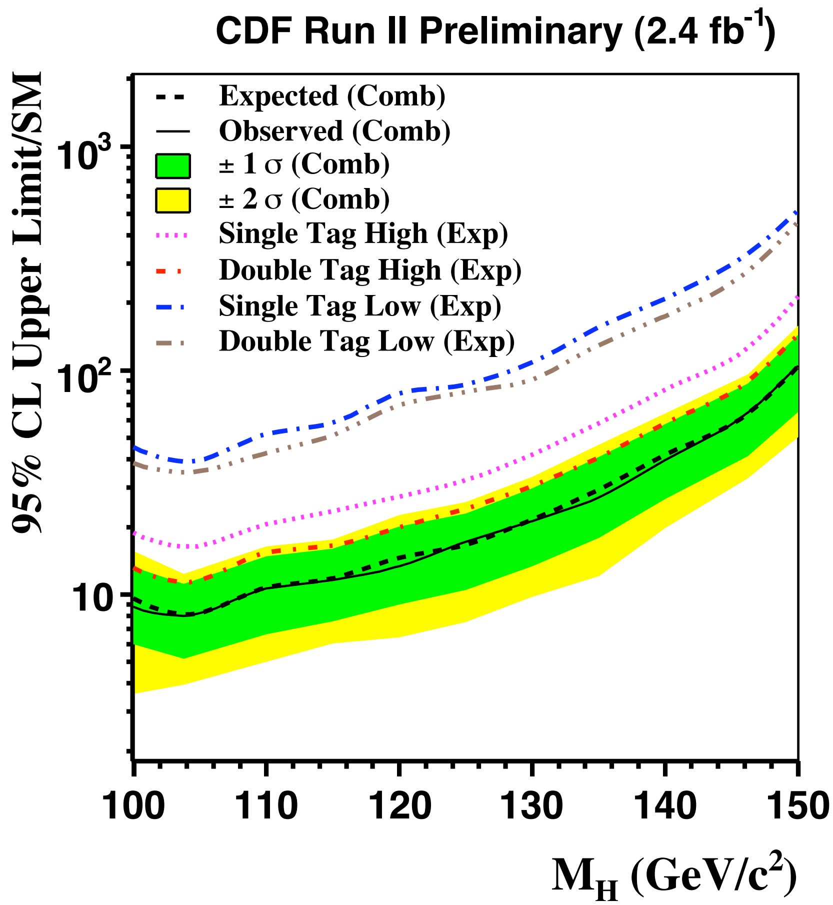

Figure 37: Expected limits for each of the individual channels and in combination.

Expected Limits						
M_H	**Single T.** (*low*)	**Double T.** (*low*)	**Single T.** (*high*)	**Double T.** (*high*)	**Comb.** (*high only*)	**Comb.** (*total*)
100	45.63	38.5	18.82	13.16	10.6	9.59
105	39.19	35.1	16.32	11.34	8.99	8.15
110	51.9	42.74	20.53	15.34	11.99	10.7
115	58.42	51.33	23.57	16.49	12.74	11.79
120	79.09	69.89	27.24	19.87	15.99	14.51
125	86.44	80.19	32.34	24.15	18.39	16.67
130	108.56	91	42.15	30.5	23.98	21.58
135	155.81	129.79	58.04	40.87	32.51	29.38
140	209.5	174.59	82.19	58.02	46.06	42.04
145	332.82	277.76	126.26	89.53	70.84	64.36
150	519.5	463.51	213.67	144.6	116.32	104.83

Table 33: Expected limits.

Expected and Observed Limits		
M_H	$Expected^{+1\sigma}_{-1\sigma}$	**Observed**
100	$9.59^{4.4}_{2.83}$	8.79
105	$8.15^{3.57}_{2.43}$	8.02
110	$10.7^{5.01}_{3.14}$	10.62
115	$11.79^{4.84}_{3.55}$	11.57
120	$14.51^{6.68}_{4.35}$	13.36
125	$16.67^{7.71}_{4.77}$	17.16
130	$21.58^{10.13}_{6.34}$	21.23
135	$29.38^{14.23}_{8.97}$	27.11
140	$42.04^{18.34}_{12.44}$	39.73
145	$64.36^{27.29}_{18.52}$	65.01
150	$104.82^{46.3}_{32.49}$	104.83

Table 34: Expected and Observed limits.

11 Conclusions

We have evaluated new limits with an updated dataset, 2.4 times larger than in the previous analysis. We have made use of new lepton categories to increase ZH acceptance. In order to gain full sensitivity from our new lepton categories we have added two additional tag categories which reduce the expected limit by $\sim 10\%$ when compared to the high $\frac{S}{\sqrt{B}}$ channels alone.

12 Appendix

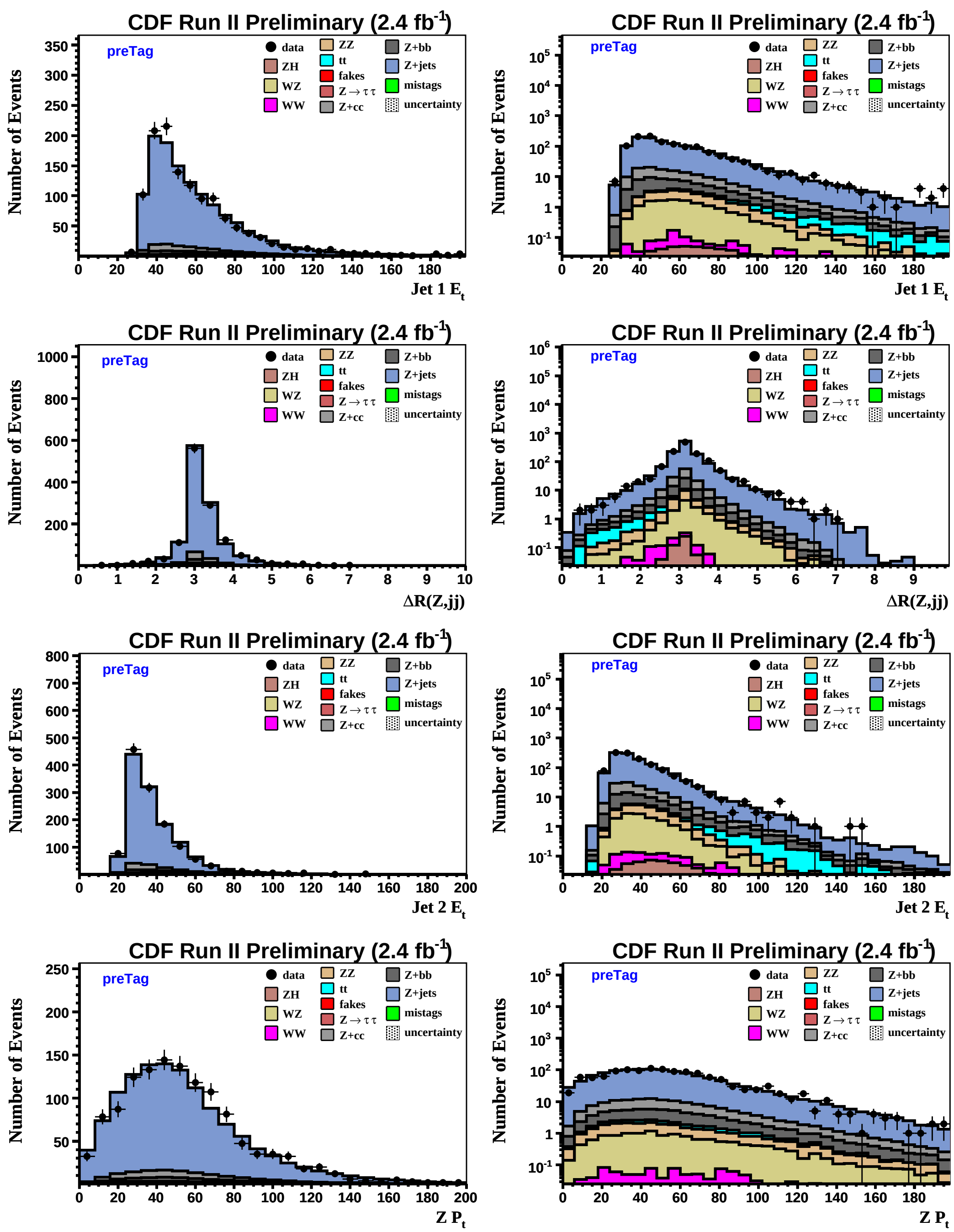

Figure 38: Pre-Tag NN inputs : Shape comparisons for TcTc Z category.

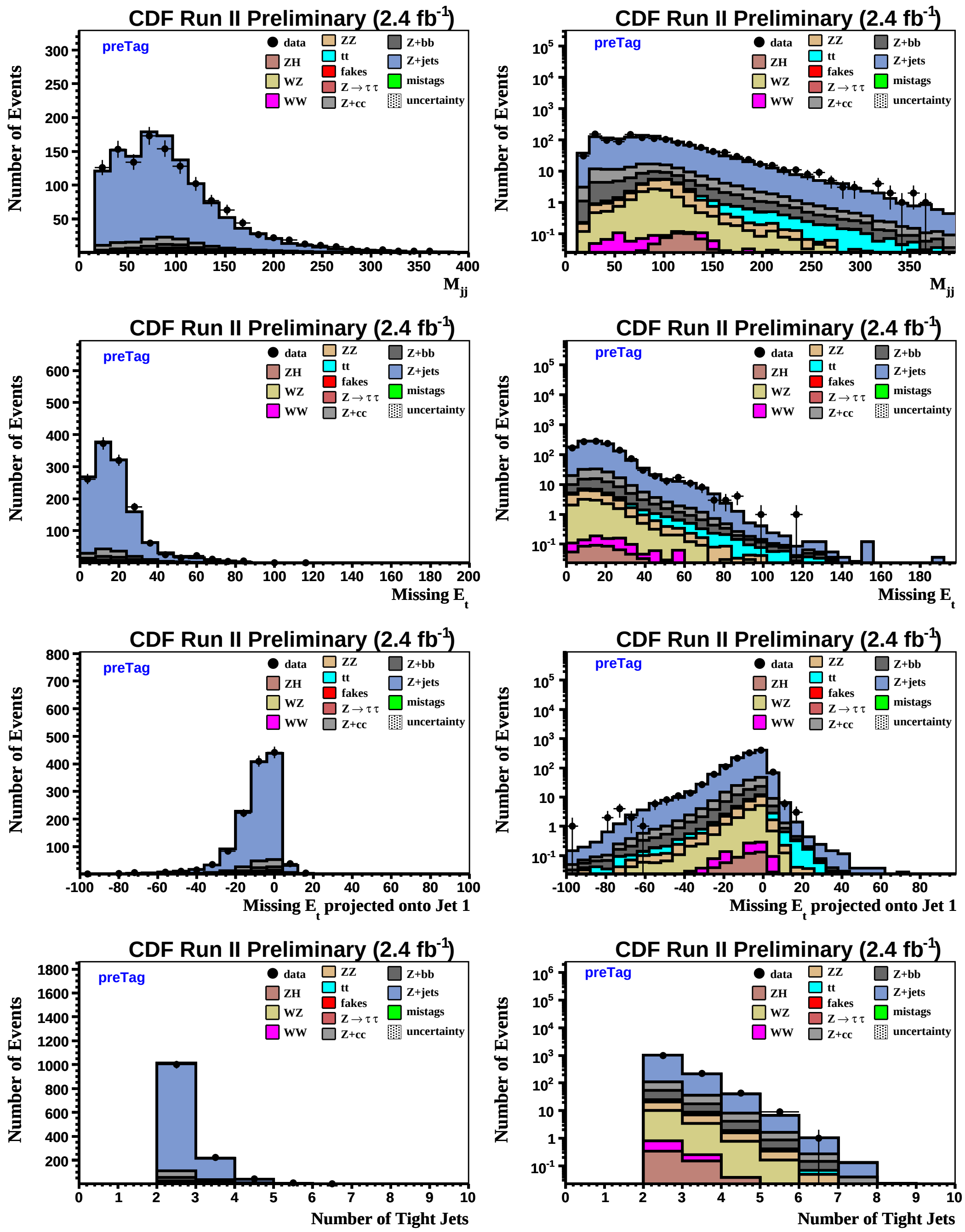

Figure 39: Pre-Tag NN inputs : Shape comparisons for TcTc Z category.

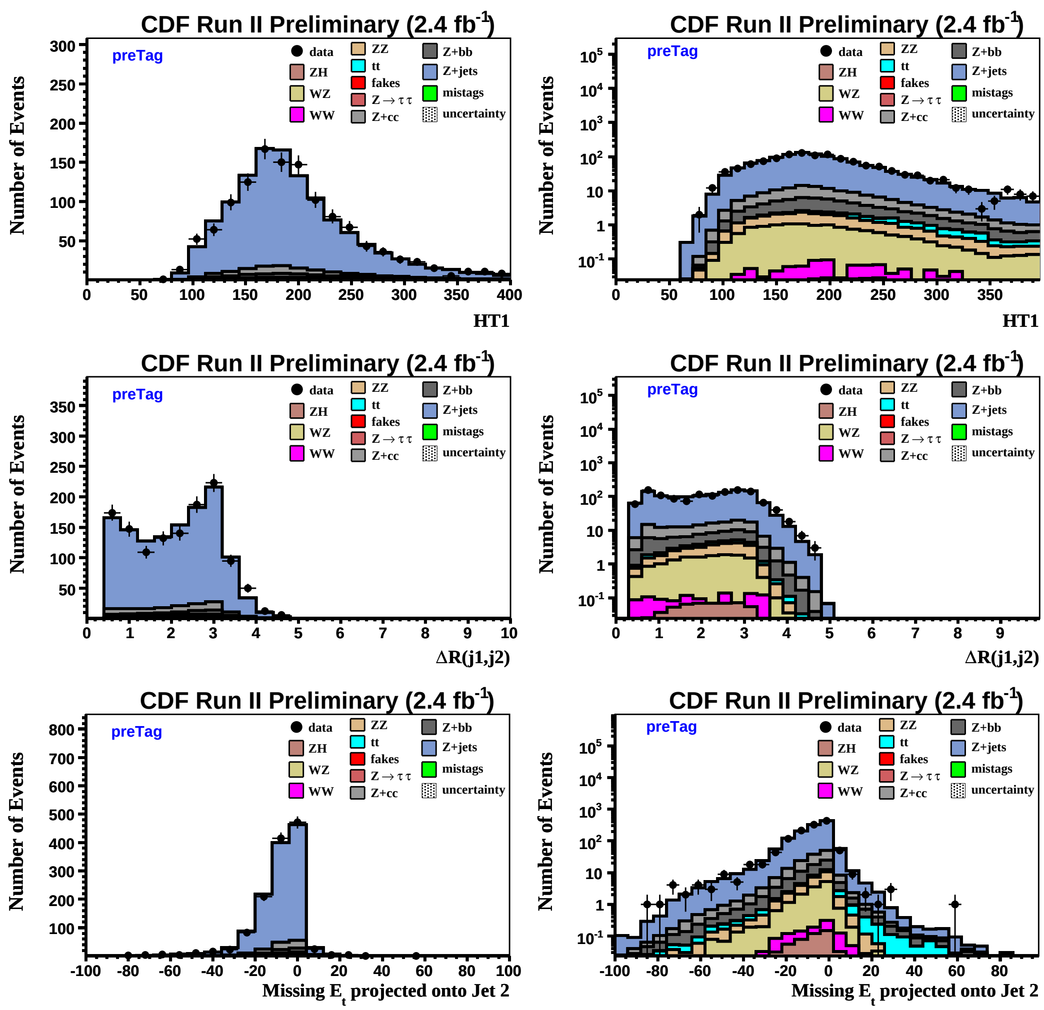

Figure 40: Pre-Tag NN inputs : Shape comparisons for TcTc Z category.

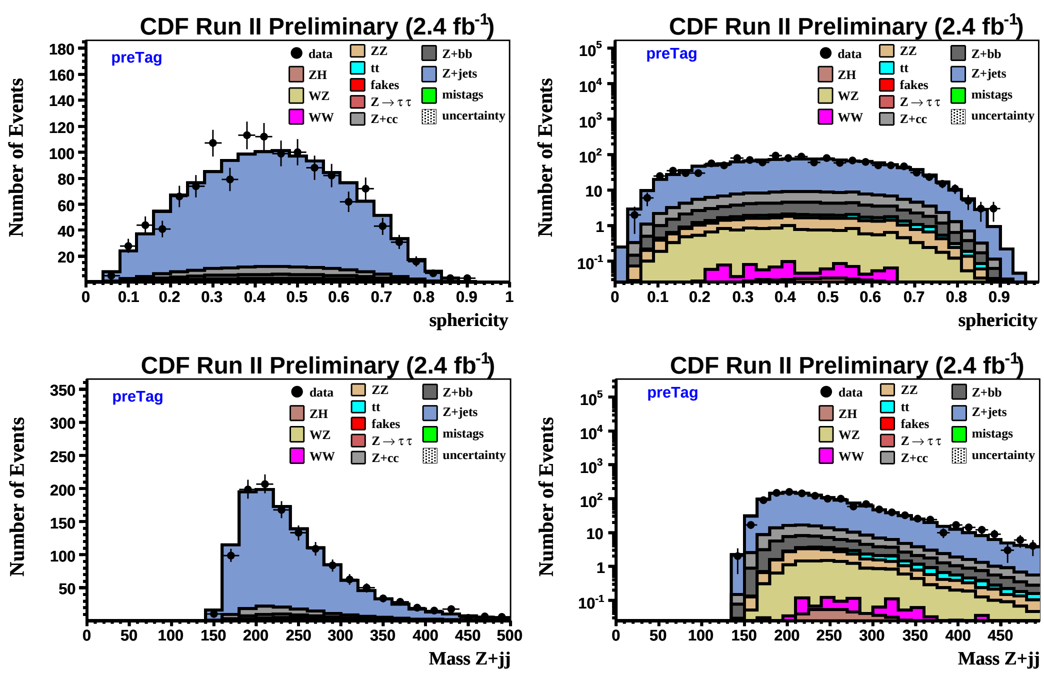

Figure 41: Pre-Tag NN inputs : Shape comparisons for TcTc Z category.

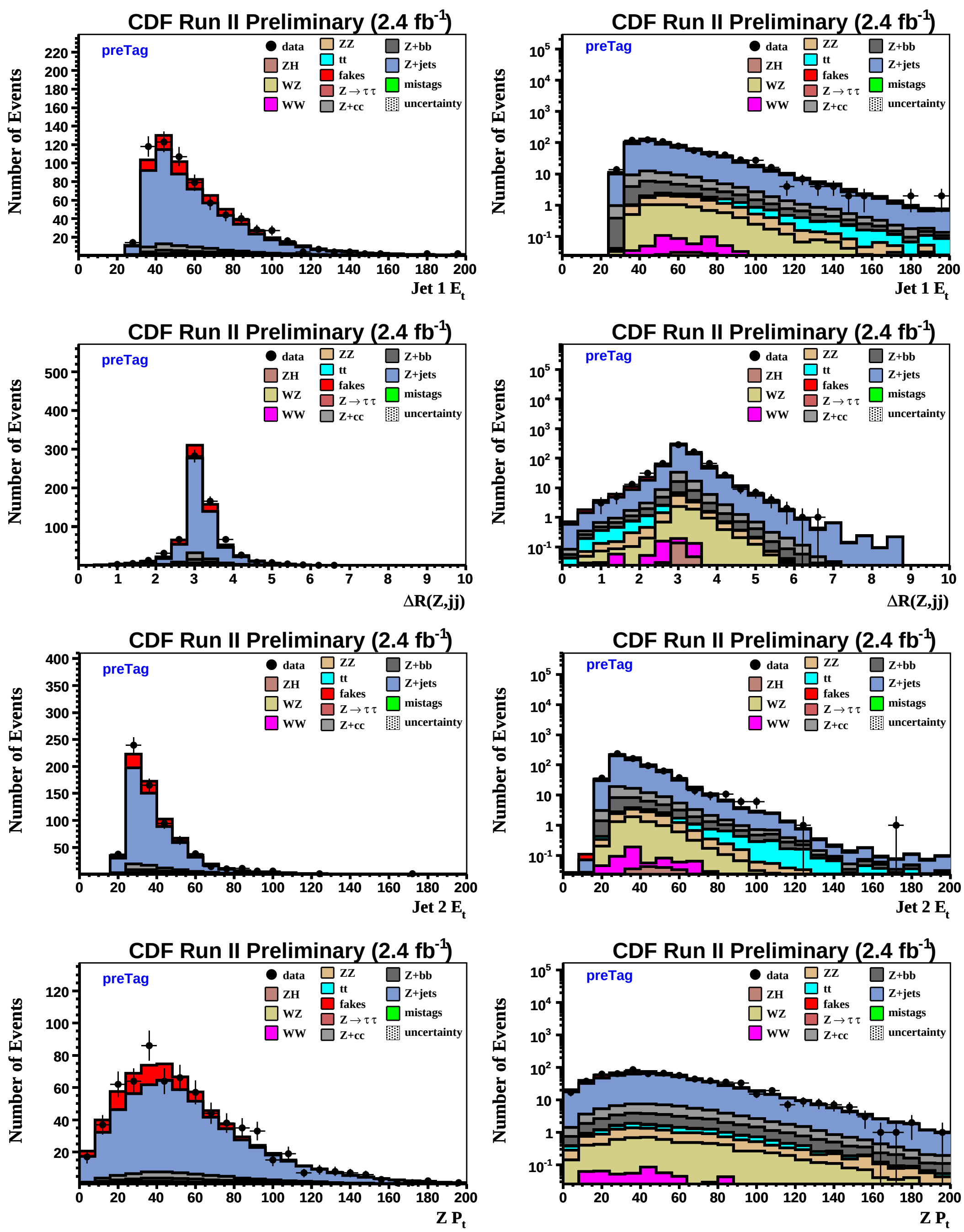

Figure 42: Pre-Tag NN inputs : Shape comparisons for TcLc Z category.

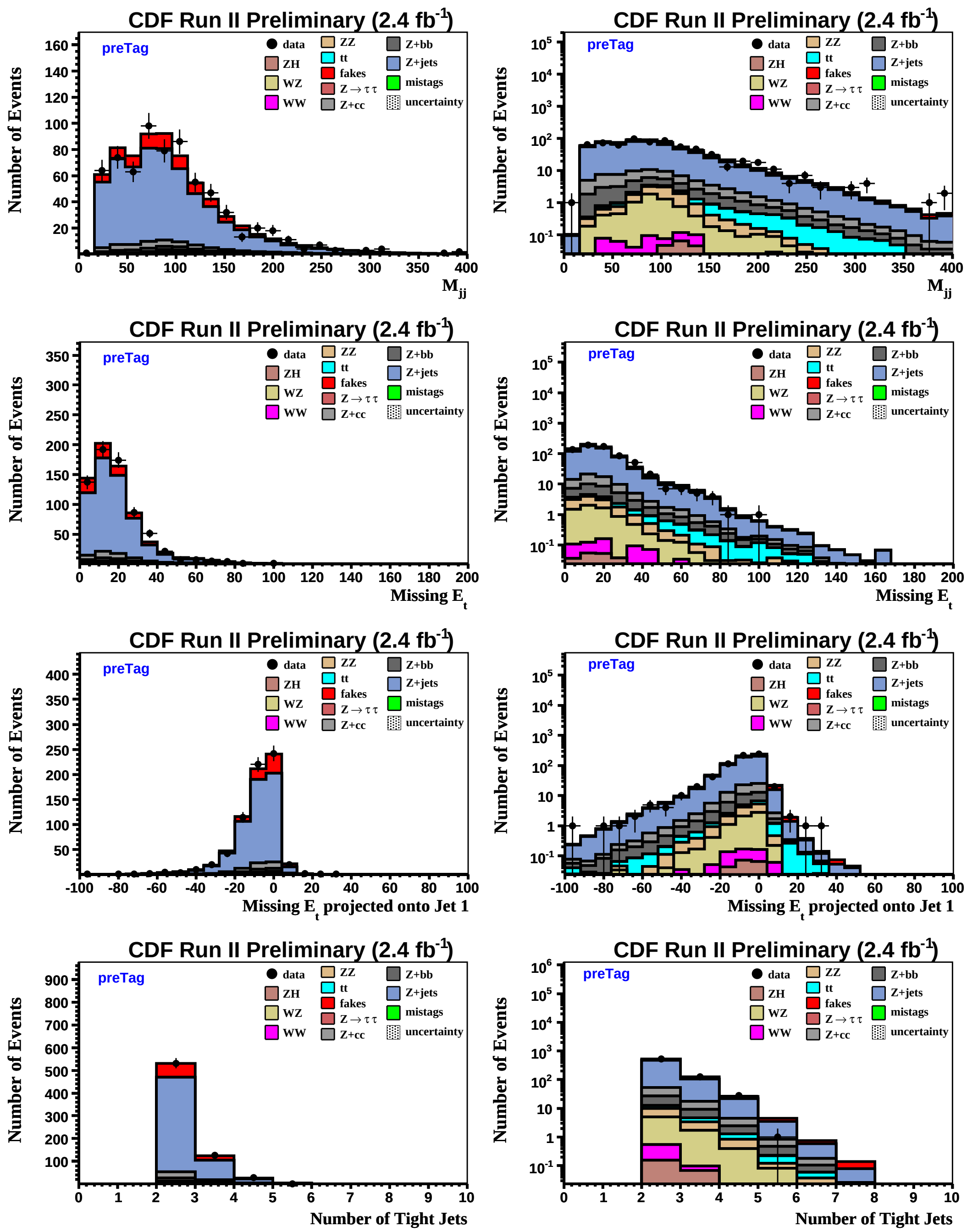

Figure 43: Pre-Tag NN inputs : Shape comparisons for TcLc Z category.

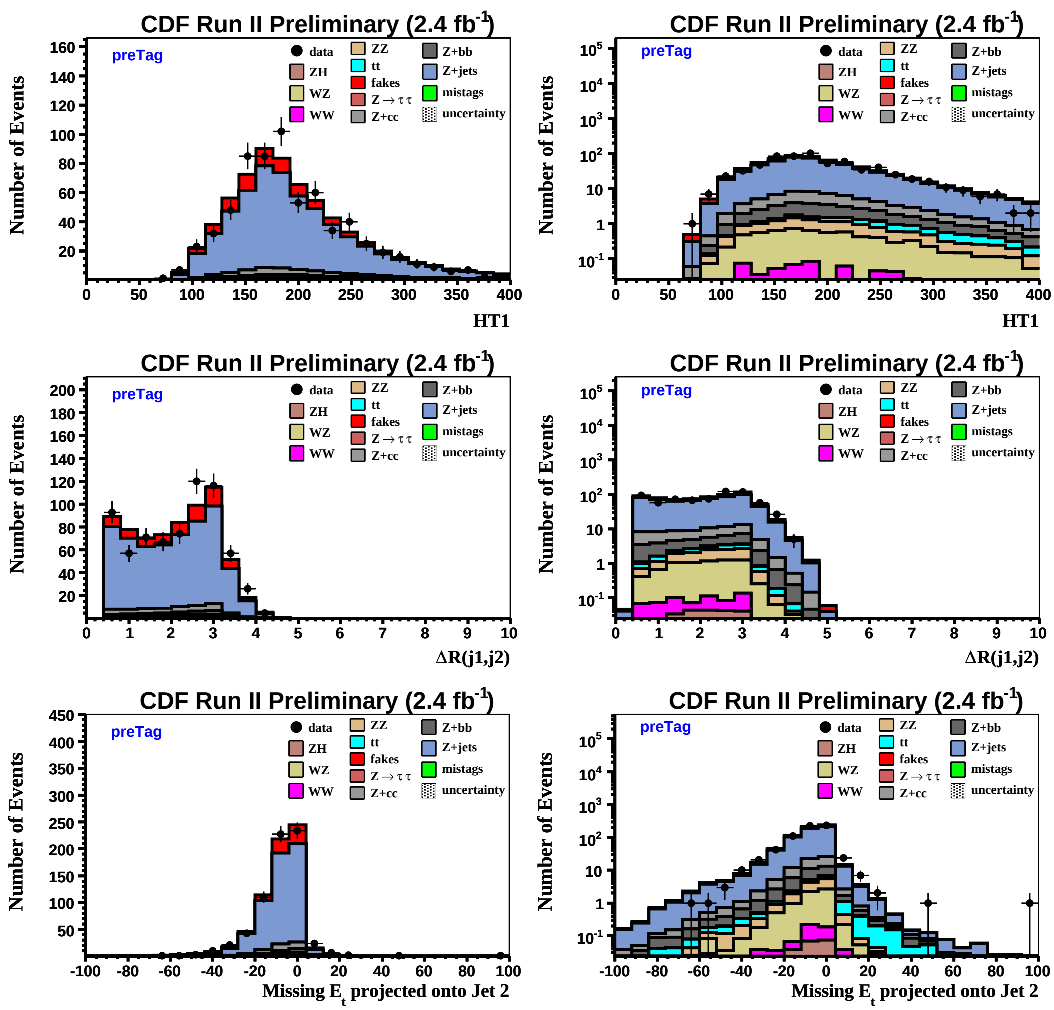

Figure 44: Pre-Tag NN inputs : Shape comparisons for TcLc Z category.

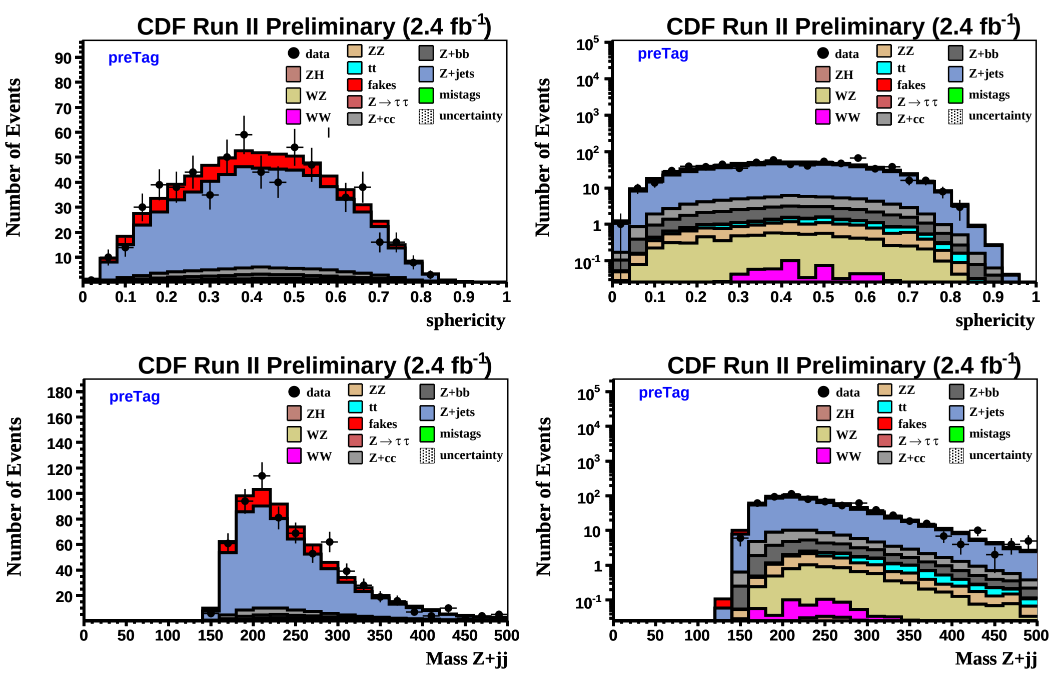

Figure 45: Pre-Tag NN inputs : Shape comparisons for TcLc Z category.

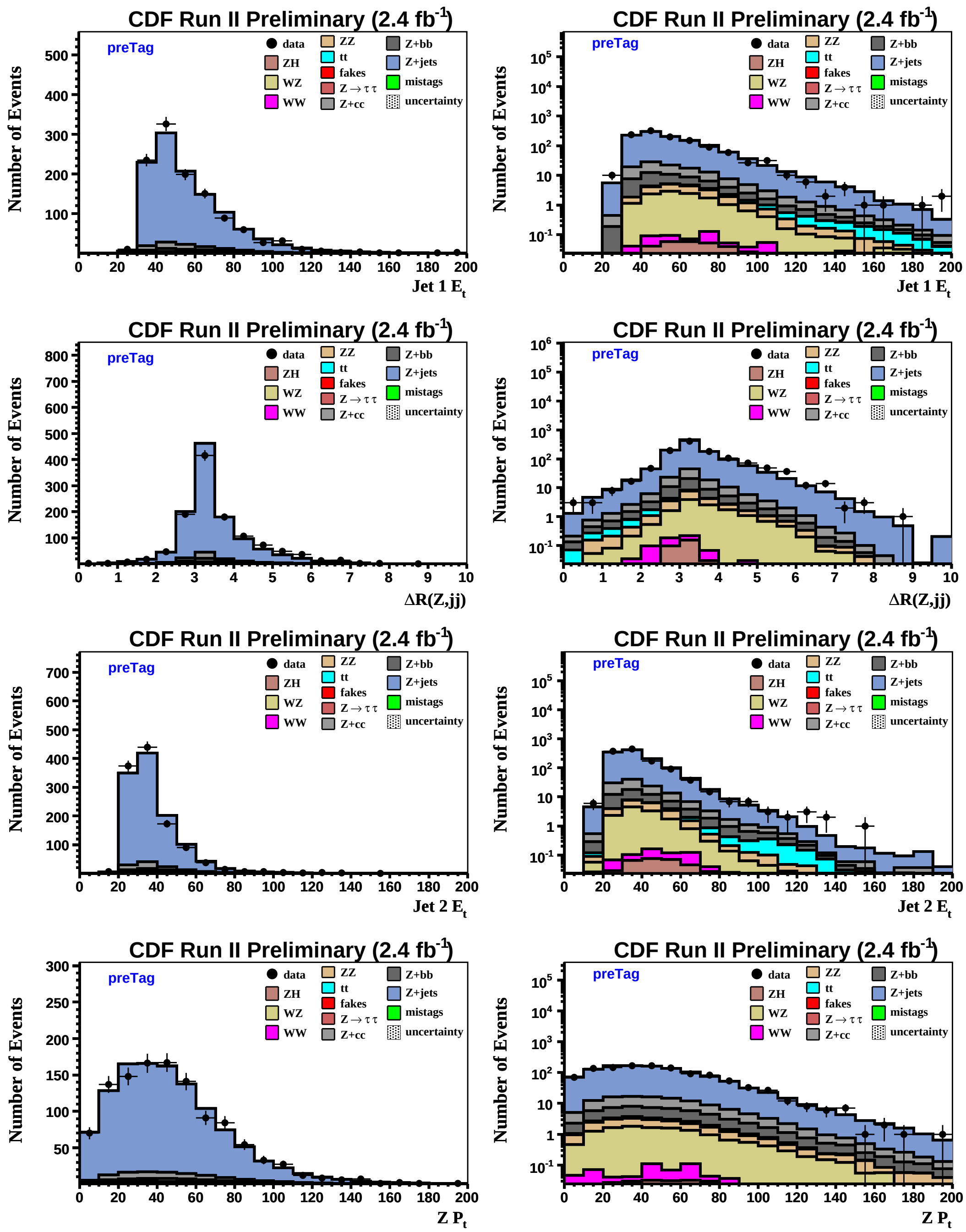

Figure 46: Pre-Tag NN inputs : Shape comparisons for TcTp Z category.

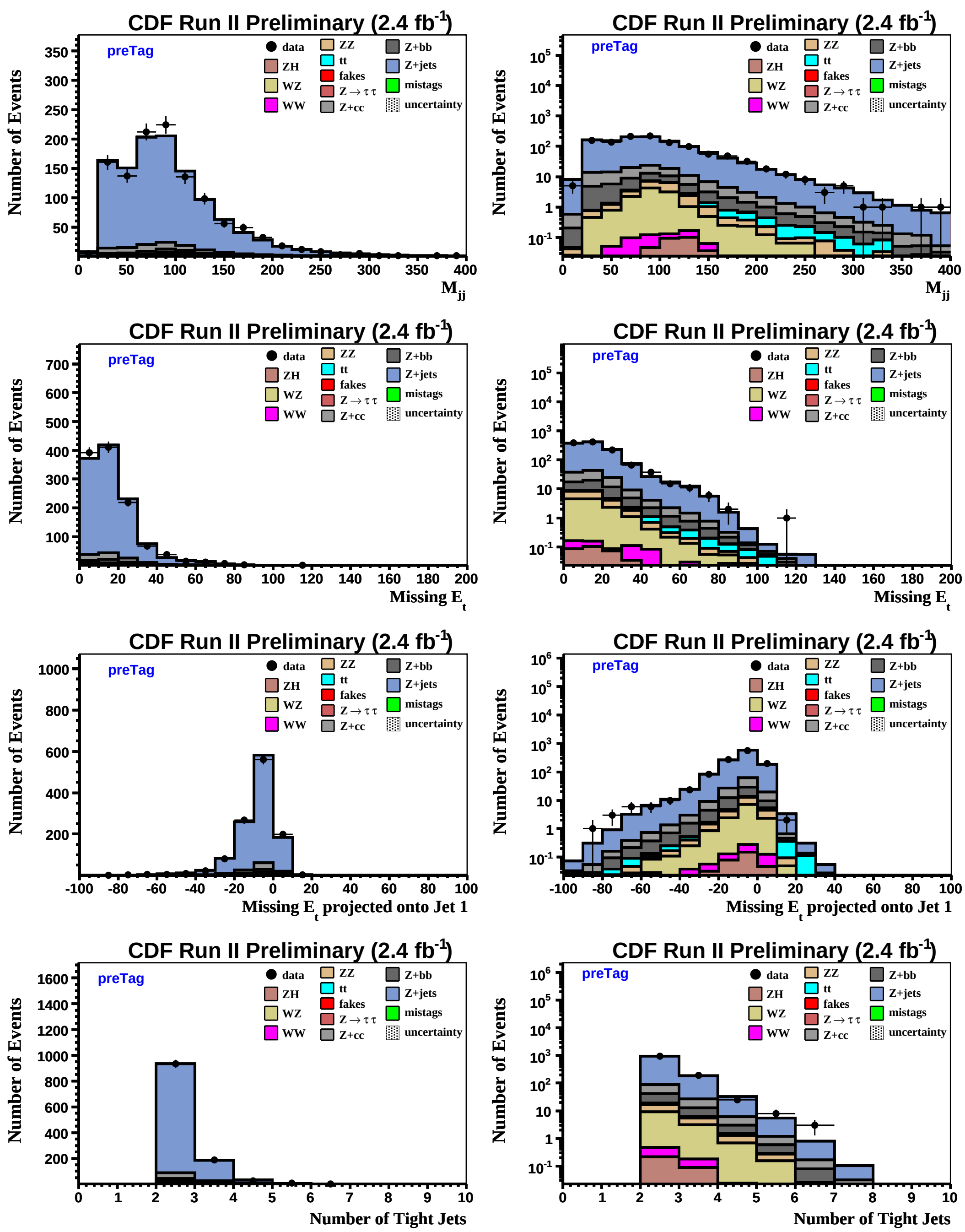

Figure 47: Pre-Tag NN inputs : Shape comparisons for TcTp Z category.

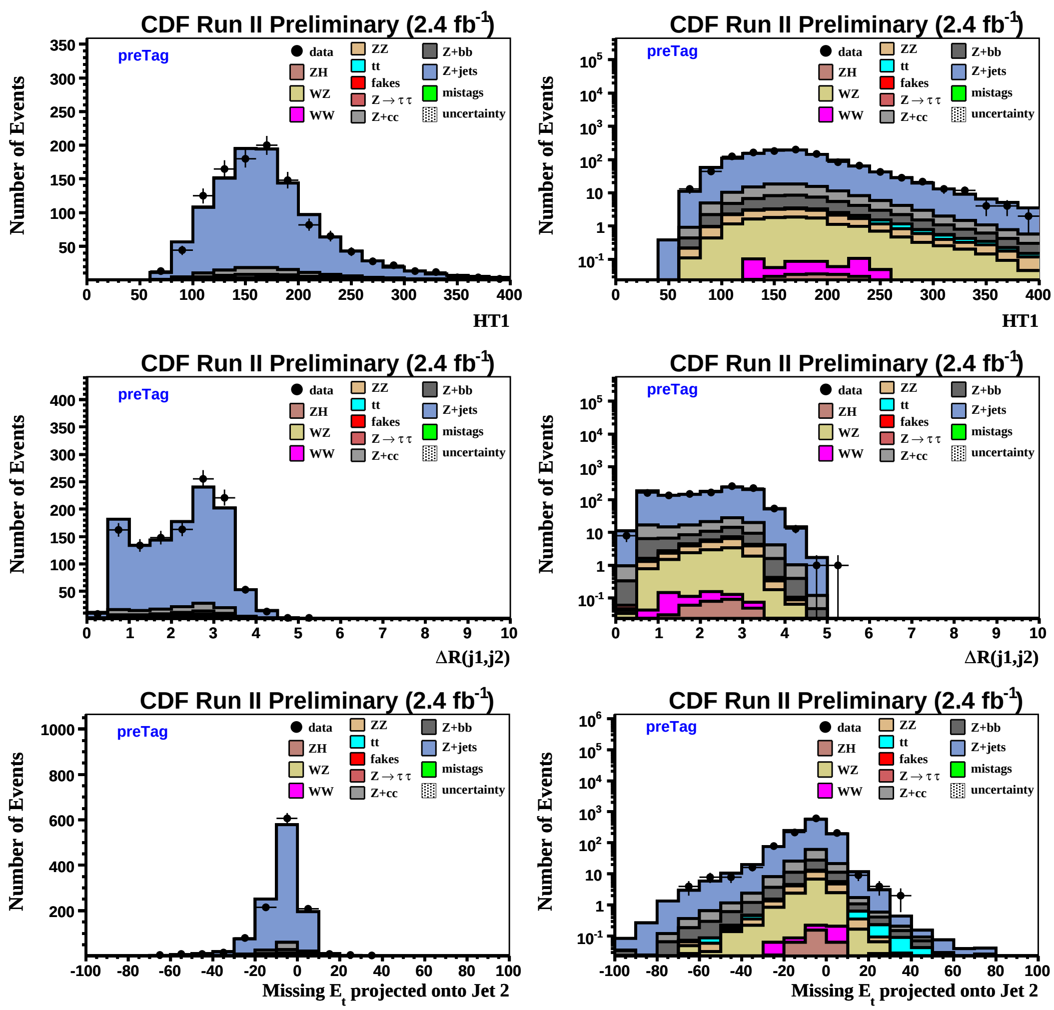

Figure 48: Pre-Tag NN inputs : Shape comparisons for TcTp Z category.

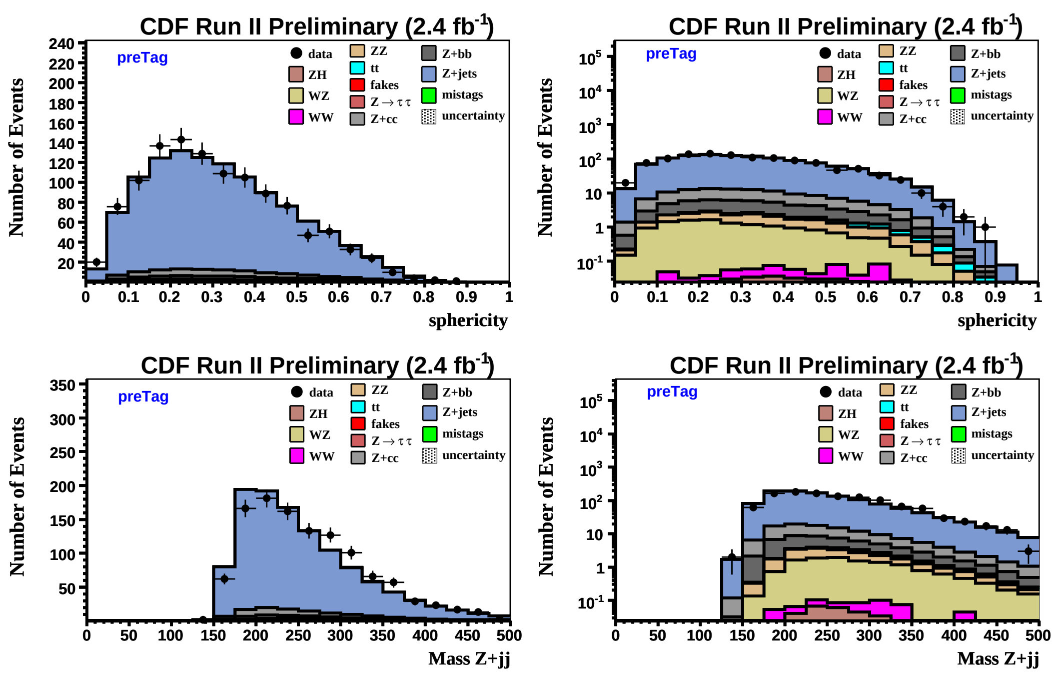

Figure 49: Pre-Tag NN inputs : Shape comparisons for TcTp Z category.

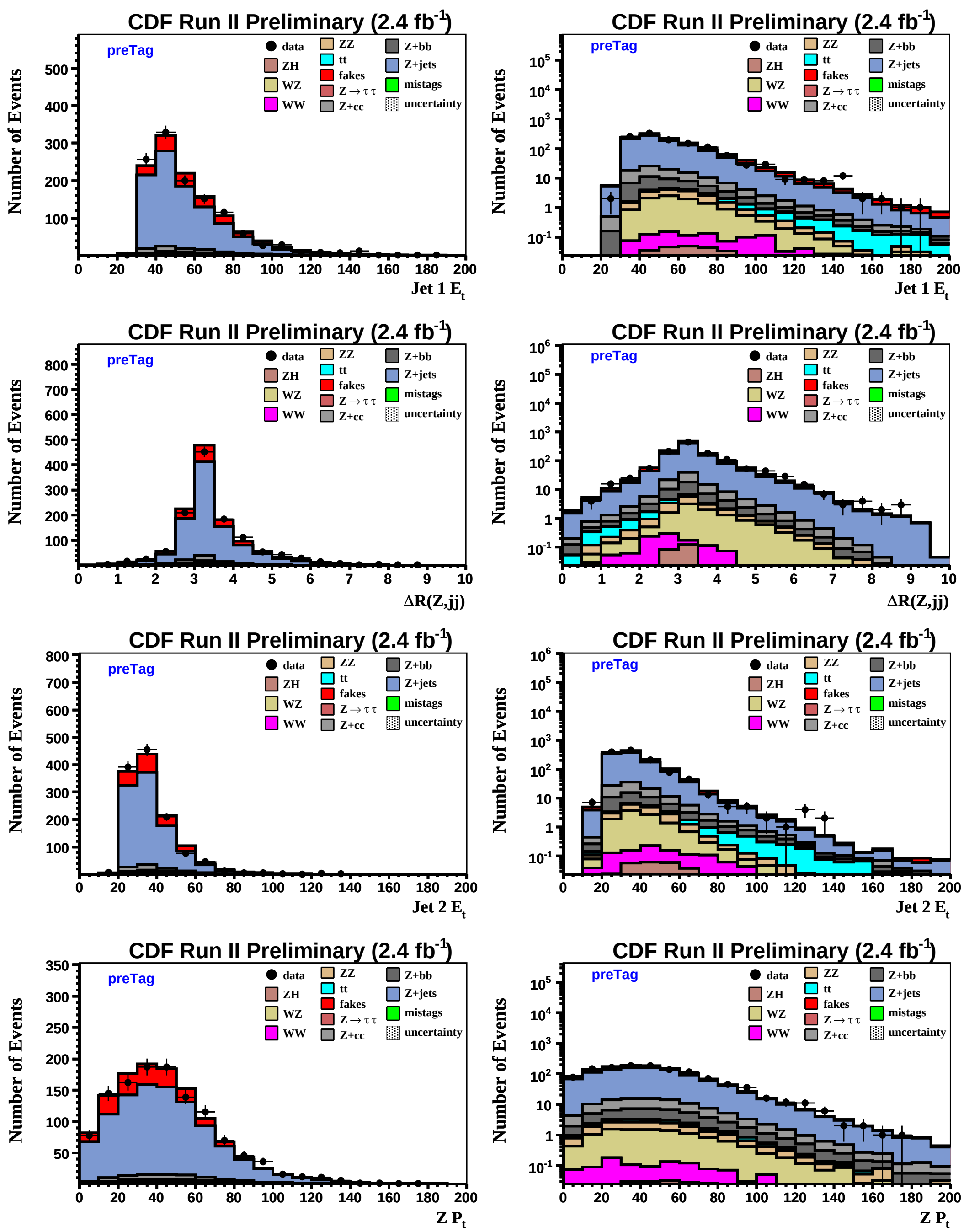

Figure 50: Pre-Tag NN inputs : Shape comparisons for TcLp Z category.

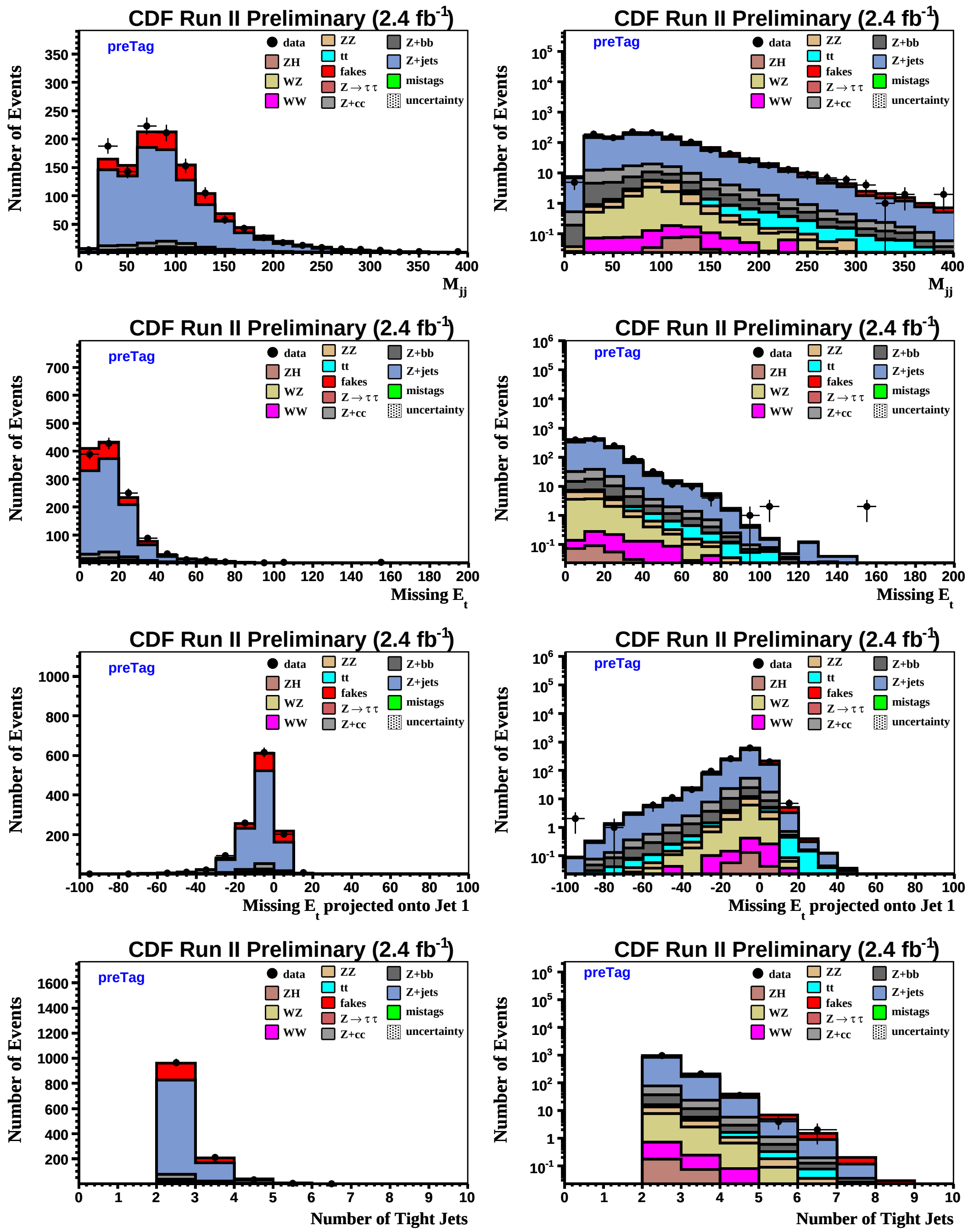

Figure 51: Pre-Tag NN inputs : Shape comparisons for TcLp Z category.

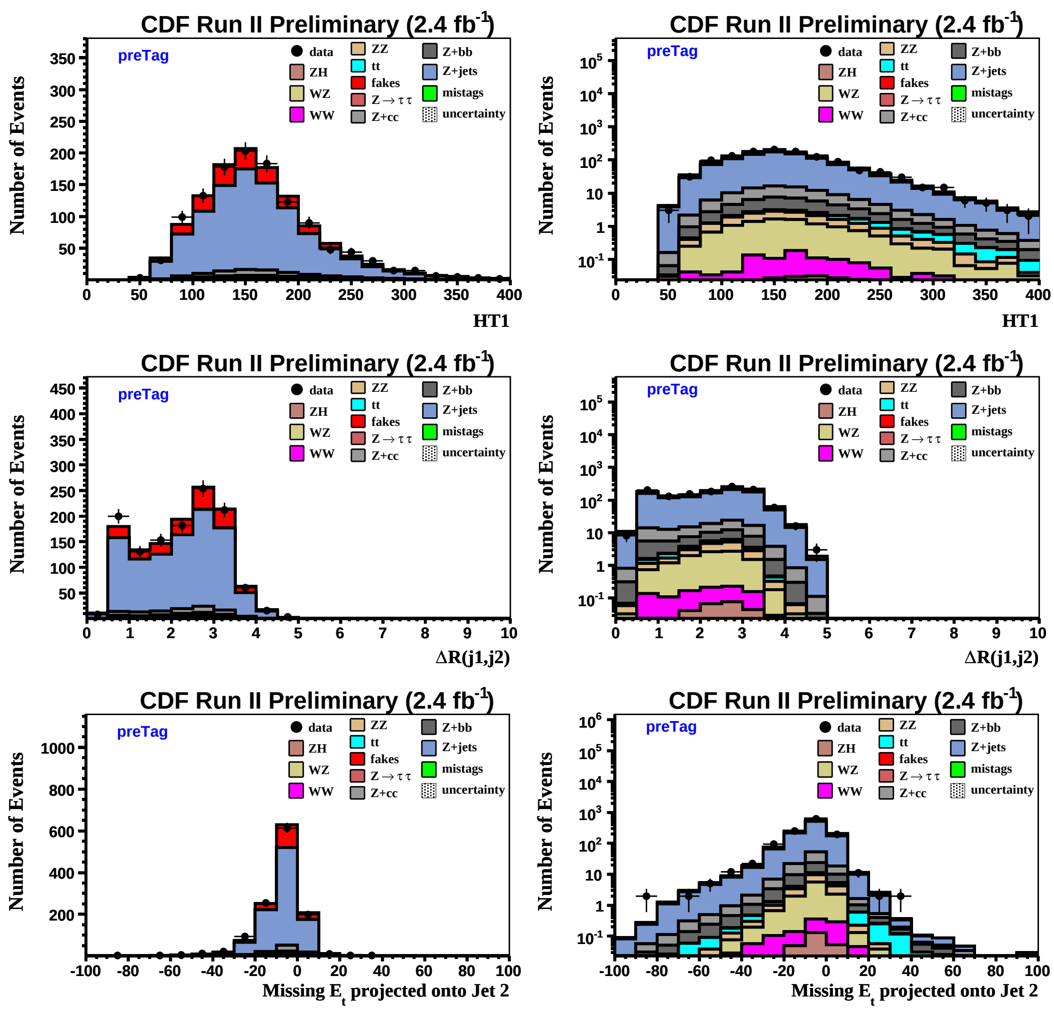

Figure 52: Pre-Tag NN inputs : Shape comparisons for TcLp Z category.

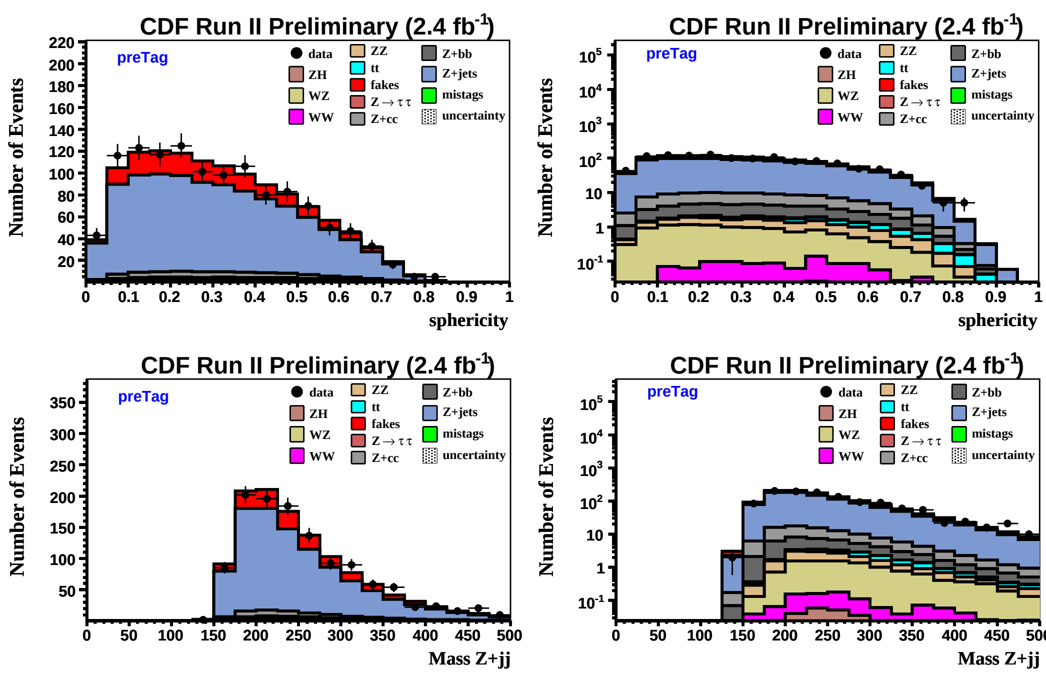

Figure 53: Pre-Tag NN inputs : Shape comparisons for TcLp Z category.

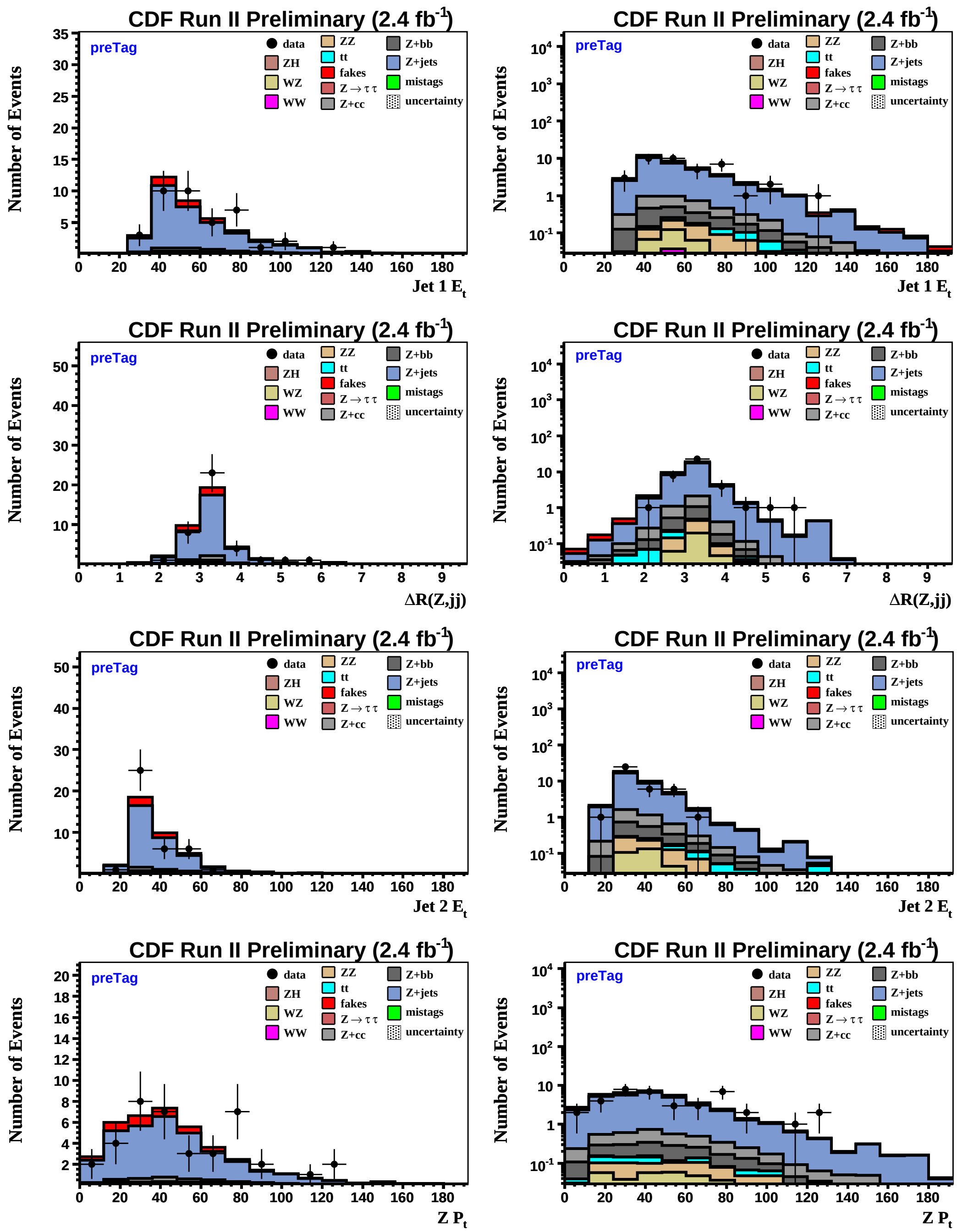

Figure 54: Pre-Tag NN inputs : Shape comparisons for Lc1Lc1 Z category.

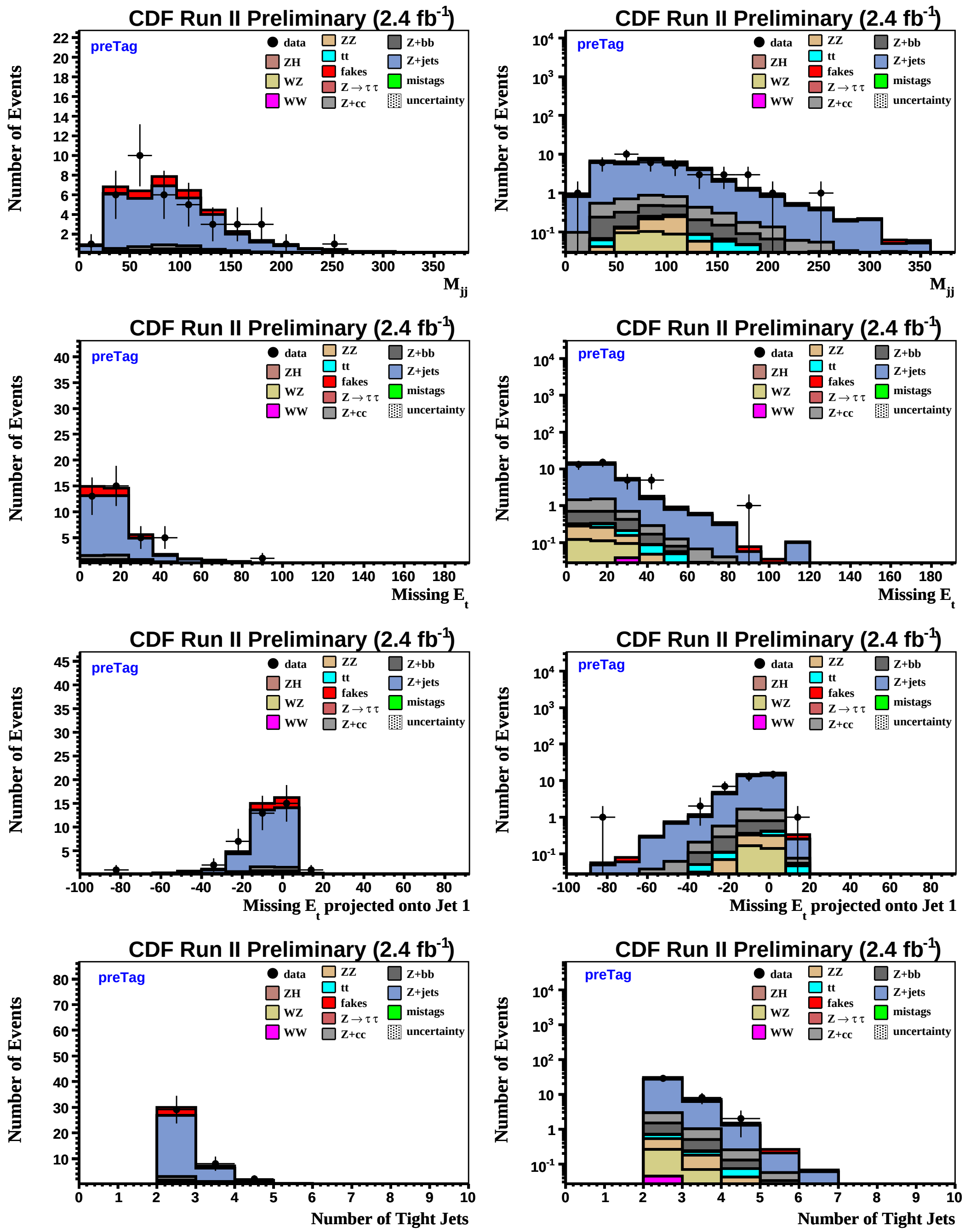

Figure 55: Pre-Tag NN inputs : Shape comparisons for Lc1Lc1 Z category.

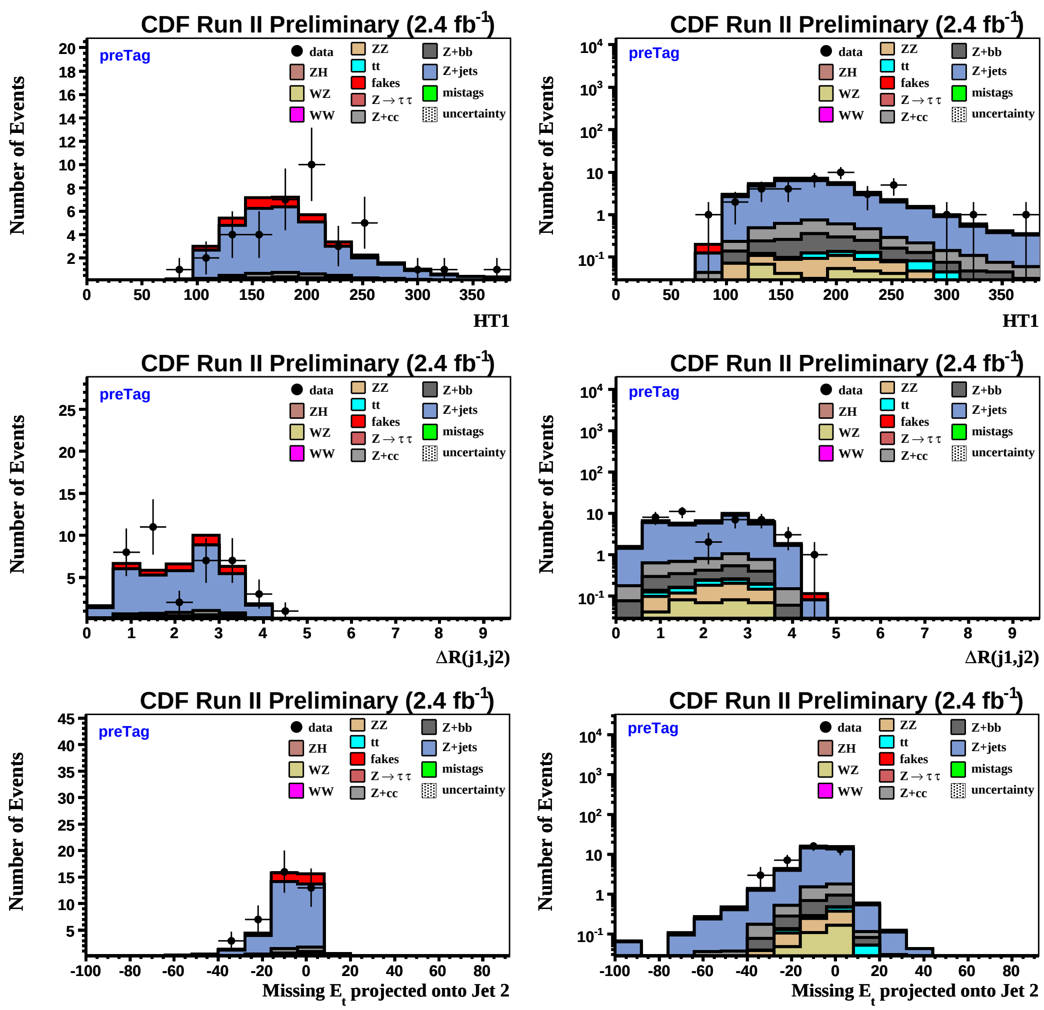

Figure 56: Pre-Tag NN inputs : Shape comparisons for Lc1Lc1 Z category.

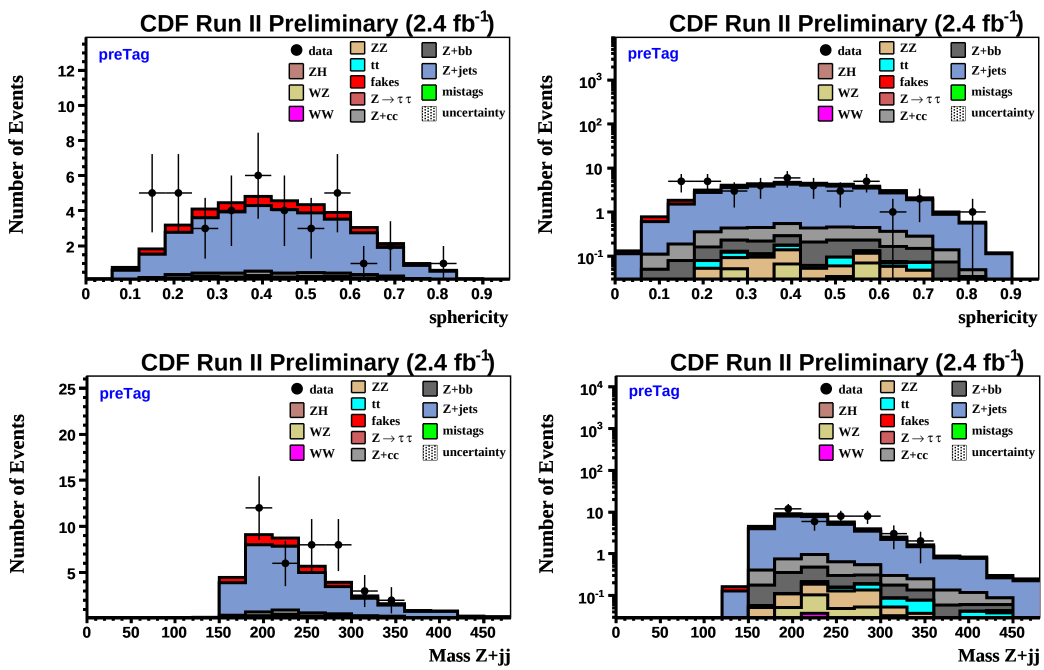

Figure 57: Pre-Tag NN inputs : Shape comparisons for Lc1Lc1 Z category.

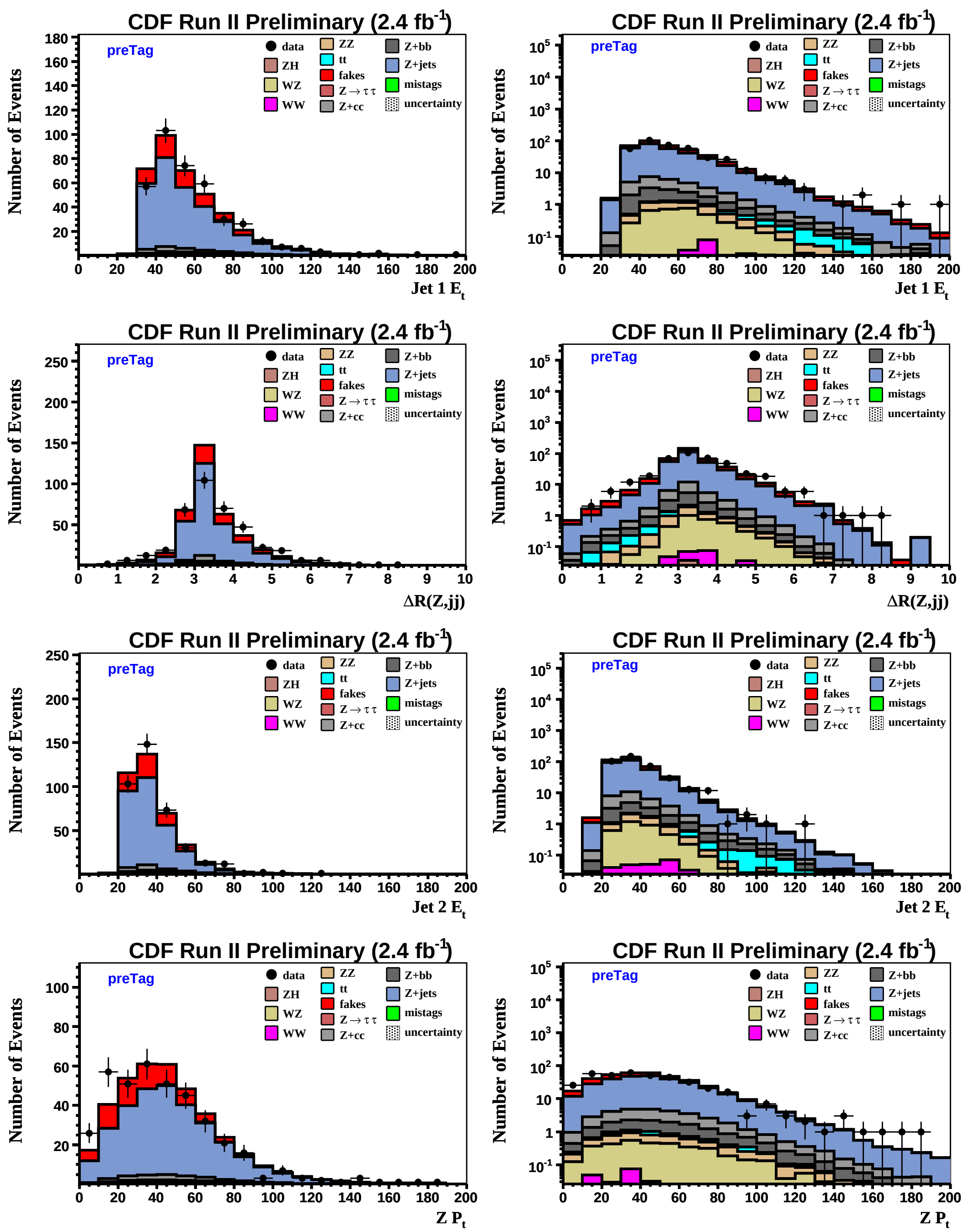

Figure 58: Pre-Tag NN inputs : Shape comparisons for TpLc Z category.

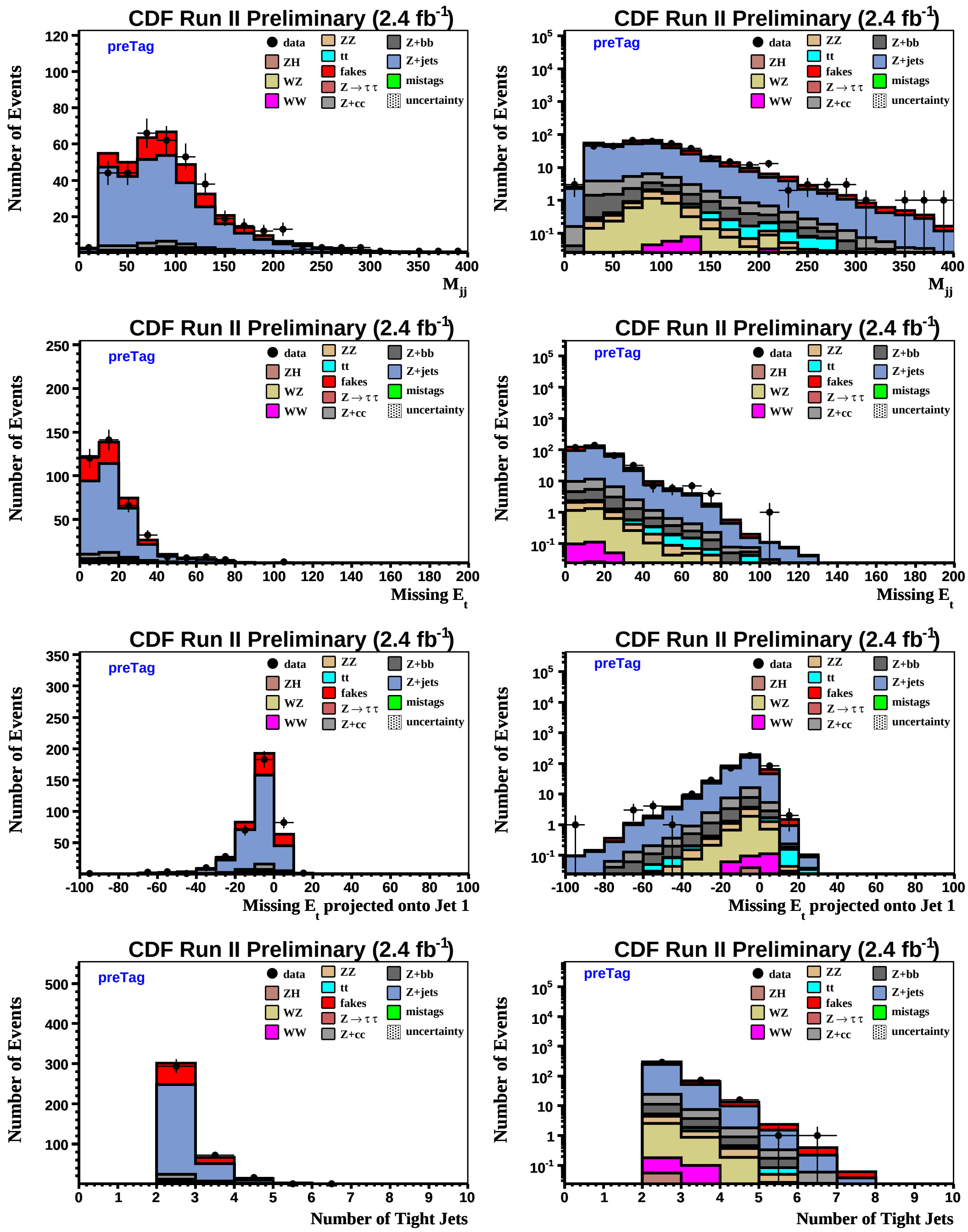

Figure 59: Pre-Tag NN inputs : Shape comparisons for TpLc Z category.

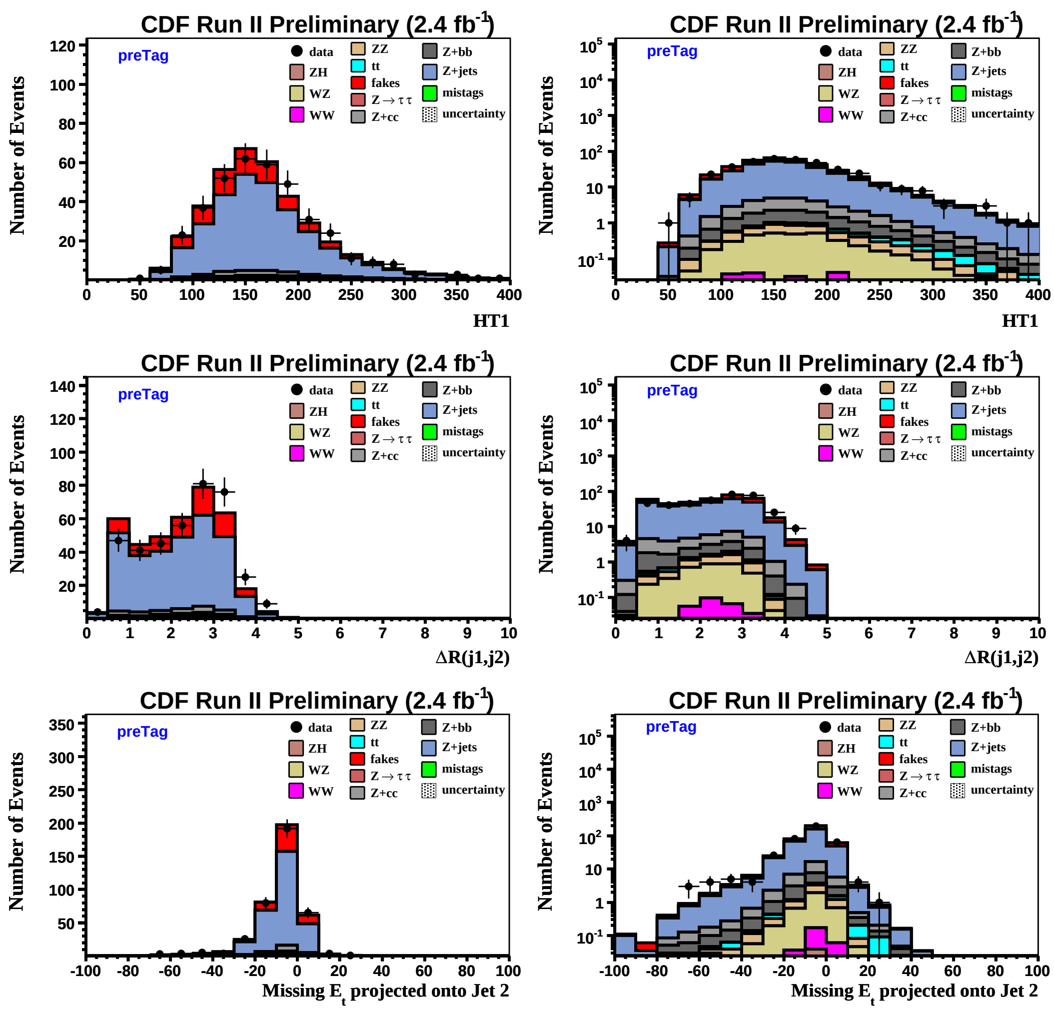

Figure 60: Pre-Tag NN inputs : Shape comparisons for TpLc Z category.

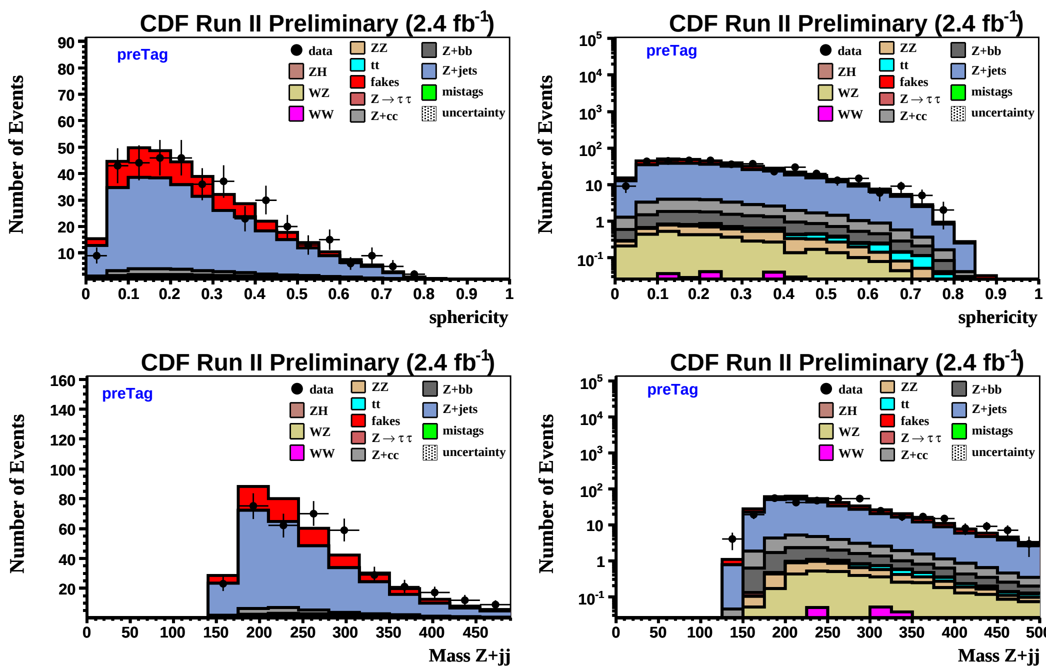

Figure 61: Pre-Tag NN inputs : Shape comparisons for TpLc Z category.

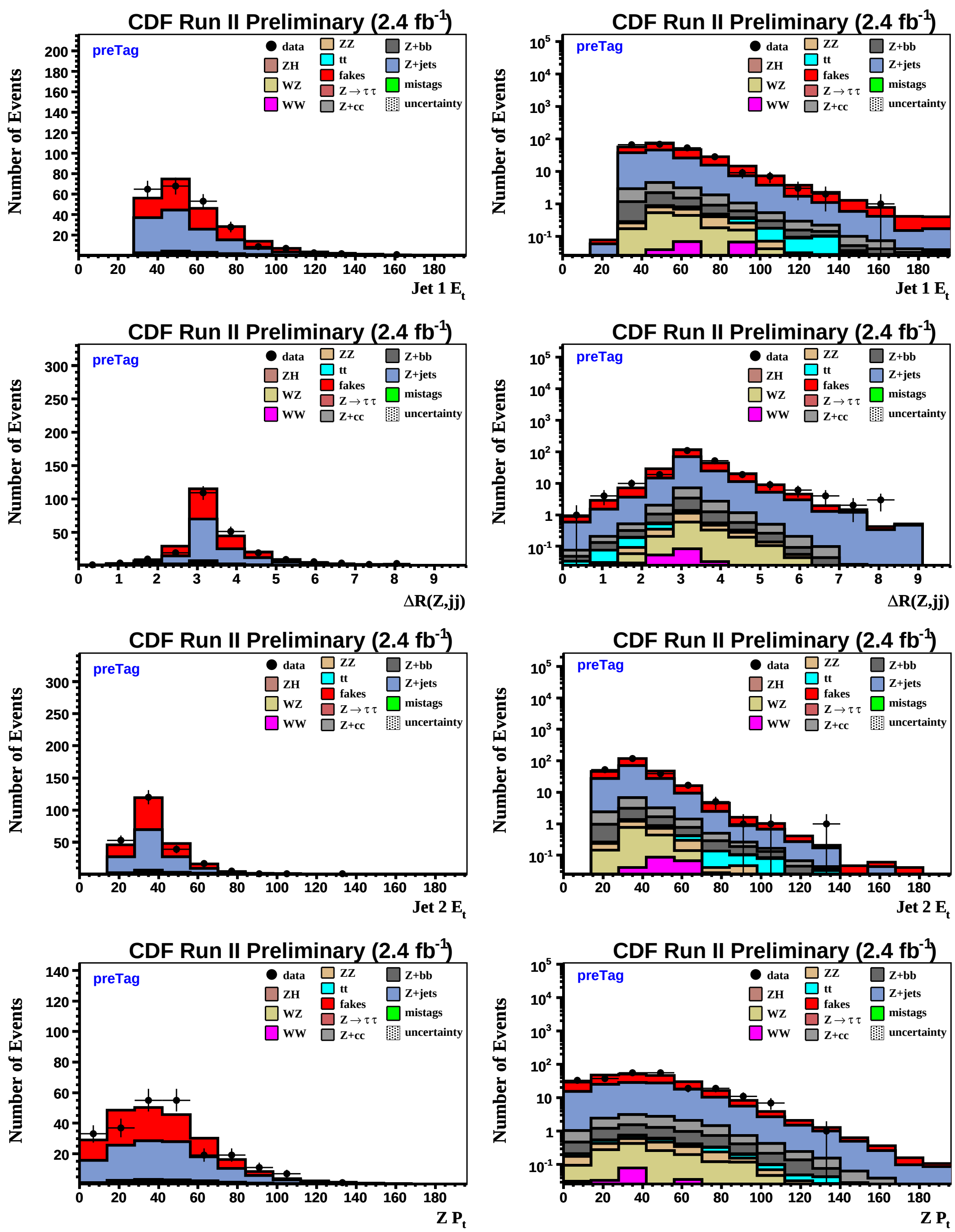

Figure 62: Pre-Tag NN inputs : Shape comparisons for Lc1Lp Z category.

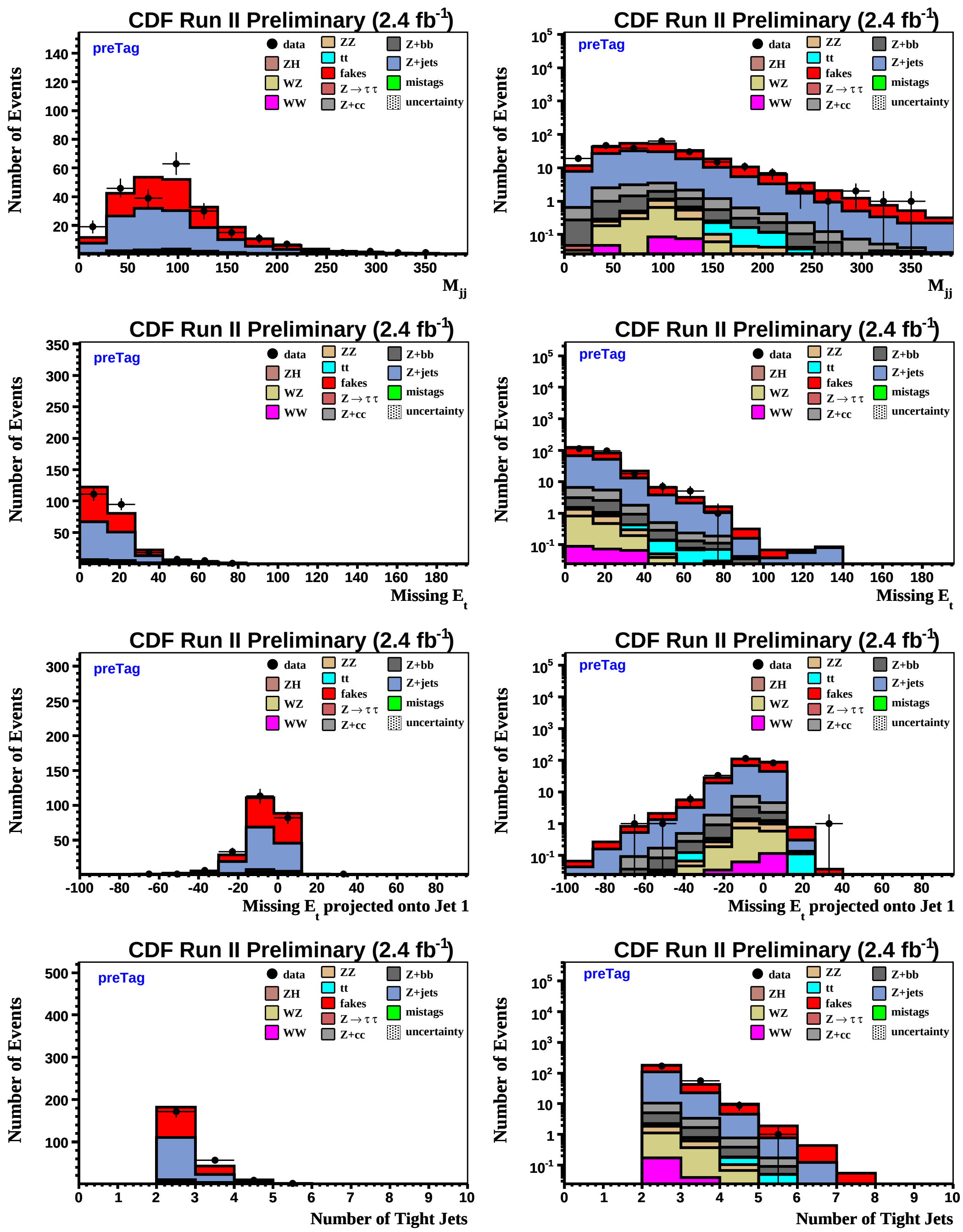

Figure 63: Pre-Tag NN inputs : Shape comparisons for Lc1Lp Z category.

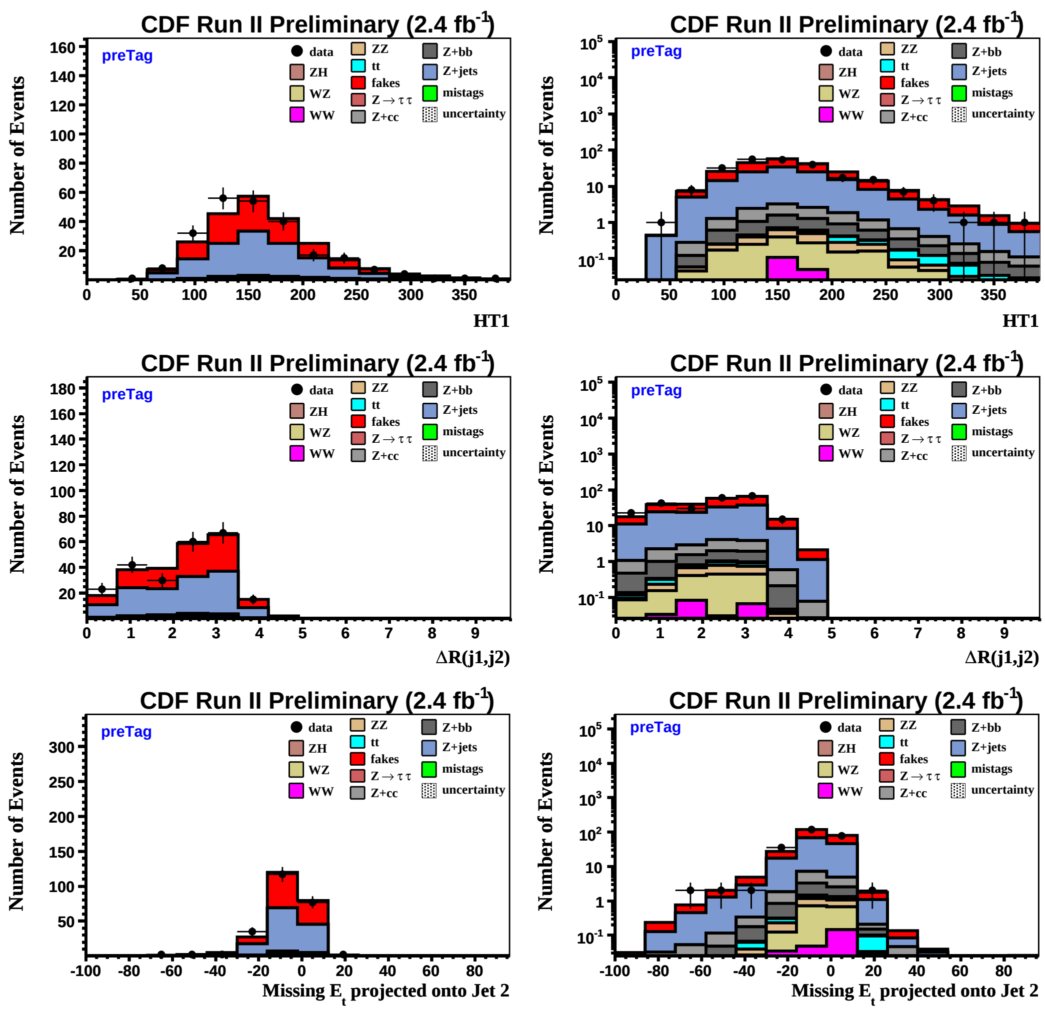

Figure 64: Pre-Tag NN inputs : Shape comparisons for Lc1Lp Z category.

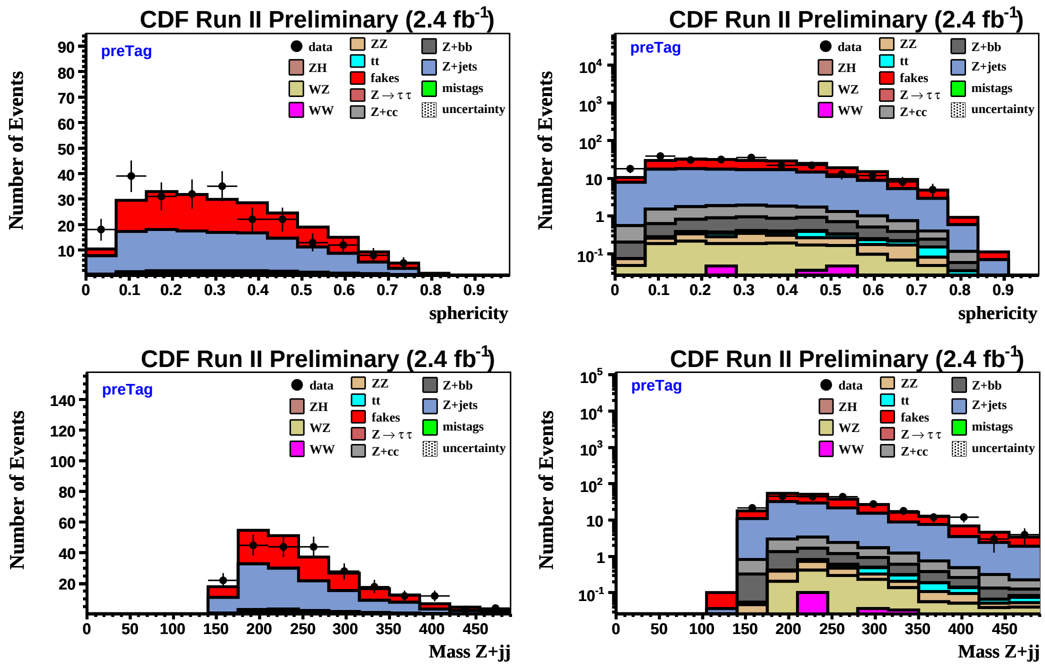

Figure 65: Pre-Tag NN inputs : Shape comparisons for Lc1Lp Z category.

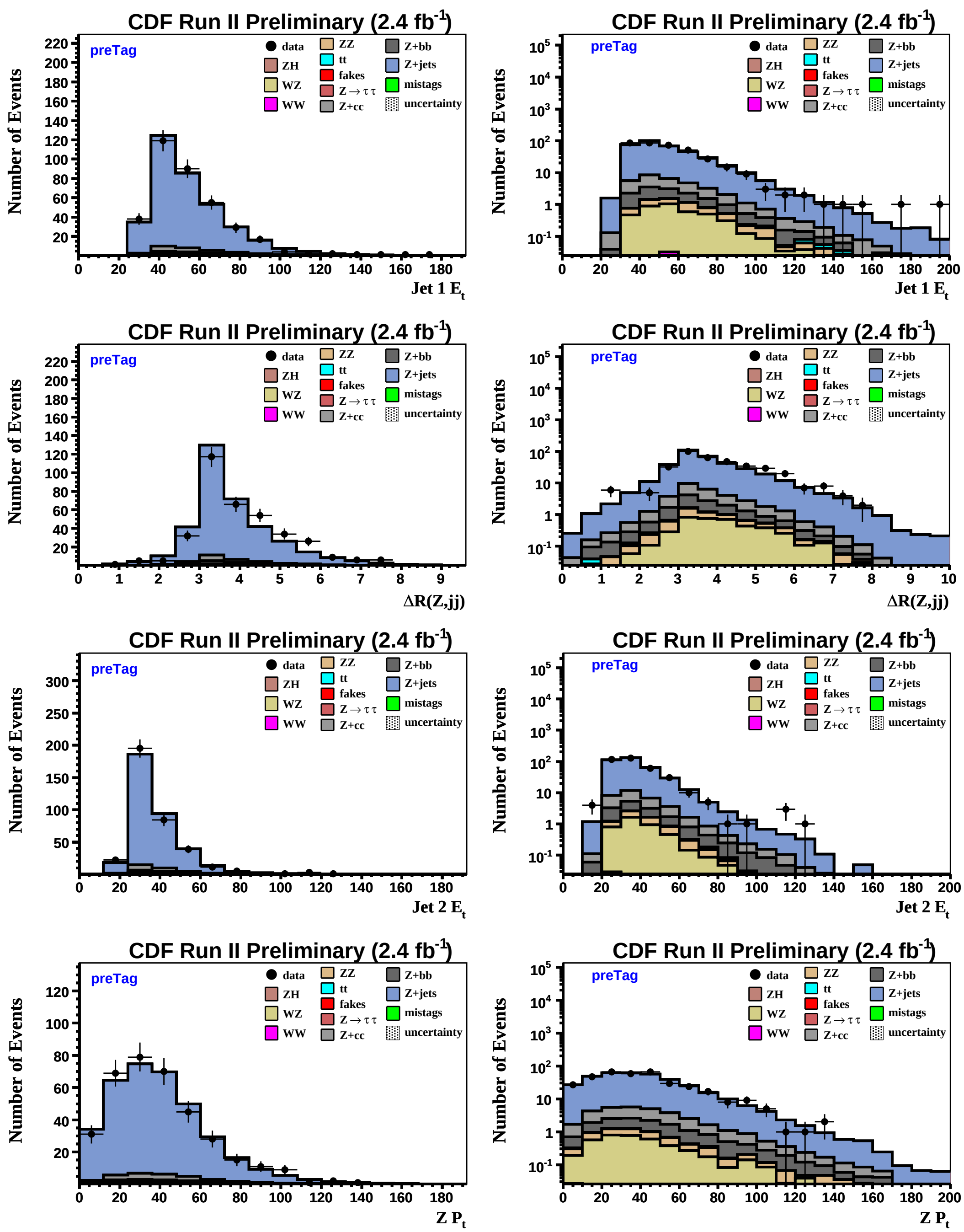

Figure 66: Pre-Tag NN inputs : Shape comparisons for TpTp Z category.

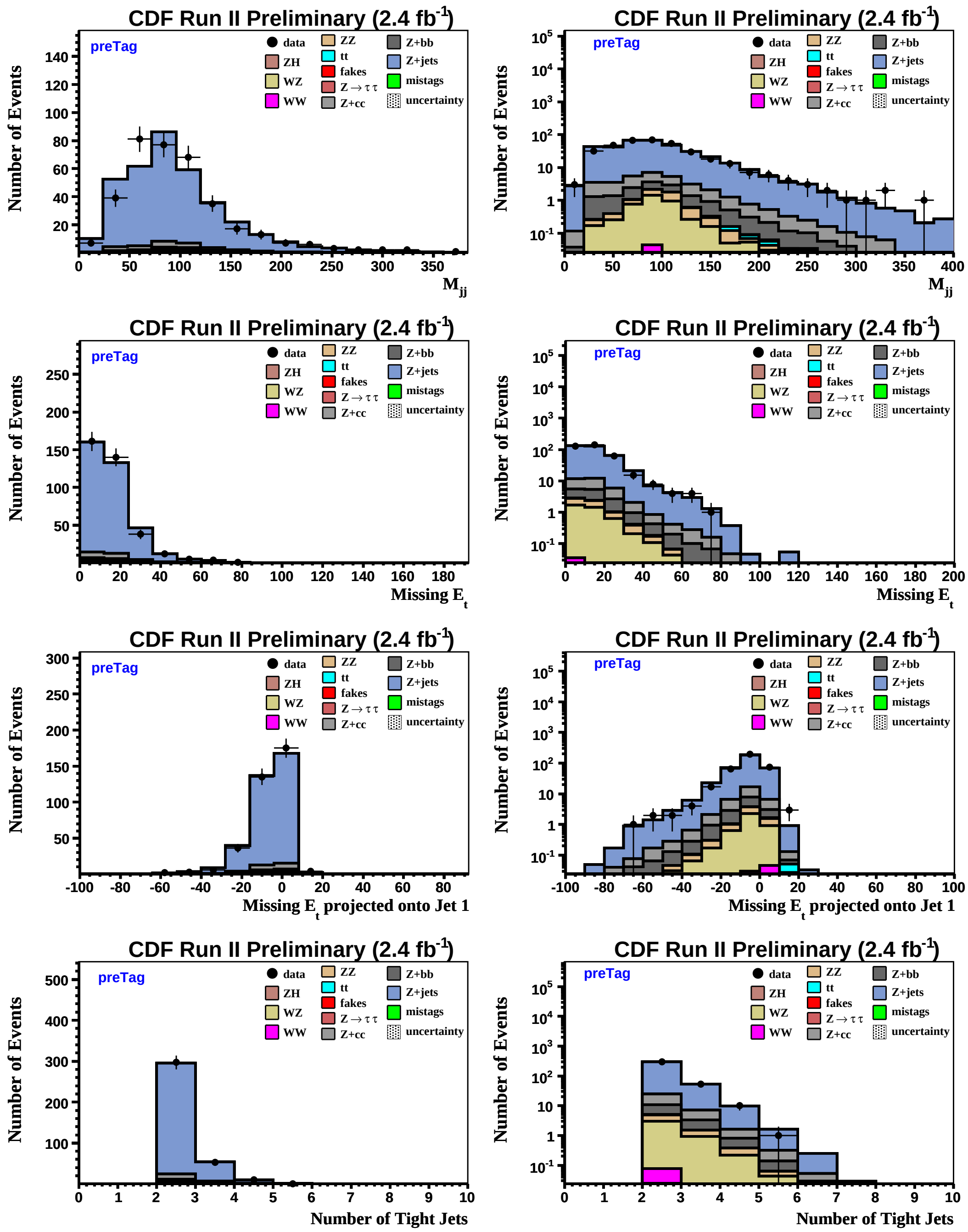

Figure 67: Pre-Tag NN inputs : Shape comparisons for TpTp Z category.

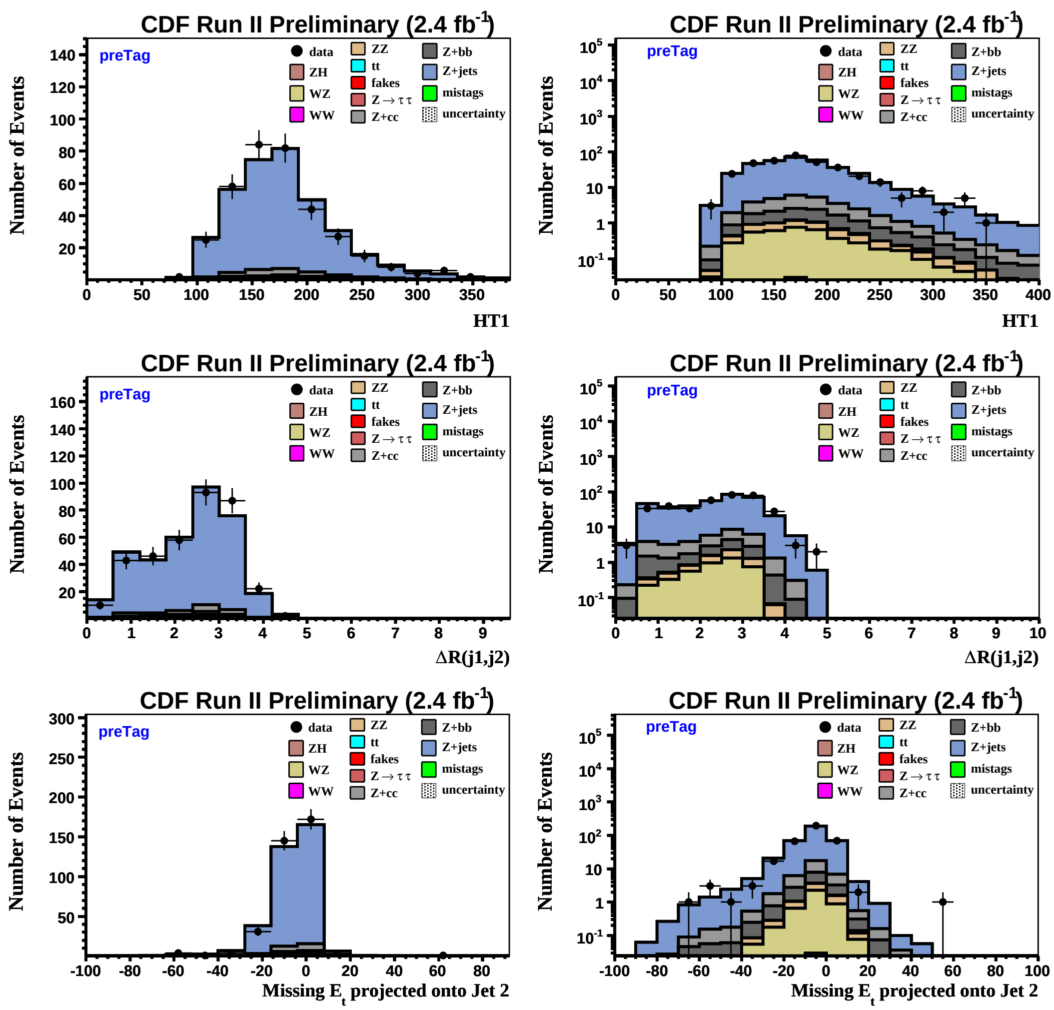

Figure 68: Pre-Tag NN inputs : Shape comparisons for TpTp Z category.

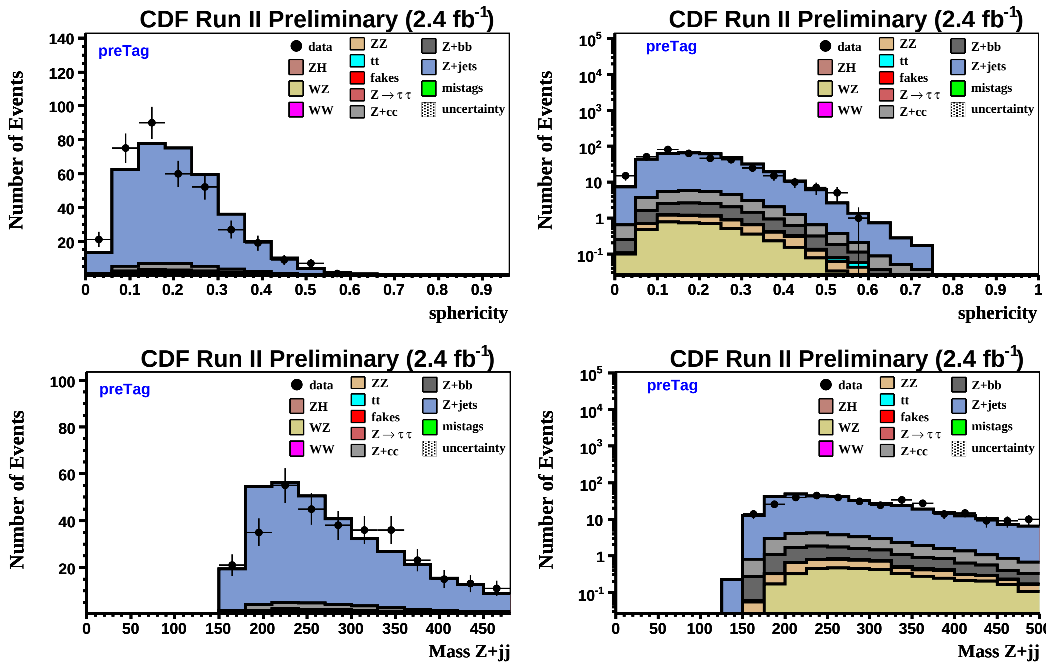

Figure 69: Pre-Tag NN inputs : Shape comparisons for TpTp Z category.

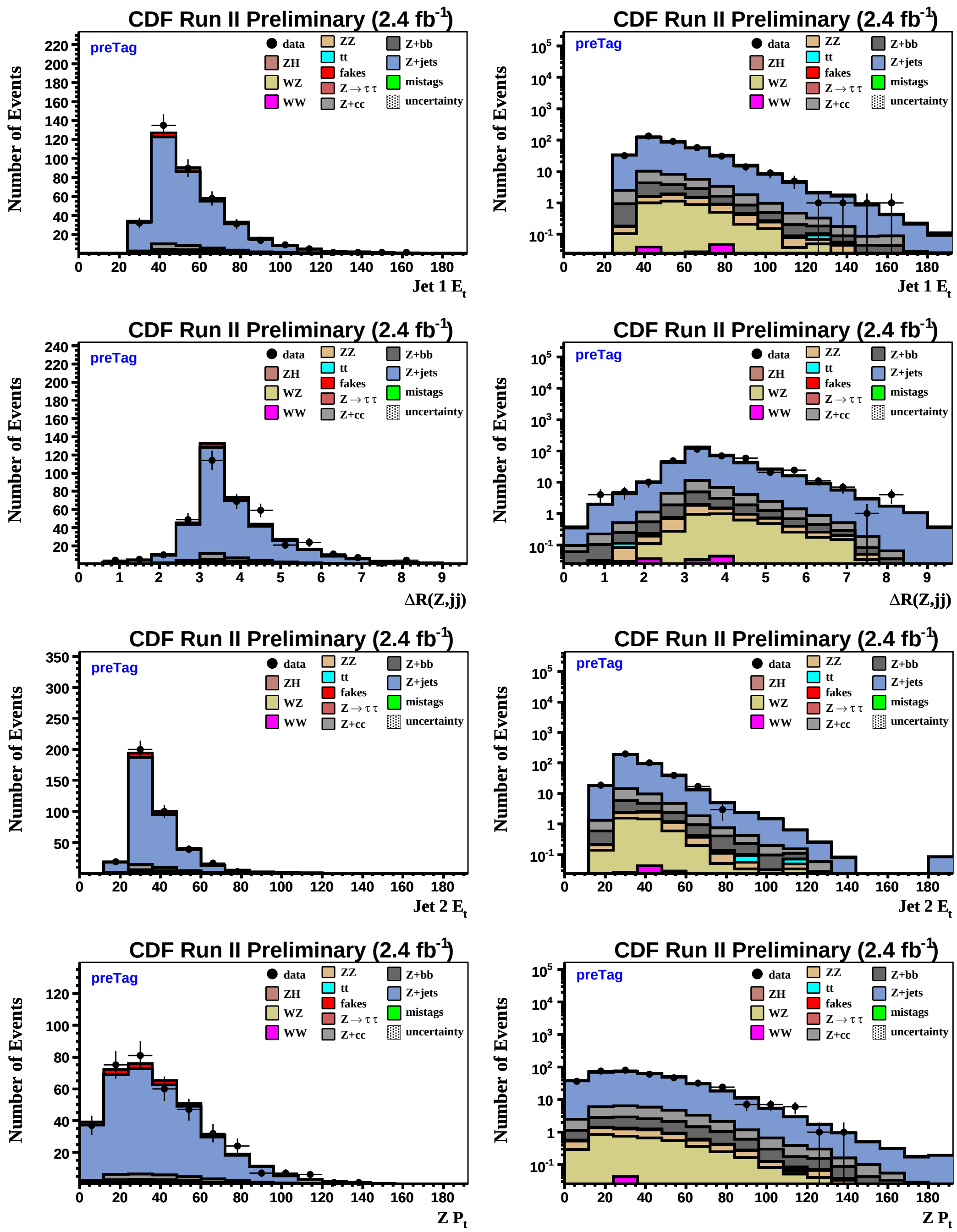

Figure 70: Pre-Tag NN inputs : Shape comparisons for TpLp Z category.

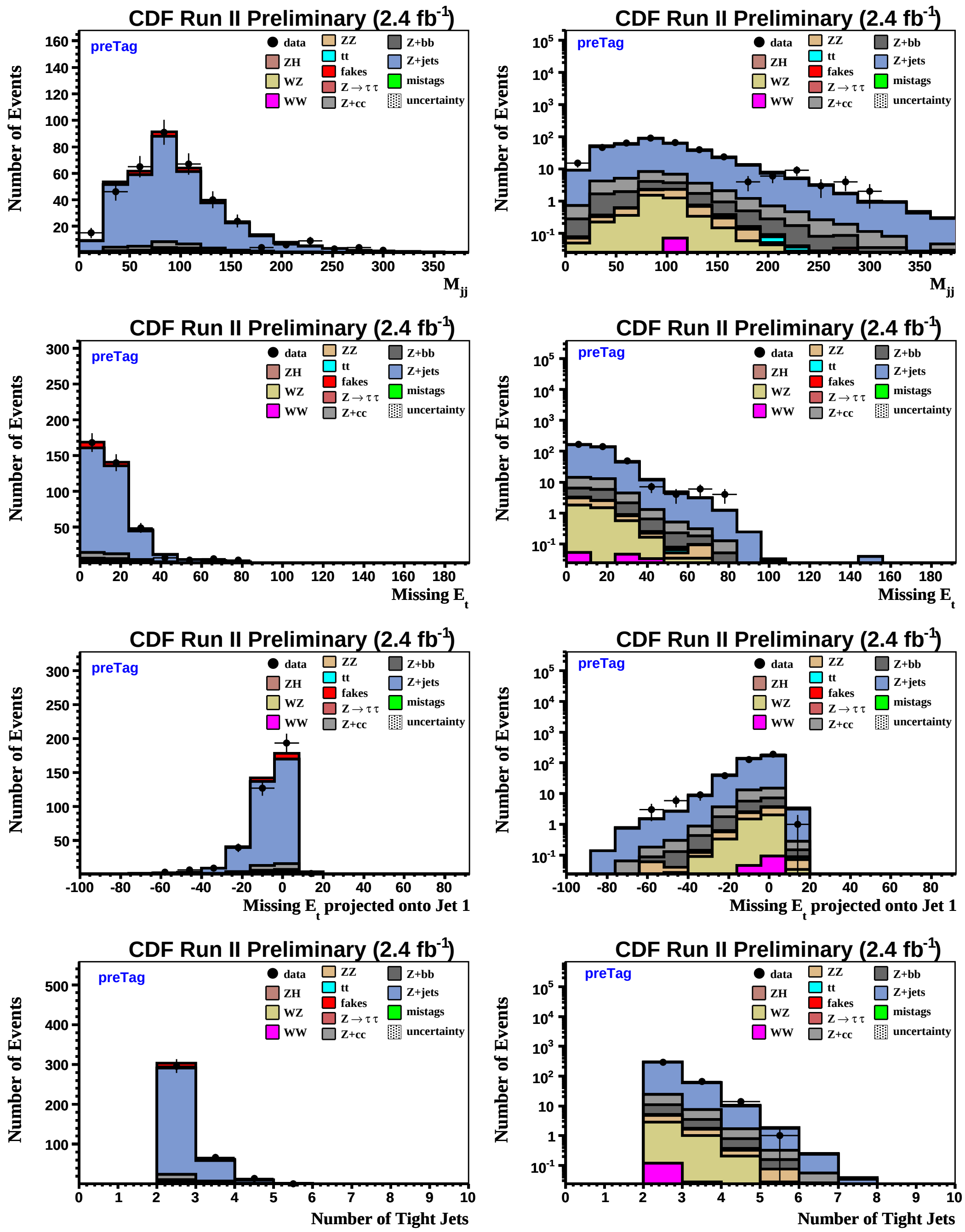

Figure 71: Pre-Tag NN inputs : Shape comparisons for TpLp Z category.

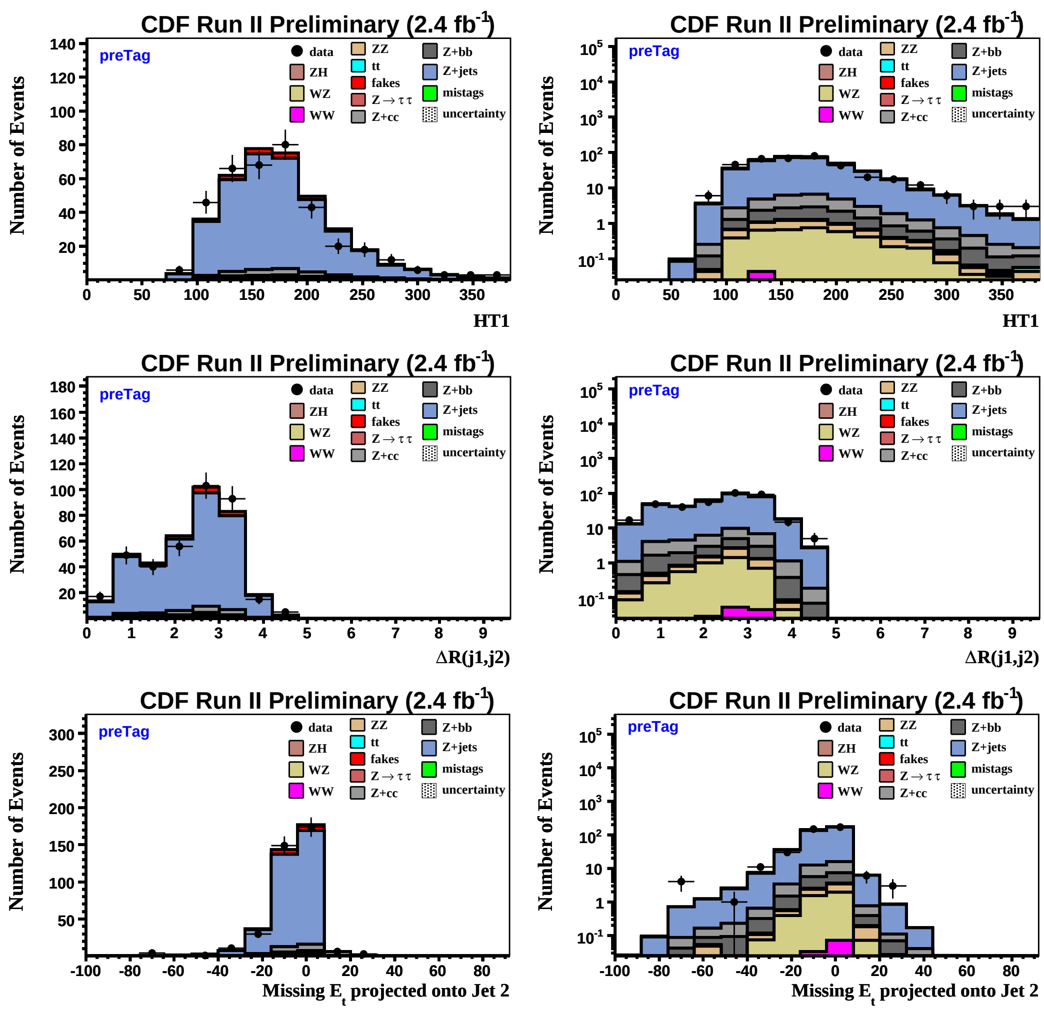

Figure 72: Pre-Tag NN inputs : Shape comparisons for TpLp Z category.

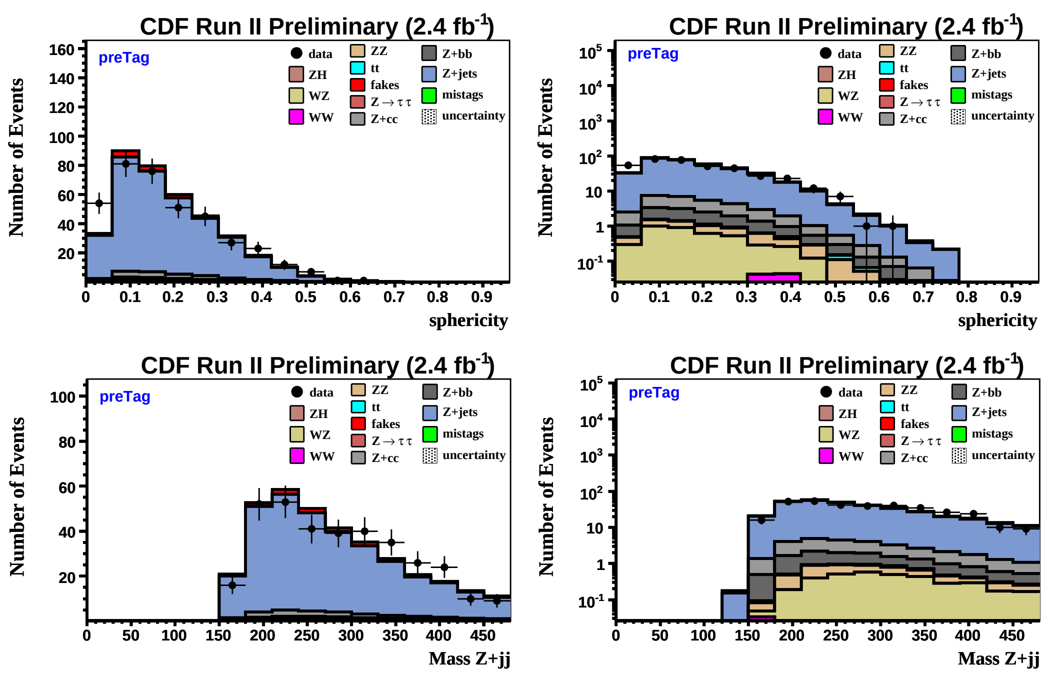

Figure 73: Pre-Tag NN inputs : Shape comparisons for TpLp Z category.

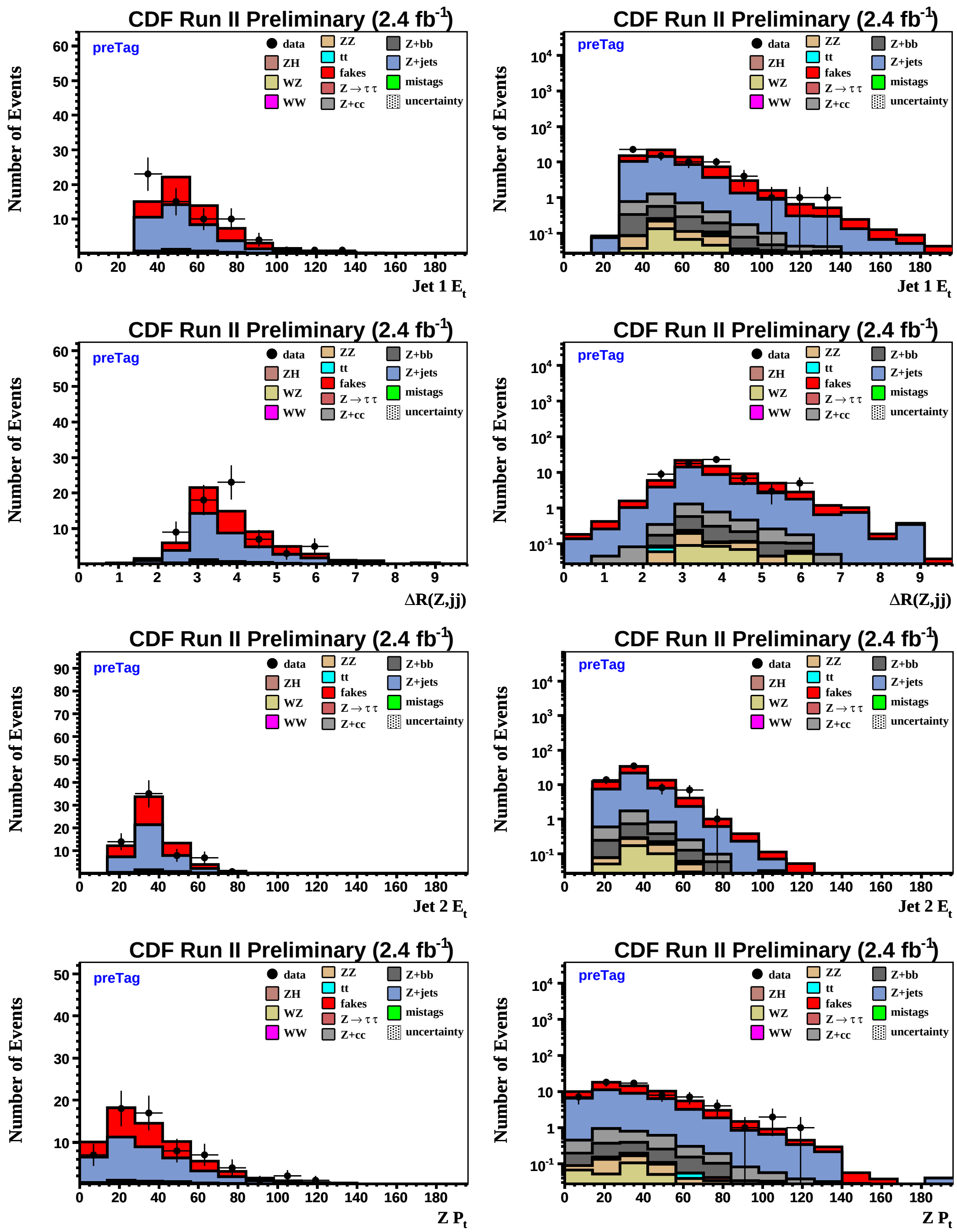

Figure 74: Pre-Tag NN inputs : Shape comparisons for LpLp Z category.

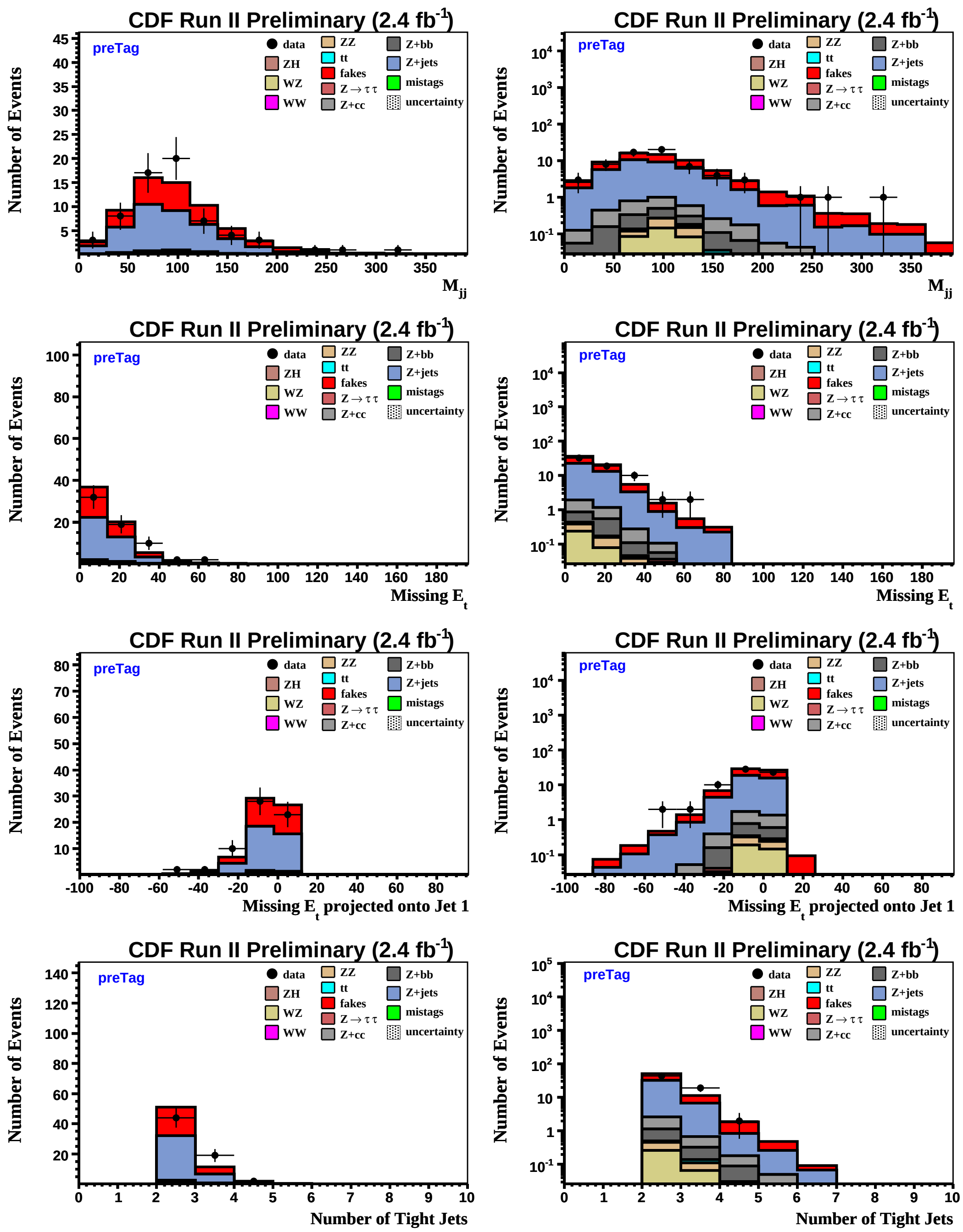

Figure 75: Pre-Tag NN inputs : Shape comparisons for LpLp Z category.

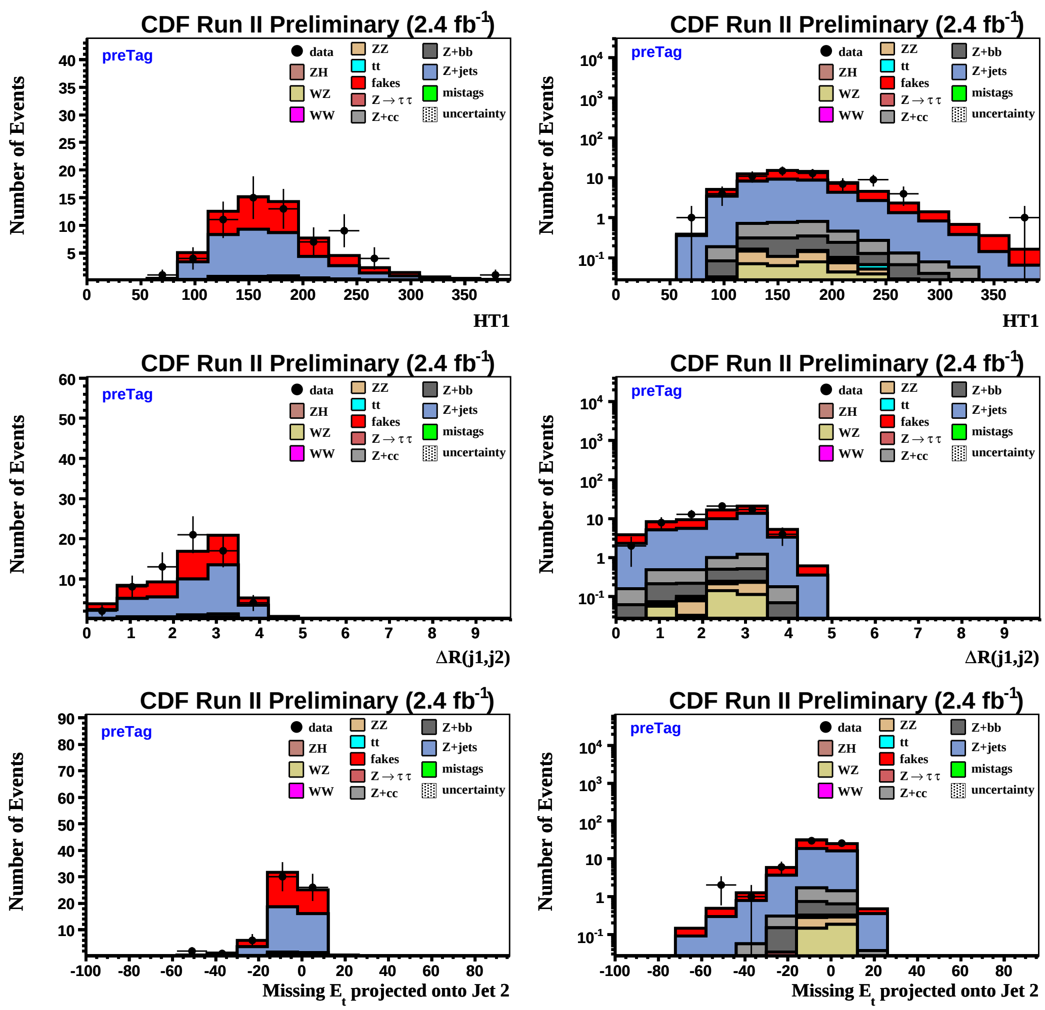

Figure 76: Pre-Tag NN inputs : Shape comparisons for LpLp Z category.

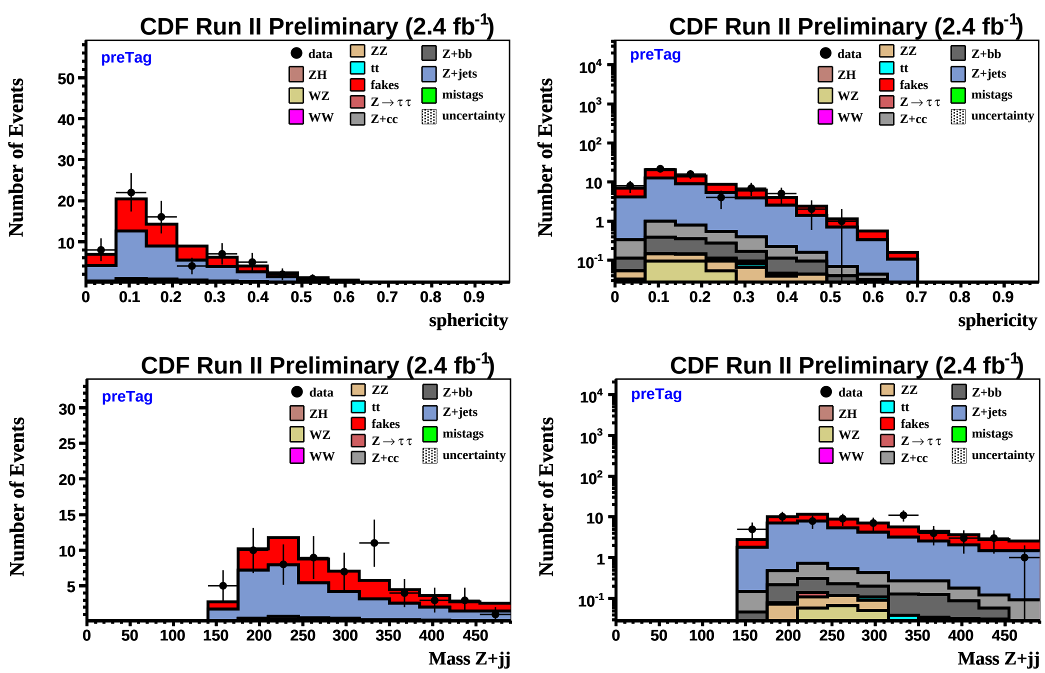

Figure 77: Pre-Tag NN inputs : Shape comparisons for LpLp Z category.

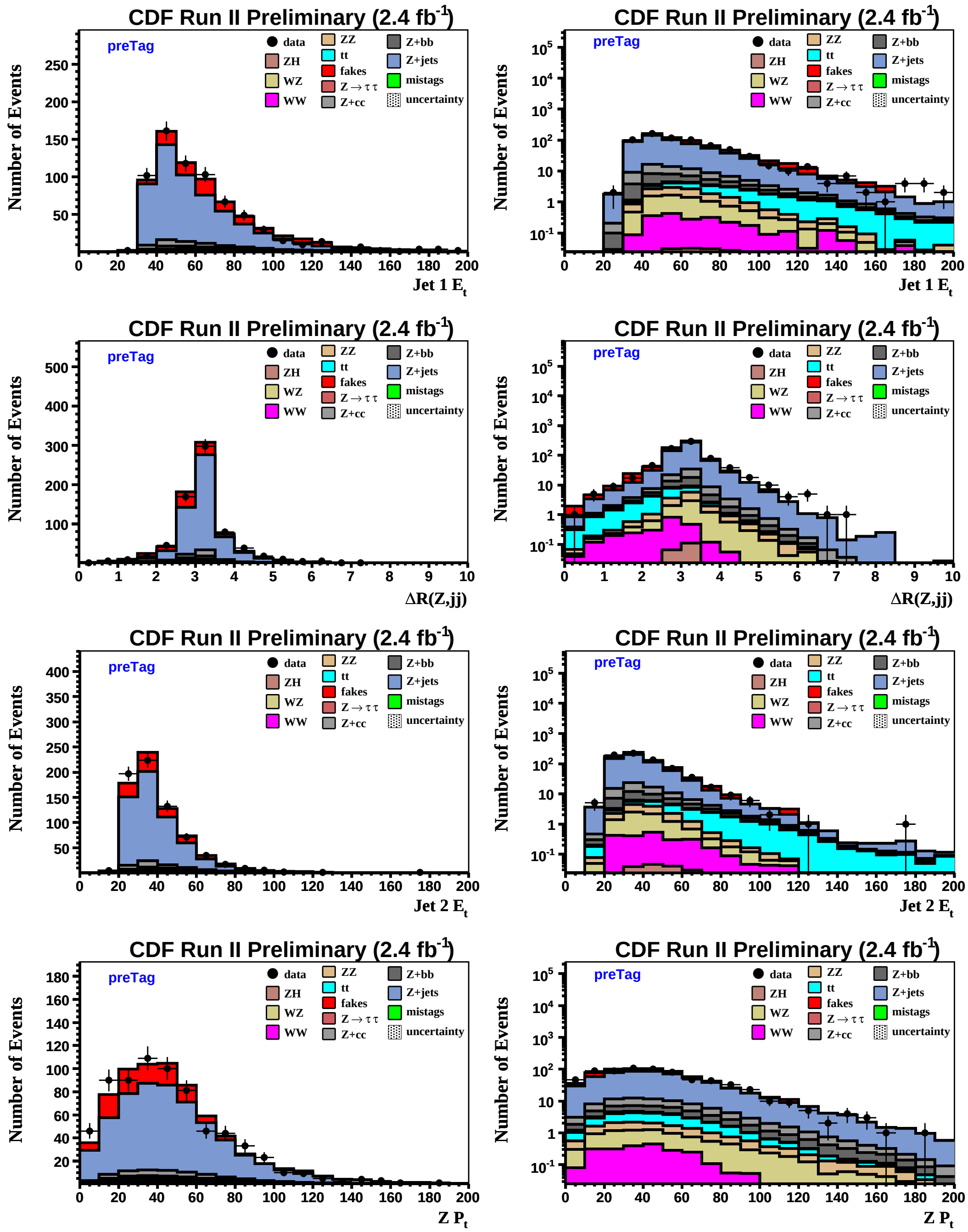

Figure 78: Pre-Tag NN inputs : Shape comparisons for TcCrkTrk Z category.

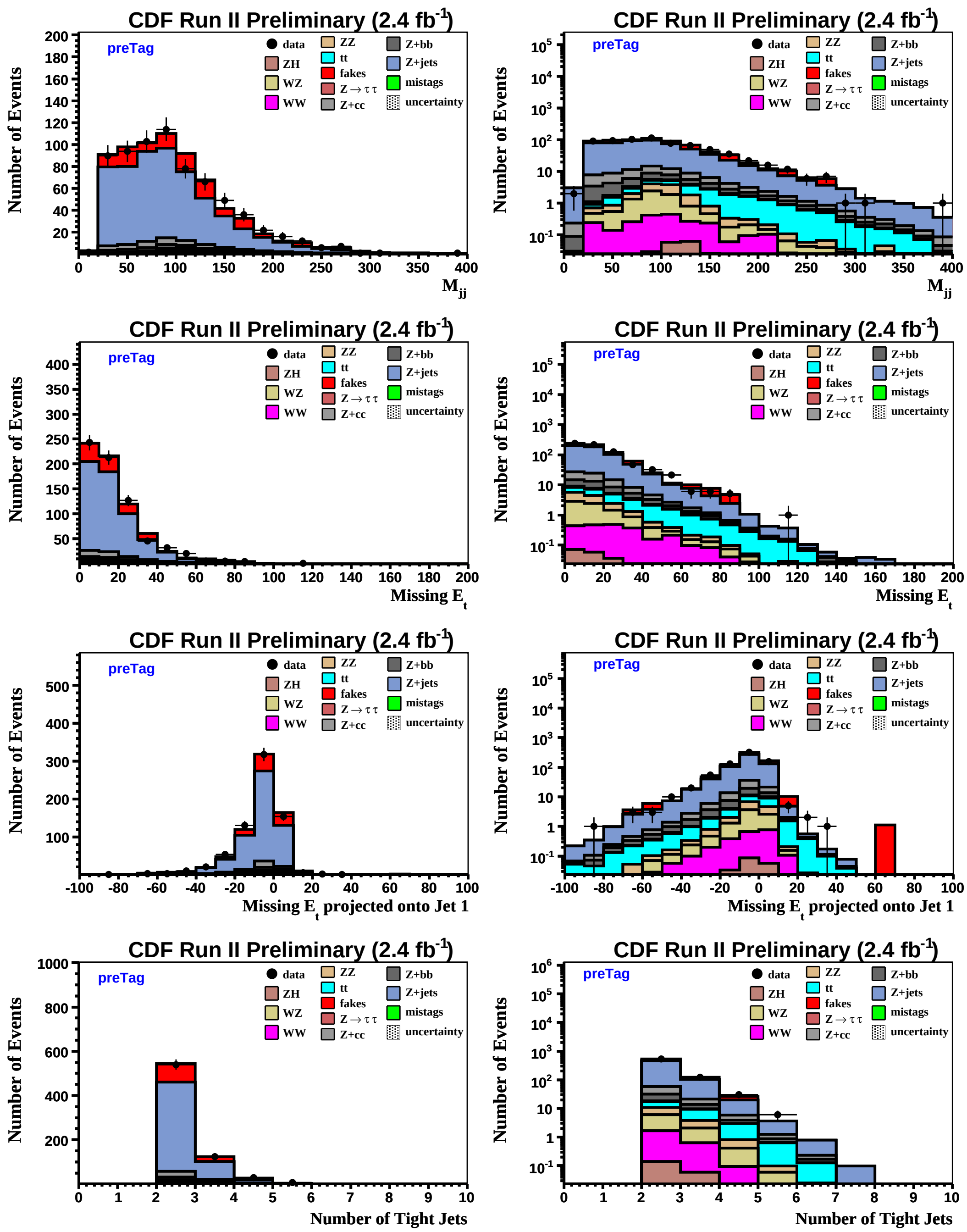

Figure 79: Pre-Tag NN inputs : Shape comparisons for TcCrkTrk Z category.

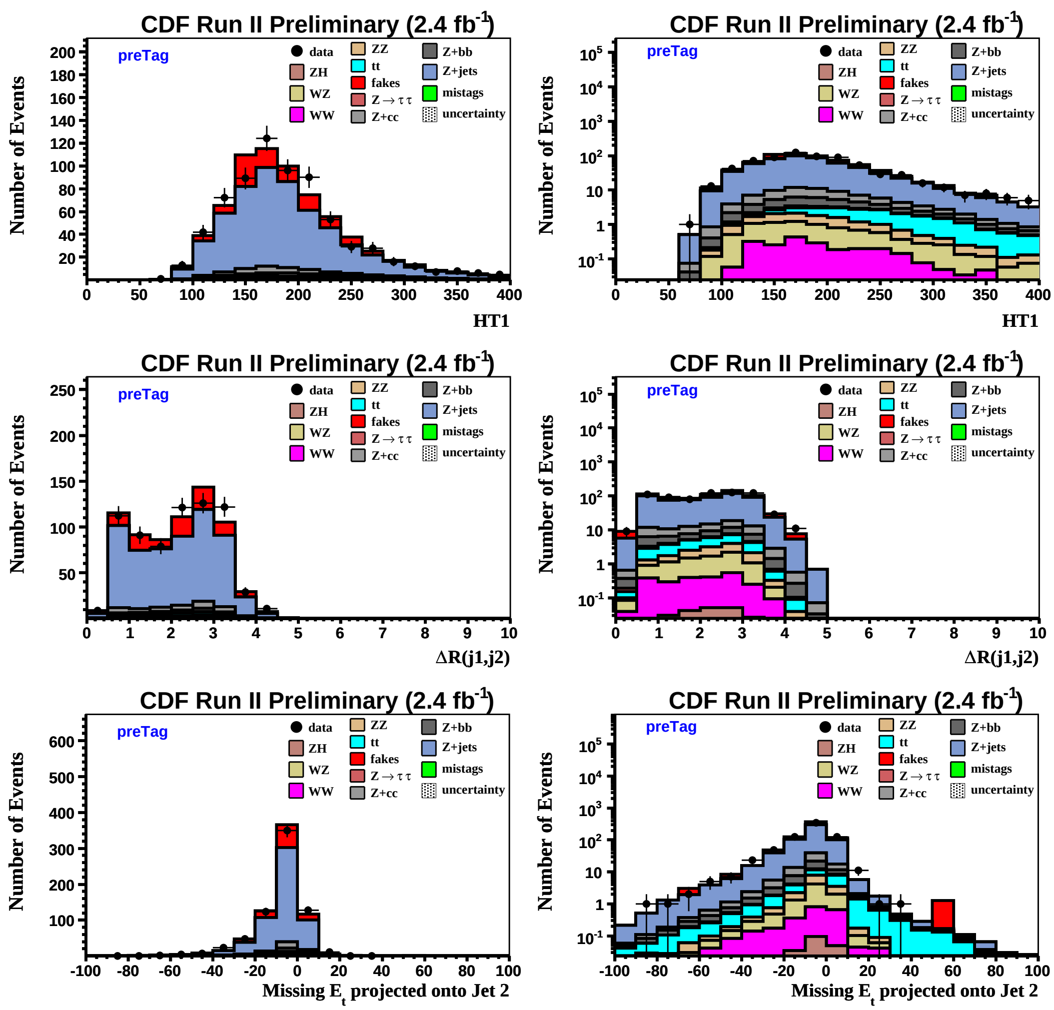

Figure 80: Pre-Tag NN inputs : Shape comparisons for TcCrkTrk Z category.

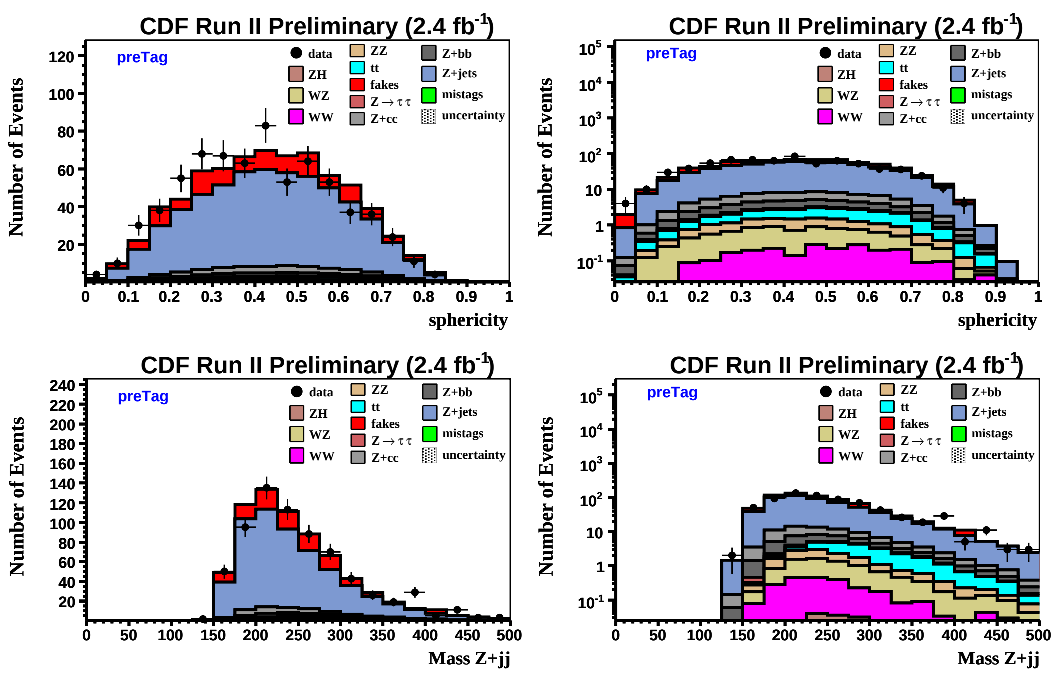

Figure 81: Pre-Tag NN inputs : Shape comparisons for TcCrkTrk Z category.

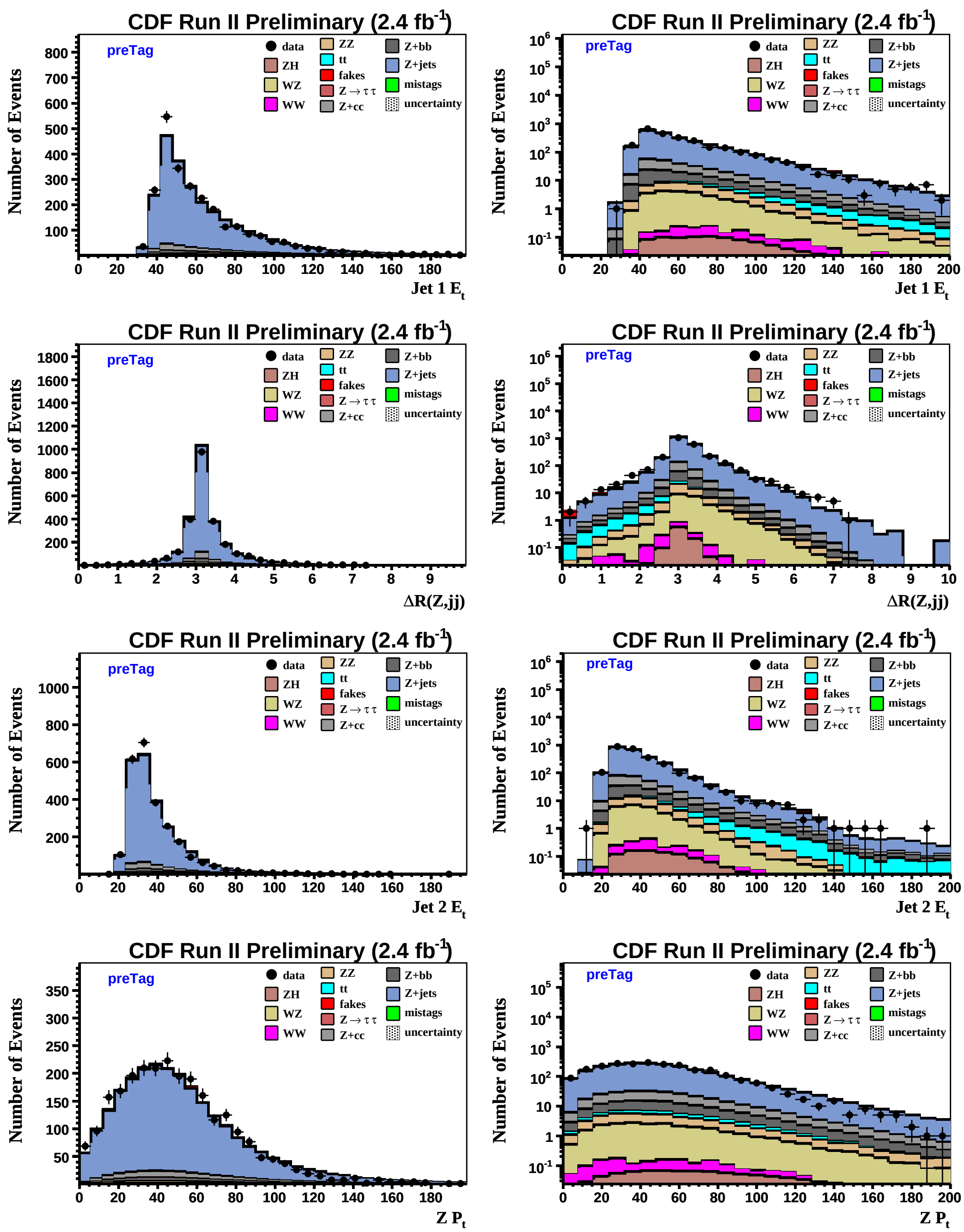

Figure 82: Pre-Tag NN inputs : Shape comparisons for $\mu\mu$ Z category.

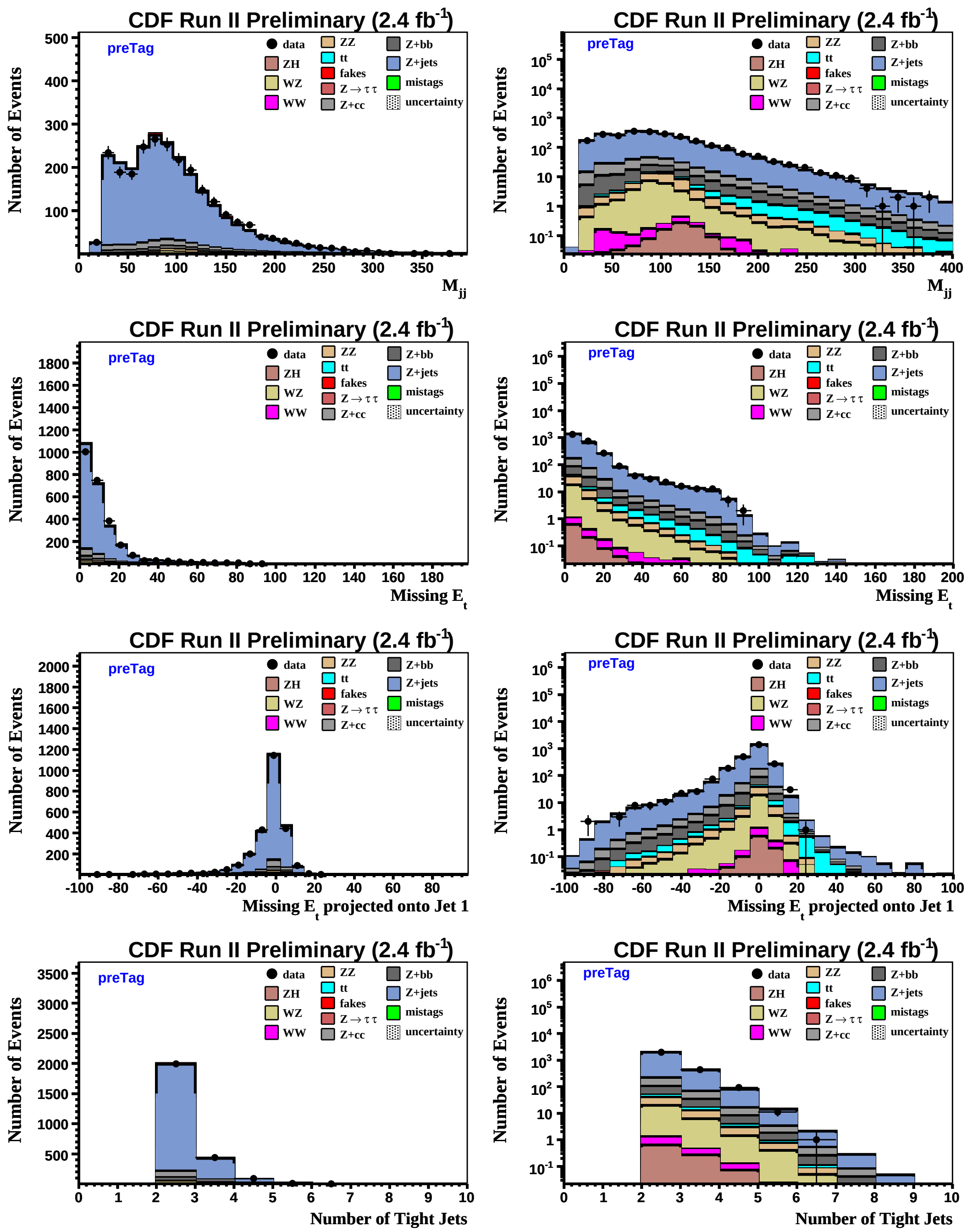

Figure 83: Pre-Tag NN inputs : Shape comparisons for $\mu\mu$ Z category.

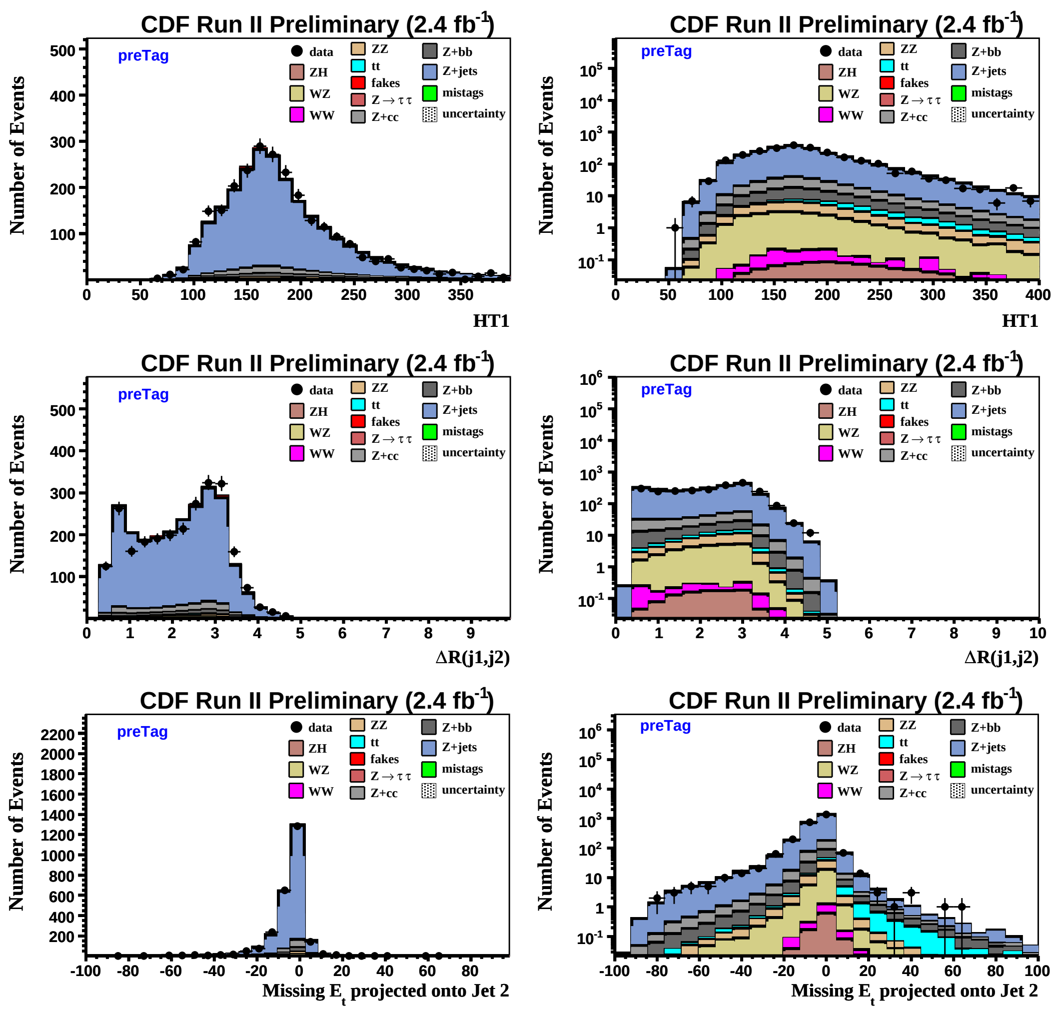

Figure 84: Pre-Tag NN inputs : Shape comparisons for $\mu\mu$ Z category.

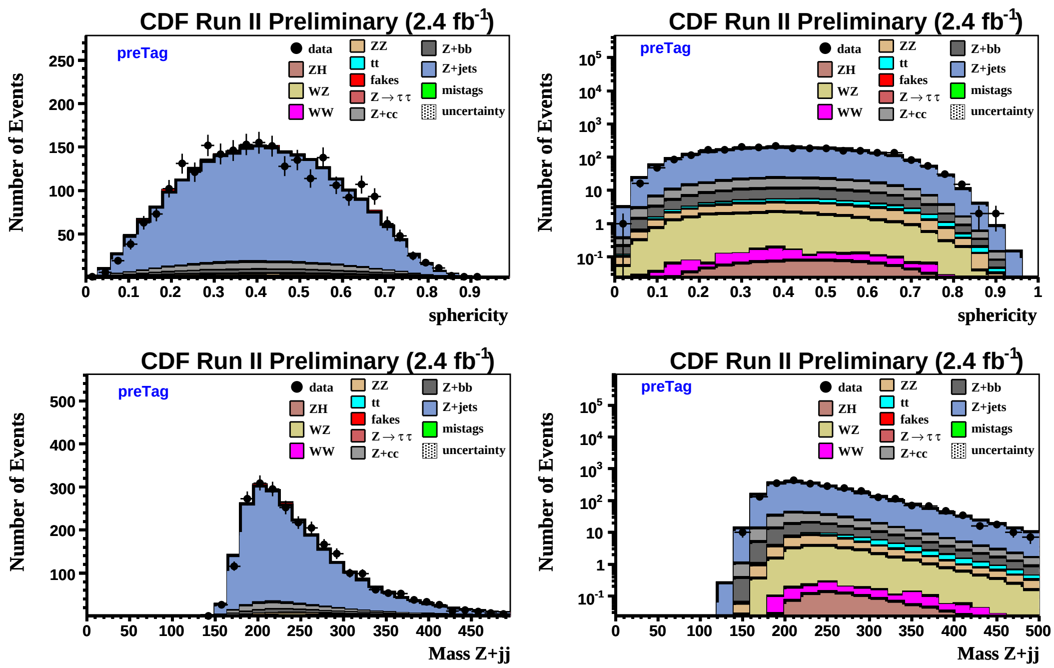

Figure 85: Pre-Tag NN inputs : Shape comparisons for $\mu\mu$ Z category.

Event Totals (All Z)					
sample	**Z**	**1 jet**	**preTag**	**Single Tag**	**double Tag**
ZH	3.5	3.46	2.76	1 ± 0.08	0.52 ± 0.04
tt	54.66	54.25	45.36	16.85 ± 3.54	8.65 ± 1.82
WW	82.09	26.01	5.5	0.16 ± 0.03	0.01 ± 0
WZ	189.92	144.74	84.86	2.99 ± 0.45	0.14 ± 0.02
ZZ	206.33	135.46	81.65	7.5 ± 1.12	2.64 ± 0.37
Z $\rightarrow \tau\tau$	158.74	28.51	4.27	0.08 ± 0.03	0 ± 0
Z+jets (bb)	1540.56	836.86	243.86	64.56 ± 27.12	16.21 ± 6.65
Z+jets (cc)	3363.1	1643.27	474.06	31.17 ± 13.09	2.29 ± 0.94
mistags / Z + jets	399711	60352.1	7140.82	113.55 ± 48.82	2.73 ± 1.2
fakes	8252.99	2697.17	591.58	25.86 ± 12.93	1.36 ± 0.68
Total Background	413563	65921.8	8674.72	263.73 ± 58.92	34.56 ± 7.1
Data	420900	70228	9035	279	39

Event Totals (TcTc Z)					
sample	**Z**	**1 jet**	**preTag**	**Single Tag**	**double Tag**
ZH	0.64	0.63	0.51	0.19 ± 0.02	0.1 ± 0.01
tt	7.37	7.31	6	2.18 ± 0.46	1.32 ± 0.28
WW	10.86	2.85	0.54	0.02 ± 0.01	0 ± 0
WZ	28.58	21.79	12.62	0.49 ± 0.07	0.04 ± 0.01
ZZ	33.62	22.99	14.16	1.35 ± 0.2	0.45 ± 0.06
Z $\rightarrow \tau\tau$	7.98	1.26	0.15	0 ± 0	0 ± 0
Z+jets (bb)	230.83	131.85	39.55	10.58 ± 4.45	2.85 ± 1.17
Z+jets (cc)	481.46	249.26	74.58	5.11 ± 2.15	0.43 ± 0.18
mistags / Z + jets	49874.1	8341.59	1065.21	15.55 ± 6.69	0.42 ± 0.18
fakes	7.84	2.59	0.48	0.03 ± 0.01	0 ± 0
Total Background	50683.2	8782.1	1213.81	35.5 ± 8.33	5.61 ± 1.23
Data	51245	9252	1275	45	5

Event Totals (TcLc Z)					
sample	**Z**	**1 jet**	**preTag**	**Single Tag**	**double Tag**
ZH	0.29	0.28	0.23	0.08 ± 0.01	0.04 ± 0
tt	5.04	5	4.21	1.58 ± 0.33	0.82 ± 0.17
WW	5.54	1.98	0.39	0 ± 0	0 ± 0
WZ	13.13	10.28	6	0.17 ± 0.03	0.01 ± 0
ZZ	14.65	10.36	6.49	0.68 ± 0.1	0.19 ± 0.03
Z $\rightarrow \tau\tau$	10.97	2	0.3	0 ± 0	0 ± 0
Z+jets (bb)	101.33	59.24	18.84	5.07 ± 2.13	1.22 ± 0.5
Z+jets (cc)	203.31	108.92	34.66	2.36 ± 0.99	0.19 ± 0.08
mistags / Z + jets	20112.2	3534.19	487.57	10.71 ± 4.61	0.27 ± 0.12
fakes	981.54	372.67	79.59	3.38 ± 1.69	0.23 ± 0.11
Total Background	21448	4104.91	638.28	24.04 ± 5.45	2.98 ± 0.56
Data	24125	4638	686	30	5

Event Totals (TcTp Z)					
sample	**Z**	**1 jet**	**preTag**	**Single Tag**	**double Tag**
ZH	0.4	0.39	0.31	0.12 ± 0.01	0.06 ± 0
tt	3.26	3.25	2.7	1.05 ± 0.22	0.61 ± 0.13
WW	9.66	2.32	0.32	0 ± 0	0 ± 0
WZ	25.05	19.26	11.58	0.45 ± 0.07	0.01 ± 0
ZZ	26.55	16.2	9.69	0.89 ± 0.13	0.33 ± 0.05
Z $\rightarrow \tau\tau$	11.1	1.25	0.18	0 ± 0	0 ± 0
Z+jets (bb)	214.81	107.45	29.11	7.76 ± 3.26	1.9 ± 0.78
Z+jets (cc)	500.12	222.46	59.7	3.83 ± 1.61	0.22 ± 0.09
mistags / Z + jets	68175.4	8952.38	954.57	14.3 ± 6.15	0.35 ± 0.15
fakes	23.67	5.38	0.84	0.04 ± 0.02	0 ± 0
Total Background	68990	9330.33	1069	28.45 ± 7.15	3.49 ± 0.81
Data	68271	10010	1159	30	0

Event Totals (TcLp Z)					
sample	**Z**	**1 jet**	**preTag**	**Single Tag**	**double Tag**
ZH	0.35	0.35	0.27	0.09 ± 0.01	0.04 ± 0
tt	4.96	4.93	4.12	1.5 ± 0.32	0.76 ± 0.16
WW	9.67	3.27	0.79	0.03 ± 0.01	0.01 ± 0
WZ	21.93	16.84	10.06	0.31 ± 0.05	0.02 ± 0
ZZ	22.96	14.16	8.04	0.67 ± 0.1	0.28 ± 0.04
Z $\rightarrow \tau\tau$	25.2	4.69	0.7	0.02 ± 0.01	0 ± 0
Z+jets (bb)	200.99	102.14	27.48	6.54 ± 2.75	1.55 ± 0.63
Z+jets (cc)	468.39	211.14	56.69	3.28 ± 1.38	0.25 ± 0.1
mistags / Z + jets	64364.8	8643.53	927.41	13.72 ± 5.9	0.34 ± 0.15
fakes	2361.85	826.96	189.91	7.06 ± 3.53	0.59 ± 0.29
Total Background	67481.1	9828.01	1225.47	33.22 ± 7.54	3.84 ± 0.74
Data	66745	10399	1218	28	2

Event Totals (Lc1Lc1 Z)					
sample	**Z**	**1 jet**	**preTag**	**Single Tag**	**double Tag**
ZH	0.01	0.01	0.01	0 ± 0	0 ± 0
tt	0.24	0.24	0.18	0.08 ± 0.02	0.02 ± 0
WW	0.35	0.09	0.03	0 ± 0	0 ± 0
WZ	0.52	0.38	0.23	0.01 ± 0	0 ± 0
ZZ	0.64	0.44	0.31	0.02 ± 0	0.01 ± 0
Z $\rightarrow \tau\tau$	0.51	0.08	0.02	0 ± 0	0 ± 0
Z+jets (bb)	5.22	2.92	0.85	0.22 ± 0.09	0.06 ± 0.02
Z+jets (cc)	10.56	5.33	1.62	0.1 ± 0.04	0 ± 0
mistags / Z + jets	1044.29	176.96	23.01	0.56 ± 0.24	0.01 ± 0
fakes	58.51	18.67	3.44	0.16 ± 0.08	0.01 ± 0.01
Total Background	1120.86	205.13	29.71	1.16 ± 0.27	0.12 ± 0.03
Data	1480	267	39	1	0

Event Totals (TpLc Z)					
sample	**Z**	**1 jet**	**preTag**	**Single Tag**	**double Tag**
ZH	0.12	0.11	0.09	0.03 ± 0	0.02 ± 0
tt	1.49	1.49	1.23	0.49 ± 0.1	0.23 ± 0.05
WW	3.52	1.17	0.23	0 ± 0	0 ± 0
WZ	8.18	6.38	3.66	0.15 ± 0.02	0 ± 0
ZZ	7.4	4.84	2.86	0.25 ± 0.04	0.09 ± 0.01
Z $\rightarrow \tau\tau$	7.53	1.67	0.24	0.01 ± 0	0 ± 0
Z+jets (bb)	59.3	32.72	9.16	2.34 ± 0.98	0.56 ± 0.23
Z+jets (cc)	130.43	66.77	19.01	1.2 ± 0.5	0.08 ± 0.03
mistags / Z + jets	14886.1	2580.3	303.83	5.32 ± 2.29	0.13 ± 0.06
fakes	1442.62	422.61	80.59	3.09 ± 1.55	0.2 ± 0.1
Total Background	16546.7	3118.06	420.91	12.87 ± 2.97	1.31 ± 0.26
Data	17877	2935	384	11	2

Event Totals (Lc1Lp Z)					
sample	**Z**	**1 jet**	**preTag**	**Single Tag**	**double Tag**
ZH	0.04	0.04	0.03	0.01 ± 0	0.01 ± 0
tt	0.64	0.63	0.55	0.19 ± 0.04	0.09 ± 0.02
WW	1.4	0.53	0.17	0 ± 0	0 ± 0
WZ	2.88	2.23	1.21	0.04 ± 0.01	0 ± 0
ZZ	2.59	1.53	0.9	0.07 ± 0.01	0.02 ± 0
Z $\rightarrow \tau\tau$	3.67	1.02	0.14	0 ± 0	0 ± 0
Z+jets (bb)	22.92	11.94	3.48	0.85 ± 0.36	0.19 ± 0.08
Z+jets (cc)	52.59	24.92	6.86	0.36 ± 0.15	0.03 ± 0.01
mistags / Z + jets	6615.27	993.51	111.7	3.23 ± 1.39	0.06 ± 0.02
fakes	1454.92	438.12	89.89	3.33 ± 1.67	0.27 ± 0.14
Total Background	8156.93	1474.47	214.93	8.09 ± 2.2	0.68 ± 0.16
Data	9875	1817	237	3	1

Event Totals (TpTp Z)					
sample	**Z**	**1 jet**	**preTag**	**Single Tag**	**double Tag**
ZH	0.04	0.04	0.03	0.01 ± 0	0.01 ± 0
tt	0.21	0.21	0.15	0.04 ± 0.01	0.03 ± 0.01
WW	1.19	0.24	0.04	0 ± 0	0 ± 0
WZ	7.44	5.77	3.43	0.12 ± 0.02	0 ± 0
ZZ	7.09	4.07	2.19	0.16 ± 0.02	0.06 ± 0.01
Z $\to \tau\tau$	3.43	0.39	0.05	0 ± 0	0 ± 0
Z+jets (bb)	52.88	26.06	6.96	1.82 ± 0.76	0.42 ± 0.17
Z+jets (cc)	134.63	58.39	15.42	0.96 ± 0.4	0.06 ± 0.03
mistags / Z + jets	22438.2	2877.04	274.46	4.5 ± 1.94	0.11 ± 0.05
fakes	5.75	1.35	0.24	0.01 ± 0	0 ± 0
Total Background	22650.8	2973.55	302.96	7.63 ± 2.12	0.68 ± 0.18
Data	21609	3318	361	15	2

Event Totals (TpLp Z)					
sample	**Z**	**1 jet**	**preTag**	**Single Tag**	**double Tag**
ZH	0.03	0.03	0.02	0.01 ± 0	0 ± 0
tt	0.18	0.17	0.14	0.04 ± 0.01	0.03 ± 0.01
WW	1.02	0.31	0.07	0 ± 0	0 ± 0
WZ	5.09	3.91	2.5	0.09 ± 0.01	0 ± 0
ZZ	5.15	3	1.74	0.17 ± 0.03	0.04 ± 0.01
Z $\to \tau\tau$	13.14	1.78	0.11	0 ± 0	0 ± 0
Z+jets (bb)	41.74	19.53	5.28	1.32 ± 0.56	0.34 ± 0.14
Z+jets (cc)	108.26	43.77	11.66	0.75 ± 0.31	0.03 ± 0.01
mistags / Z + jets	18701.9	2228.85	208.78	4.37 ± 1.88	0.08 ± 0.04
fakes	197.27	52.88	10.42	0.32 ± 0.16	0.02 ± 0.01
Total Background	19073.8	2354.23	240.73	7.07 ± 1.99	0.54 ± 0.14
Data	21912	3146	378	8	3

Event Totals (LpLp Z)					
sample	**Z**	**1 jet**	**preTag**	**Single Tag**	**double Tag**
ZH	0	0	0	0 ± 0	0 ± 0
tt	0.03	0.03	0.03	0.01 ± 0	0.01 ± 0
WW	0.06	0.01	0.01	0 ± 0	0 ± 0
WZ	0.39	0.3	0.19	0 ± 0	0 ± 0
ZZ	0.44	0.25	0.14	0.01 ± 0	0.01 ± 0
Z $\rightarrow \tau\tau$	2.76	0.43	0.02	0 ± 0	0 ± 0
Z+jets (bb)	4.59	2.12	0.51	0.13 ± 0.05	0.03 ± 0.01
Z+jets (cc)	11.2	4.59	1.12	0.05 ± 0.02	0 ± 0
mistags / Z + jets	1863.05	226.43	20.77	0.85 ± 0.36	0.01 ± 0.01
fakes	269.02	72.94	14.18	0.44 ± 0.22	0.03 ± 0.02
Total Background	2151.55	307.11	36.96	1.49 ± 0.43	0.1 ± 0.02
Data	4525	641	65	3	0

Event Totals (TcCrkTrk Z)					
sample	**Z**	**1 jet**	**preTag**	**Single Tag**	**double Tag**
ZH	0.25	0.25	0.2	0.07 ± 0.01	0.04 ± 0
tt	15.45	15.31	13.03	4.64 ± 0.98	2.1 ± 0.44
WW	14.81	7.3	1.94	0.06 ± 0.01	0 ± 0
WZ	13.22	10.07	5.62	0.2 ± 0.03	0.01 ± 0
ZZ	14.32	9.82	5.91	0.51 ± 0.08	0.17 ± 0.02
Z $\rightarrow \tau\tau$	56.18	11.44	1.96	0.04 ± 0.02	0 ± 0
Z+jets (bb)	100.85	56.71	16.77	4.48 ± 1.88	1.21 ± 0.49
Z+jets (cc)	207.94	106.3	31.18	2.09 ± 0.88	0.17 ± 0.07
mistags / Z + jets	21550.5	3600.85	448.21	10.51 ± 4.52	0.22 ± 0.1
fakes	1161	399	100	5 ± 2.5	0 ± 0
Total Background	23134.5	4217.06	624.81	27.59 ± 5.65	3.91 ± 0.67
Data	24155	4661	700	33	7

Event Totals ($\mu\mu$ Z)					
sample	**Z**	**1 jet**	**preTag**	**Single Tag**	**double Tag**
ZH	1.33	1.31	1.05	0.38 ± 0.03	0.2 ± 0.02
tt	15.79	15.68	13.02	5.05 ± 1.06	2.63 ± 0.55
WW	24.01	5.93	0.97	0.05 ± 0.01	0 ± 0
WZ	63.51	47.53	27.77	0.94 ± 0.14	0.05 ± 0.01
ZZ	70.94	47.81	29.21	2.71 ± 0.41	0.97 ± 0.14
Z $\rightarrow \tau\tau$	16.26	2.51	0.39	0.01 ± 0	0 ± 0
Z+jets (bb)	505.1	284.19	85.87	23.46 ± 9.85	5.89 ± 2.42
Z+jets (cc)	1054.22	541.42	161.56	11.09 ± 4.66	0.82 ± 0.34
mistags / Z + jets	110085	18196.5	2315.3	29.93 ± 12.87	0.74 ± 0.32
fakes	289	84	22	3 ± 1.5	0 ± 0
Total Background	112126	19226.9	2657.14	76.63 ± 16.97	11.31 ± 2.53
Data	109081	19144	2533	72	12

References

[1] J. Efron, B. Heinemann, R. Hughes, B. Kilminster, A. Mehta, B. Parks, B. Winer, *Improved search for ZH in llbb with 1 fb^{-1}* , CDF note 8704. 2, 6

[2] B. Parks, R. Hughes, B. Kilminster, K. Lannon, B. Winer, *Multi-jet Energy corrections using a Neural Net*, CDF note 8124. 3, 26

[3] B. Parks, B. Kilminster, R. Hughes, B. Winer, *Low Mass Higgs Search in Met Plus Jets Data Sample with 1.7 fb^{-1}*, CDF note 8678.

[4] http://www-cdf.fnal.gov/internal/dqm/goodrun/good.html 4

[5] A. Mehta, B. Heinemann, *Measurement of the b jet cross section for events with a Z^0 boson*, CDF note 7780. 6

[6] T. Spreitzer, C. Mills, J. Incandela, *Electron Identification in offline release 6.1.2*, CDF 7950. 8

[7] E. Lipeles, M. Neubauer, S. Hsu, F. Wurthwein, *Lepton ID for multilepton Diboson Analyses*, CDF 8538. 8